Road Embankment and Slope Stabilization

By

Dr. Mohamed Ashour and Mr. Hamed Ardalan
Department of Civil and Environmental Engineering
The University of Alabama in Huntsville
Huntsville, Alabama

Prepared by

UTCA

University Transportation Center for Alabama

Technical Report Documentation Page

1. Report No FHWA/CA/OR-	2. Government Accession No.	3. Recipient Catalog No.
4. Title and Subtitle Road Embankment and Slope Stabilization		**5. Report Date** July 31, 2010
		6. Performing Organization Code
7. Authors Dr. Mohamed Ashour and Mr. Hamed Ardalan		**8. Performing Organization Report No.** UTCA Final Report Number 09305
9. Performing Organization Name and Address Department of Civil and Environmental Engineering S201 Technology Hall The University of Alabama in Huntsville Huntsville, Alabama 35899		**10. Work Unit No.**
		11. Contract or Grant No.
12. Sponsoring Agency Name and Address University Transportation Center for Alabama The University of Alabama; Box 870205 Tuscaloosa, AL 35487-0205		**13. Type of Report and Period Covered** Final Report: January 1, 2009–July 31, 2010
		14. Sponsoring Agency Code
15. Supplementary Notes		

16. Abstract

This report and the accompanying software are part of efforts to improve the characterization and analysis of pile-stabilized slopes using one or two rows of driven piles. A combination of the limit equilibrium analysis and strain wedge (SW) model technique is employed to assess the stability of vulnerable slopes before and after using driven piles to improve the slope stability. This report focuses on the entry of input data, interpretation of the output results, and description of the employed technique. In addition to a comparison study with a full-scale load test, the finite element (FE) analysis using a general-purpose FE package, "PLAXIS," is performed to verify the results.

The characterization of lateral load induced by slipping mass of soils can be accomplished using the modified SW model technique. The SW model for laterally loaded pile behavior is a new predictive method (recommended as an alternative method by AASHTO [2007]) that relates the stress-strain behavior of soil in the developing three-dimensional passive wedge in front of the pile (denoted as the strain wedge) under lateral load to the one-dimensional beam-on-elastic foundation parameters.

Two failure scenarios are employed in the developed computer program to include pile stabilization for 1) existing slip surface of failed slope and 2) potential failure surface. The two scenarios evaluate the distribution of the soil driving forces with the consideration of the soil flow-around failure, soil strength, and pile spacing. The developed procedure can also account for the external pile head lateral load and moment along with the driving force induced by the sliding mass of soil.

The developed computer program is a design tool in which the designer can select an economic pile size to stabilize slopes. In addition to the external lateral loads applied at the pile head, the presented research work determines the mobilized driving force caused by sliding mass of soil that needs to be transferred via installed piles to stable soil layers below the slip surface. The side and front interaction between piles and sliding mass of soil is one of the main features of this project. The work presented also evaluates the appropriate pile spacing between the piles in the same pile row (wall) and the spacing between the pile rows. The computer program provides a flexible graphical user interface that facilitates entering data and analyzing/plotting the results.

The finite element analysis (using PLAXIS) was used to investigate the results. A field test for pile-stabilized slope is used to validate the results obtained from the finite element analysis and the developed technique.

17. Key Words		18. Distribution Statement	
heuristics, simulation, traffic, decision support systems, strategic planning, practice of OR			
19. Security Classif. (of this report) Unclassified	**20. Security Classif. (of this page)** Unclassified	**21. No of Pages** 87	**22. Price**

iii

Table of Contents

Tables

Figures

Executive Summary

This report and the accompanying software are part of efforts to improve the characterization and analysis of pile-stabilized slopes using one or two rows of driven piles. A combination of the limit equilibrium analysis and strain wedge (SW) model technique is employed to assess the stability of vulnerable slopes before and after using driven piles to improve the slope stability. This report focuses on the entry of input data, interpretation of the output results, and description of the employed technique. In addition to a comparison study with a full-scale load test, the finite element (FE) analysis using a general-purpose FE package, "PLAXIS," is performed to verify the results.

The characterization of lateral load induced by slipping mass of soils can be accomplished using the modified SW model technique. The SW model for laterally loaded pile behavior is a new predictive method (recommended as an alternative method by AASHTO [2007]) that relates the stress-strain behavior of soil in the developing three-dimensional passive wedge in front of the pile (denoted as the strain wedge) under lateral load to the one-dimensional beam-on-elastic foundation parameters.

Two failure scenarios are employed in the developed computer program to include pile stabilization for 1) existing slip surface of failed slope and 2) potential failure surface. The two scenarios evaluate the distribution of the soil driving forces with the consideration of the soil flow-around failure, soil strength, and pile spacing. The developed procedure can also account for the external pile head lateral load and moment along with the driving force induced by the sliding mass of soil.

The developed computer program is a design tool in which the designer can select an economic pile size to stabilize slopes. In addition to the external lateral loads applied at the pile head, the presented research work determines the mobilized driving force caused by sliding mass of soil that needs to be transferred via installed piles to stable soil layers below the slip surface. The side and front interaction between piles and sliding mass of soil is one of the main features of this project. The work presented also evaluates the appropriate pile spacing between the piles in the same pile row (wall) and the spacing between the pile rows. The computer program provides a flexible graphical user interface that facilitates entering data and analyzing/plotting the results.

The finite element analysis (using PLAXIS) was used to investigate the results. A field test for pile-stabilized slope is used to validate the results obtained from the finite element analysis and the developed technique.

Section 1
Introduction

Problem Description

Landslides (slope failures) are a critical issue likely to result from poor land management or seasonal changes in soil moisture. Driven piles, drilled shafts, or micropiles can be installed to reduce the likelihood of slope failure or landslides. At present, simplified methods are used to design the driven piles/drilled shafts/micropiles needed to stabilize slopes of bridge embankments or to reduce the potential for landslides from one season to another. The major challenge lies in the evaluation of lateral loads (pressure) from moving soil acting on the piles/pile groups. The interaction among piles including the lateral effective range of pile resistance is complex and depends on soil and pile properties and the level of soil-induced driving force. The Naval Facilities Engineering (NAVFAC 1982) design manual recommends an empirical value for the driving force of the soil on the piles based on the full passive resistance of soil. There may be considerable error in this assumption. A more sophisticated and accurate technique is needed to more realistically assess the destructive effect of sliding soil on the performance of the bridge foundation. The use of piles for slope stabilization is a common and favorable practice, especially when stiff soil deposits lie close to the ground surface (Figure 1-1).
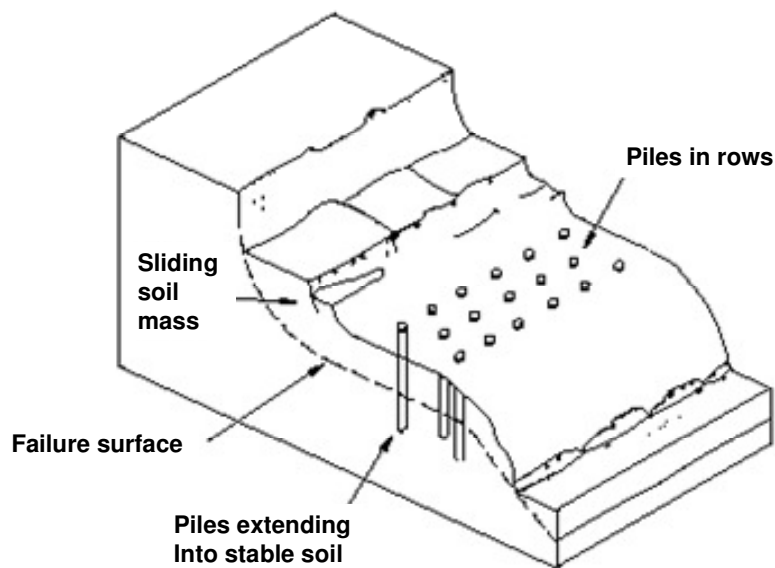
Figure 1-1. Pile rows for slope stabilization (after White, *et al.* 2005)

The problem of landslides and the use of piles to improve the stability of such slopes require better characterization of the integrated effect of laterally loaded pile behavior and the interaction of the pile structure. The lateral driving load (P_D) caused by the sliding soil mass needs a representative model for the soil-pile interaction above the failure surface that describes the actual distribution for the soil driving force along that particular portion of the pile. Flow-around failure of soil around the pile is a significant phenomenon considered in the presented methodology. It should be noted that for piling without lagging, the flow-around failure governs the amount of soil mass driving force applied on the pile, along with the pile spacing on the slope.

One approach has been used to calculate the (soil passive resistance) driving force based on Broms' method (1964) as characterized in DM.7-2 (NAVFAC 1982). Another alternative is to use the soil reaction from the traditional (Matlock and Reese) p-y curve. Neither of these ultimate resistances is envisioned for sloping ground; and neither considers group interference effects in a fundamental way for sloping ground. Since the traditional (Matlock-Reese) p-y curves were developed for long piles beneath level ground with the concentrated lateral load at the pile head, the use of these curves in the soil mass above the slip surface for the envisioned failure mechanism is not as robust as the current model.

Employed Methodology

The procedure developed deals with the problem of slope/landslide stabilization using driven piles/drilled shafts/micropiles (Driven piles, drilled shafts, or micropiles) to account for the mentioned limitations of current practices. The designer cannot evaluate the developing deformations (i.e. the strain accompanying the mobilized stress) in the soil mass until slope failure takes place and infinite strain occurs. Such analysis lacks the link between the shape of the deformed pile under mobilized conditions and the deformed/strained soil mass. The proposed design procedure does not assume that the stabilized slope moves sufficiently to mobilize the limiting soil pressure along the pile element. Rather, it considers the use of a sufficient number of installed piles to arrest slope movement before the ultimate pressure develops. This requires the incremental assessment of the developing driving force and the induced soil-pile resistance. During the incremental solution, pile and soil failure, flow-around soil failure, and in-between pile soil slip should be investigated.

The strain wedge (SW) model technique (Ashour, *et al.* 1998) for laterally loaded piles based on soil-structure interaction is modified to evaluate the mobilized non-uniformly distributed soil driving force (F_D) along the length of the pile located above the anticipated failure surface. However, the force F_D is governed by the soil-pile interaction (i.e. soil and pile properties) and by the developing flow-around failure above (no lagging) and below the slip surface. The SW model can capture the developing flow-around response and the interaction among adjacent piles.

The result of the completed research provides a new technique (analytical method/design guidelines) to deal with slope stabilization using piles. The realistic characterization and

2

determination of loads induced by lateral soil movement and transferred to stable soil layers via stabilizing piles is the core of this work.

This research provides a reliable design procedure compiled into computer code for the analysis of pile-stabilized slopes. In many cases, pile stabilization may be more effective and more appropriate than the other stabilization practices.

The utilized design methodology demonstrates the suitability of pile-stabilized slopes to assist with incorporating pile-stabilization systems into slope remediation (mitigation) practices. Therefore, a mitigation plan for vulnerable slopes and bridge embankments can be established based on such knowledge. Nevertheless, the designer has the ability to enter pre-existing landslide geometry and to estimate the resulting driving forces and the impact of external shear forces and moments applied at the pile head. The employment of this technology is often more appropriate for stabilizing potential shallow slope failure.

A full-scale pile-stabilized slope test along with the FE analysis using PLAXIS are used to show the reliability of the results obtained from the developed technique. The case study using the proposed technique also highlights the simple characterization and limited amount of data that are required to perform this type of analysis.

Section 2
Slope-Stability Analysis and Stabilizing Pile Data

Slope Section

Slope-stability analysis should be performed to estimate the risk level of the slope in question. Before the data can be entered into the program, a cross section should be prepared using a reasonable number of line segments that will represent the cross section. For existing slope failure, the developed slope geometry is used to calculate the soil parameters on the failure plane that led to that failure.

Each location where your line segments intersect, or end, is called a point and each line segment is called a line (boundary). Use lines to show the ground surface, different soil zones, and water table surface. Plot the core boring soil and rock layers on the cross section and determine the soil boundaries. Number each line from left to right starting at the top boundary (see Figure 2-1). Do not number the water surface boundary at this time.

Determine and record on the cross section the coordinates x and y (offsets and elevations) for the endpoints of all line segments, including those for the water surface, if any (Figure 2-1). Notice all boundaries have the same beginning and ending edges. Extend the water surface to the same beginning and ending edges. No vertical or overhanging boundaries are allowed. The program always sets the starting point for the graph at x, y = 0, 0. Consequently, when preparing the cross section, adjust the values of the coordinates so that the lower left starting point is at least x, y = (10, 10) to allow room for the slip plane below the lowest surface. Also, if the actual elevations are used, the program will plot the actual distance from zero, producing an impracticably small graph (e.g. if the lower left starting point on Figure 2-1 were imputed at the actual elevation, the graph would be scaled to fit the screen in such a manner that it would be hard to see the geometry shown below).
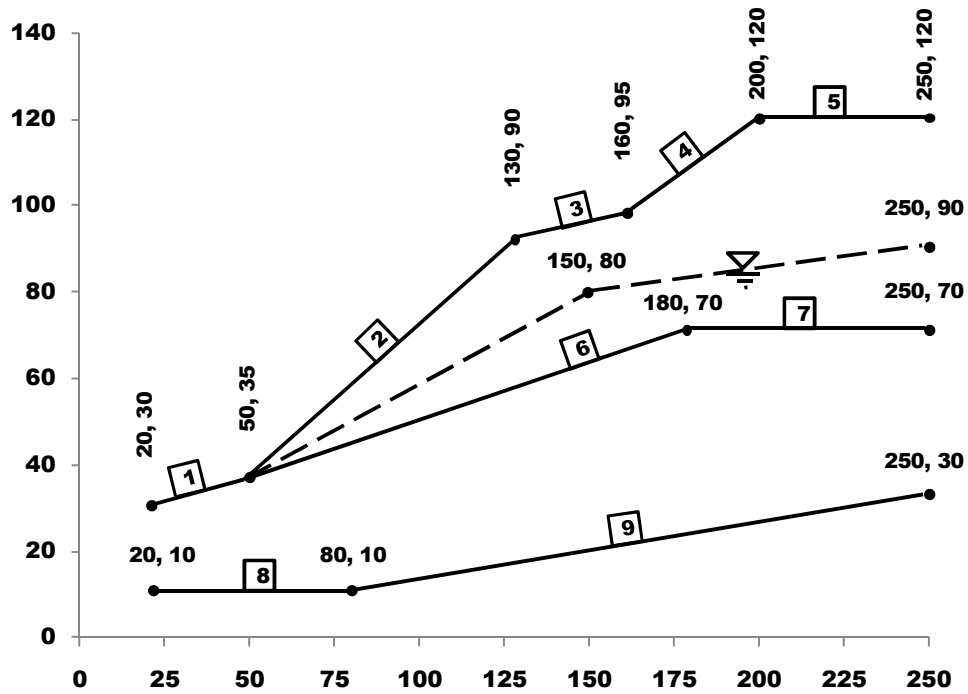
Figure 2-1. Flagged lines and point coordinates
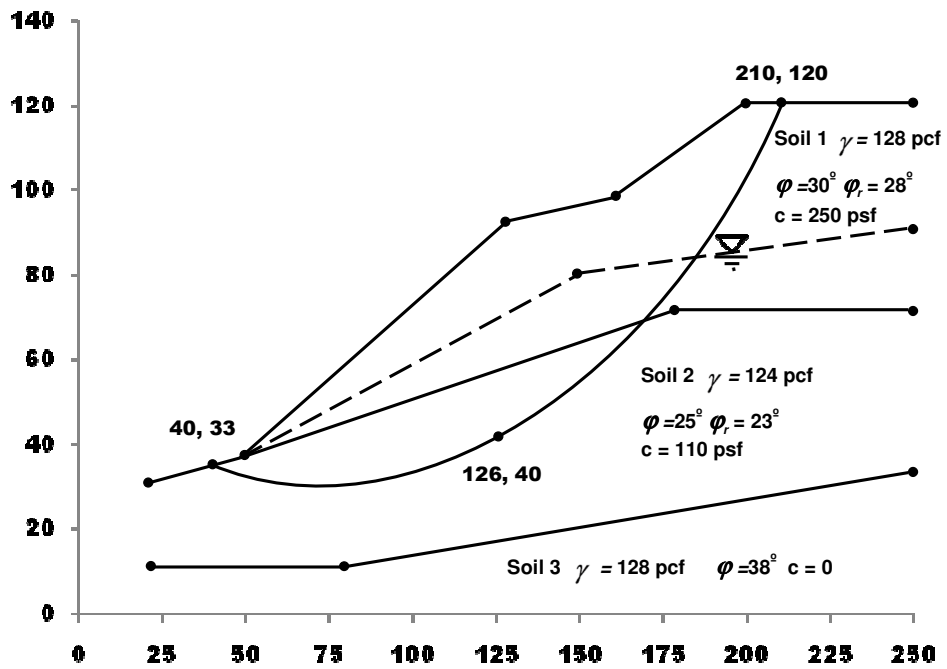
Figure 2-2. Cross section showing typical required data

5

Prepare Soil Data

Number the soil (rock) zones on the cross section and record the properties of the soil in each zone (Figure 2-2). The soil below each line is accounted for in the program as will be discussed. The program can use the average Standard Penetration Test (SPT) N-values to estimate the undisturbed soil parameters for each layer (for soil-pile analysis). Unit weight, saturated unit weight, residual friction angle, peak friction angle, disturbed cohesion, and undisturbed cohesion can be estimated based on the soil type or from laboratory testing. The Rock Mass Rating (RMR) can be used to estimate rock properties. Selecting soil parameters and using RMR and N-values will be discussed later.

Select Coordinates for the Failure Surface

For existing failure surface use the boring information to determine or estimate the failure surface location. The program uses a circular failure surface. Based on the three failure-surface points entered into the program, plot the predicted failure surface on the soil profile (see the three points on Figure 2-2). Alternatively, for potential failure surface, if a range for the initiation point near the toe and ending point near the scarp is entered, the program will search for the worst failure surface out of the ten worst failure surfaces in the selected range. Make sure your circle does not intersect the ground surface in more than two points or an error message will be generated. You may have to slightly change some points, or lines, on the cross section to correct this problem.

Input Data

When entering data, refer to Figure 2-3 (Input Table).
1. Enter a title.
2. Enter a number for Number of Soil Types; this must be greater than zero.
3. Change the SPT Hammer Efficiency if the hammer used has a different efficiency than the standard 60% for rope and cathead hammer. The program internally adjusts the SPT blow-counts to the standard (N_{60}) to determine the soil properties needed for soil-pile analysis.
4. Click the Update Screen button to generate the required rows for the number soils entered. After making changes to a table/section, and prior to selecting another table/section or to running the analysis, the screen must be updated).
5. Select the Soil Type. There are four choices: three soil types and one rock. When selecting Soil Type, it is important to understand how the program uses each in its calculations.
    a. **Sand**: This soil has zero cohesion, only friction; therefore, the program ignores any values entered into the Cohesion Intercept undisturbed column. This soil would be recognized as fairly clean sand with not enough binder soil to stick together.
    b. **Clay**: This soil has zero friction, only cohesion; therefore, the program ignores any values entered into the Friction Angle peak column. This soil would be

classified as clay with only a trace of sand of silt, and it can be rolled into a thin thread between the fingers.

   c. **C-Phi (Silt)**: This soil contains both friction and cohesion properties. This selection will use both soil properties in the calculation. This soil should be selected unless it can be determined the soil is either a pure sand or pure clay.

   d. **Rock**: Used for bedrock of all types, including an intermediate geomaterial (IGM) of extremely weathered rock.

6. Input the disturbed cohesion intercept and friction angle. Cohesive Intercept <u>Disturbed</u> and Friction Angle <u>Residual</u> represent the soil strength parameters along the failure surface. <u>These values are used in the initial slope-stability analysis without piles</u>.

7. The last four columns of the soil properties, <u>Blowcounts</u>, <u>RMR</u> (rock mass rating), <u>Cohesion Intercept</u>, <u>Friction Angle</u>, represent the data needed for the soil-pile analysis. These represent the soil strength parameters above and below the failure surface and are considered undisturbed.

8. The program defaults to the columns labeled <u>Blowcounts and RMR</u> when running the soil-pile analysis. If values are entered into the Blowcounts (N Value) or RMR columns, the program ignores any value entered in the last two columns: Cohesion Intercept and Friction Angle.

Soil Number	Soil Type	Unit Wt. pcf	Saturated Unit Wt. pcf	Cohesion Intercept (Disturbed) psf	Friction Angle (Residual) deg	Blowcounts N	RMR (Rock)	Cohesion Intercept (Undisturbed) psf	Friction Angle (Peak) deg
1	Sand	124	128	0	28	17	0	0	0
2	Rock	138	140	500	34		12	0	0

Problem Title: Jordan Run Road Slide #3, 3802 Station 22+50

Number of Soil Types: 2   SPT Hammer Efficiency % 60   Update Screen

Figure 2-3. Soil input table

Boundaries

1. There are two failure scenarios used to analyze slope stability as follows:
   a. Existing Failure Surface
   b. Potential Failure Surface

   The input of the boundary layers is the same for the two scenarios mentioned—**Existing** and **Potential** Failure Surface—both require a detailed input of boundaries, soil profile, water surface, and slip plane.

   This section covers only slope failure scenario a. When inputting the data into this section, refer to Figure 2-4.

2. Input the total number of boundaries and the number of top boundaries and click Update Screen. In the example in Figure 2-1, the number of top boundaries is 5 and the total number of boundaries is 9.

3. Input the boundary line segments <u>starting from the left and top most boundary</u> and working to the right and down through the layers. Input line segments using the x and y coordinates for the start and end of each line segment. Notice that the <u>ending coordinates are repeated as the starting coordinates</u> for the next line segment.

4. When entering the line segments, it is required to define which soil type underlies which line segment by giving the soil a number corresponding to the soil type. This Soil Number is entered in the same row as the line segment for which it underlies.

5. It is important to accurately estimate where the water surface was at the time of failure. Enter the number of water surface points that make up the total number of line segments. Do not forget the last ending point. For example, 9 line segments will require 10 points. Enter the x and y coordinates that make up the line segments. The program only accepts one water surface.

Boundary	X-Left	Y-Left	X-Right	Y-Right	Soil Number		Total number of boundaries:	9	Input Data for
Number	ft.	ft.	ft.	ft.	Below Bnd		Number of top boundaries:	5	○ Existing Failure Surface
1	20	30	50	35	1				⦿ Potential Failure Surface
2	50	35	130	90	1				
3	130	90	160	95	1				
4	160	95	200	120	1				

Water Surf.	X(1)	Y(1)	X(2)	Y(2)	X(3)	Y(3)	X(4)	Y(4)	X(5)	Y(5)	X(6)
No. of pts	ft	ft	ft	ft	ft	ft	ft	ft	ft	ft	ft
3	50	35	150	80	250	90					

Figure 2-4. Input table for boundary line and water surface segments

6. It is possible to enter the data for either or both Existing Failure Surface or Potential Failure Surface and to switch between the two methods. Switching to one of the other methods will require re-entry of the boundary data. Therefore, it is recommended that the user <u>save the file after entering the boundary data and prior to switching methods of analysis</u>.

Performing Stability Analysis

1. **Existing Failure Surface**: This method requires inputting the slip surface, utilizing a three-point method. The failure surface is determined by the slope geometry, the scarp, the toe, and the depth to slip plane as indicated by the borings. This requires the x and y coordinates for the starting, ending, and middle points by entered in a table (see Figure 2-5) that opens when the Existing Failure Surface button is selected. The slope geometry and the failure surface can be viewed by selecting the Plot Failure Surface button. This option is useful to determine if adjustments are needed to the failure surface or boundaries.

Figure 2-5. Existing failure surface input box

If the table is closed without inputting data, the program will generate the warning box shown in Figure 2-6. Ignore this warning; it is just indicating there is no data to plot.
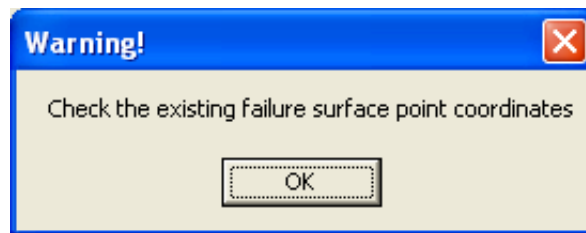
Figure 2-6. Warning box

2. **Potential Failure Surface**: This method requires entering the slip surface by inputting the Leftmost Initiation Point, Rightmost Initiation Point, Left Termination Limit, Right Termination Limit, and Minimum Elevation of Surface Development (Figure 2-7). The table will open when the 2nd button is selected (Figure 2-4). This method is used when the exact failure surface is unknown or when searching for the most critical slip surface. It is also used when analyzing a slope that has not failed for stability. It is common to first conduct a preliminary search for the critical slip surface. It is usually found that most of the slip surfaces occur within a defined range. It is possible after the first run to more precisely define the search limits or force the critical surface to a predetermined location.

Figure 2-7. Potential failure surface input box

3. **Modified Bishop Method**: The method used in the program is the Modified Bishop Method, which simulates a circular failure surface. When the factor of safety of a slide is 0.99—or for practical purposes 1.0—failure has occurred. (It is commonly observed that failures can occur with a factor of safety of 1.10 using this method. More on factors of safety will be discussed later.) Other methods are available that simulate sliding block failures, which may be more accurate for the type of failure, although the Bishop method is believed adequate for pile wall design and estimating soil parameters.

4. **The Goal for the Initial Stability Analysis**: The goal of the initial stability analysis is to establish the soil parameters (strength parameters and water surface) to obtain a factor of safety of 1.0. In this form of back-analysis, the <u>soil parameter values do not have to be exact</u>, just *reasonably correct*. If you are running the program for an existing slide, the factor of safety should be 1.0. If the factor of safety does not reach 1.0, adjust the strength parameters, the water table data, or both until it is. Do not waste time making the slide factor of safety <u>exactly</u> 1.0 if the factor of safety rounds to 1.0 (i.e. is 0.96 to 1.04; use two decimal places only). Use soil parameters and water surface in subsequent stability analyses to evaluate the pile wall design (discussed later).

5. **Run the Stability Analysis**: At the top in the menu, select **Run, Slope Stability**. The following note will appear if all inputs were entered correctly (Figure 2-8).
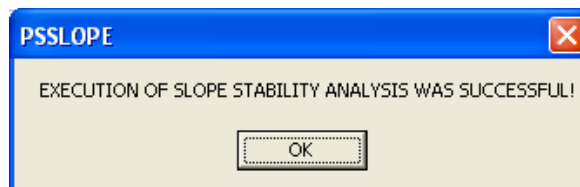
Figure 2-8. Notification message of successful stability analysis

6. **Viewing Results**
    a. The program offers two methods to view the profile of the input parameters prior to running the stability analysis (this function is not available in the Simple Wedge Analysis). This function can be used to check the soil, water table, and failure surfaces and make adjustments prior to running the analysis (Figure 2-9). A small sketch of the surface, water, and slip plane boundaries will be generated (Figure 2-9).
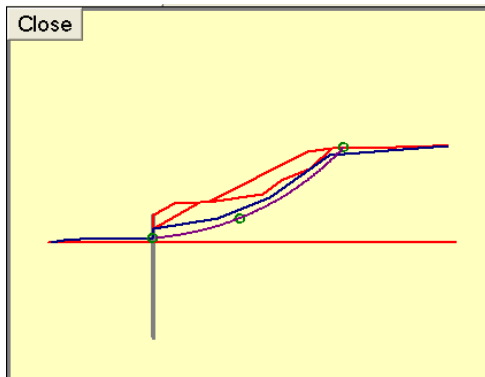
Figure 2-9. Preview

    In the Existing Failure Surface, press the Plot Failure Surface button (Figure 2-10). This button is not available in the Potential Failure Surface.

Points of Failure	X-Coordinate	Y-Coordinate
Surface	ft	ft
Point No. 1	13.11	11.88
Point No. 2	52.02	19.56
Point No. 3	85.29	33.36

Figure 2-10. Plotting failure surface

    b. To view the preview sketch (Figure 2-9), select Profile on the main menu bar at the top of the screen (Figure 2-11).

Slide3680 at 500

File   Run   Graph   Profile   Manual   Pile Output Data
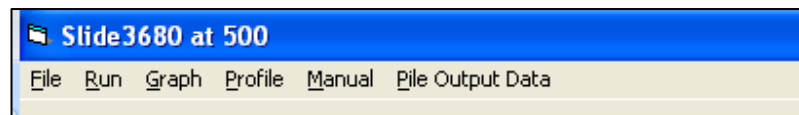
Figure 2-11. Profile on main menu bar

    c. Once the stability analysis has run successfully, the user has the option to view a graph of the geometry and failure surfaces (Figure 2-12). The graph displays the factor of safety (F.S.), water table, soil layers, and slide name. If the mouse

11

pointer is moved over the graph, the x and y coordinates are displayed on the lower border of the graph. Please note that the order of the coordinates are reversed: y and x.

In addition to the information displayed on the graph, other information can be printed or viewed on the additional two tabs:

c.1   **Output Data**
        Detailed failure surface coordinates (circle center coordinates and radius), soil profile and properties, water surface coordinates, driving and resistance forces along the failure surface, and stability factor of safety are presented in the output data file.
c.2   **Input Data**
        ASCII (numerical) code for all input data prepared as required by the program read format.
c.3   **Print**
        Plot/graph failure surface with the slope-embankment profile, water surface, and pile location.
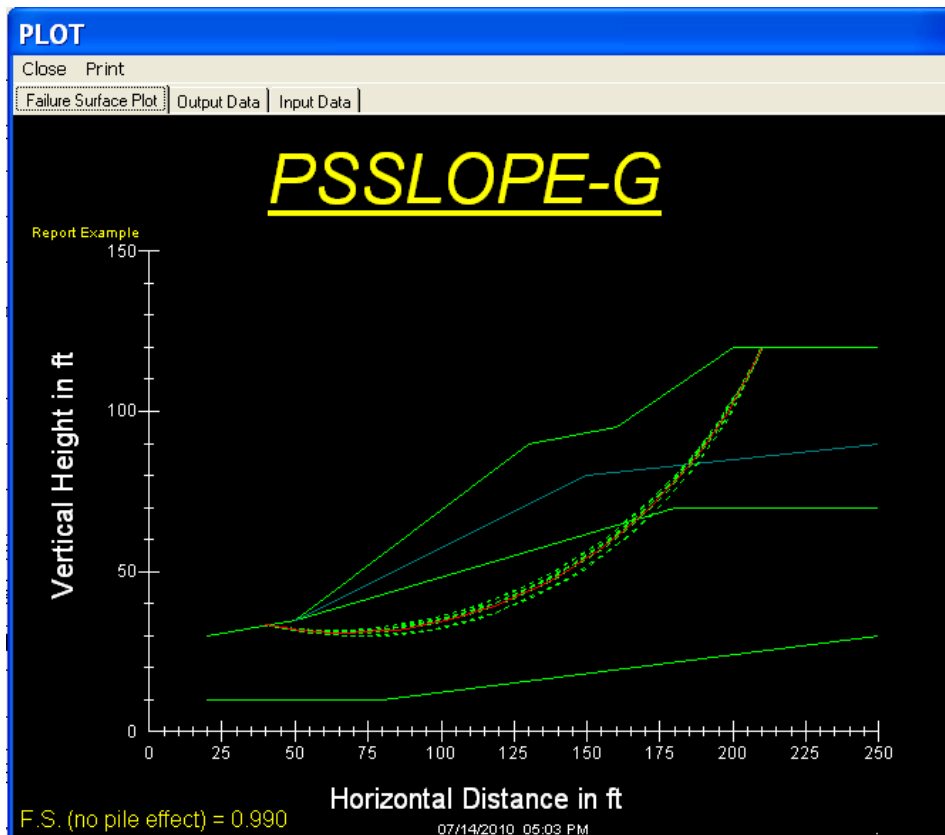
Figure 2-12. Stability graph/plot

Pile Properties

Pile Data Input

1. Select from the drop down menu the appropriate pile (Figure 2-13) and enter the pile properties (Figure 2-14):

    a. Flange Width: Column Width (b_f) for H-Pile or diameter for pipe pile
    b. Depth: Column Depth (d), from manual
    c. EI: E = Modulus of Elasticity
                             I = Moment of Inertia (I) in the strong axis
    d. Unfactored Plastic Moment: Yield stress (psi) ^{x} S in the strong
                                   direction (S = section modulus)

H-Pile	Lagging Depth	Total Length	Pile Spacings	Pile-Head	Pile-Head	Pile Rows	Pile Row
Section	ft	of the Pile, ft	ft	X-Coordinate, ft	Y-Coordinate, ft	⊙ One row	Spacing, ft
Pile Type ▾	0	60	4	160	95	○ Two rows (Staggard)	0
Pile Type							
H-Pile	ported Portion of the Slope	1		Pile-Head Lateral Load (Kips)	8.16	Pile-Head Moment (Kips-ft)	8.02
Steel Pipe Pile							
Concrete Pile							

Figure 2-13. Pile input table

Figure 2-14. H-pile input

Selection of the proper pile size will come with experience and will only need minor adjustment to achieve the proper performance and deflection. A good practice is to select a pile size a little larger than anticipated and run the program to determine the smallest size needed. Selecting a pile size that is too small results in an error message (see Figure 2-15) that the pile failed under the moment and produces no quantifying results by which to gauge how much larger the pile needs to be.
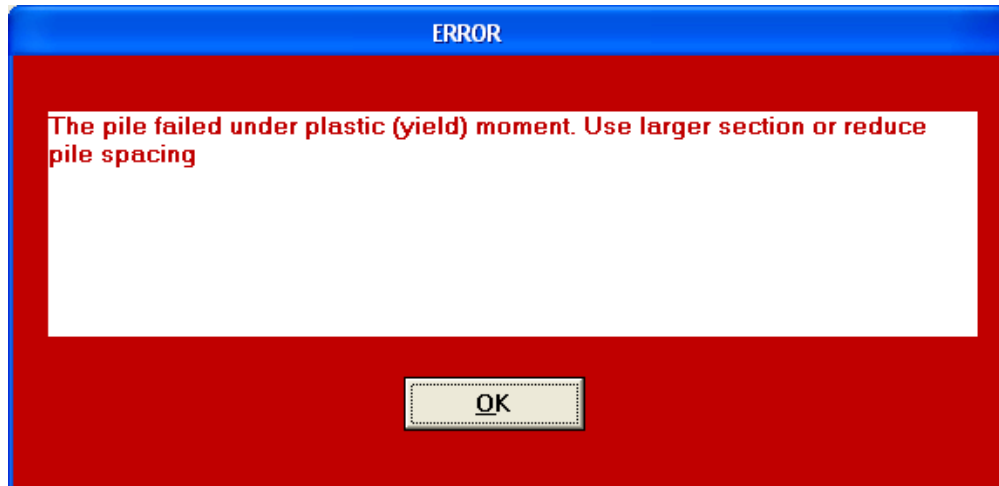
Figure 2-15. Pile failure warning message

2. Enter the desired **Lagging Depth**. Keep in mind that the slope on the downhill side may continue to move.
3. Enter the estimated **Total Length** of the pile in feet.
4. Enter the **Pile Spacing** (center-to-center) in a row.
5. Enter the **Pile Head** x and y coordinates. These must be the same coordinates as at the top of the pile, which were entered into the boundary input table.
6. Select the number of pile rows (one or two).
7. Select the **FS**. For the initial analysis of the supported portion of the slope, use 1.0.
8. Enter the shear force (lateral load) applied at the pile head.
9. Enter the value of the moment applied at the pile head.

By entering the pile properties and coordinates, the pile can be plotted on the slope graph with the slope failure surface (Figure 2-16). The user can check the appropriate location of the pile on that plot and change it (by changing the pile coordinates) as needed.
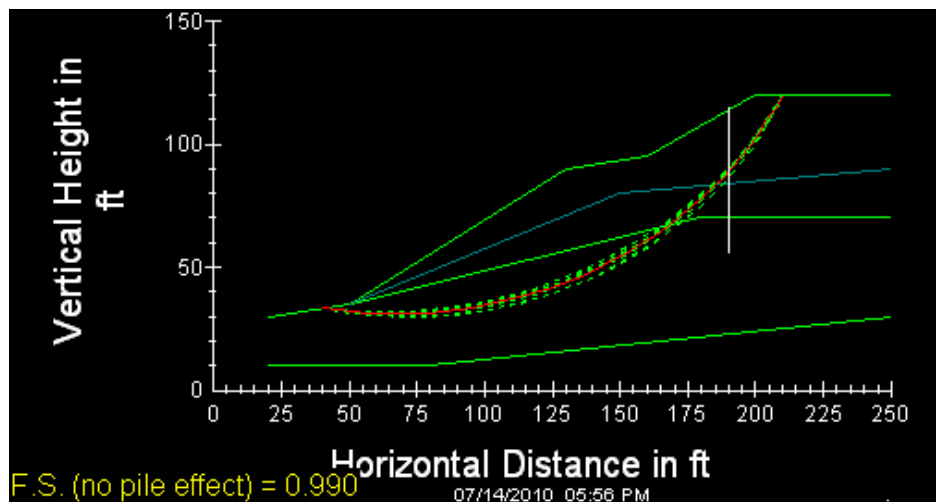
Figure 2-16. Failure surface with the location of the stabilizing pile

14

Section 3
Pile Analysis and Results

Performing Pile Analysis

1. It is important to remember that <u>Slope Stability</u> must be run prior to running <u>Slope with Piles</u> ***EVERY TIME*** a change is made. If a change is made to ***ANY*** input data, then the slope stability must be run again. So it is recommended as a practice to run the Slope Stability and then run the Slope with Piles every time. To run the program, select Run the Slope with Piles.
2. Once the program has successfully run, pile performance information will be displayed on the main page and the user has the option of viewing several files and graphs. The Factor of Safety and the Pile Performance Ratio will be displayed at the far lower right of the main page (Figure 3-1).

Water Surf.	X (1)	Y(1)	X (2)	Y(2)	X (3)	Y(3)	X (4)	Y(4)	X (5)	Y(5)	X (6)
No. of pts	ft	ft	ft	ft	ft	ft	ft	ft	ft	ft	ft
3	50	35	150	80	250	90					

H-Pile	Lagging Depth	Total Length	Pile Spacings	Pile-Head	Pile-Head	Pile Rows		Pile Row	
Section	ft	of the Pile, ft	ft	X-Coordinate, ft	Y-Coordinate, ft	⊙ One row		Spacing, ft	FS of the Unsupported Portion of Slope = 1.030
H-Pile	0	60	4	190	115	○ Two rows (Staggard)		0	Pile Performance Ratio= 0.273

Desired FS of the Supported Portion of the Slope [1]   Pile-Head Lateral Load (Kips) [0]   Pile-Head Moment (Kips-ft) [0]

Figure 3-1. Pile analysis output

   a. **FS of the Unsupported Portion of Slope**: This is the FS for the portion of the slide that is downhill from the pile wall, which is not supported by the pile wall. By stabilizing the upper portion of the slide, the driving force could be reduced or even eliminated, thereby stabilizing the lower portion. This information is of concern if there is something downhill of the slide that may be in jeopardy such as structures, roads, and train tracks.

   b. **Pile Performance Ratio**: This is a percentage of the factored pile strength being used. This information can be utilized several ways. When sizing the pile up or down, this percentage can help in determining how much to adjust the pile size. It is important to remember that the final correction requires a factor of safety of 1.3 for general slides and 1.5 around structures (per AASHTO LRFD Bridge Design Specifications). The higher FS will use a greater percentage of the pile strength. Also, if the pile is not long enough and rotates over (fence post), the performance ratio <u>will be low</u>. This number should always be used in conjunction with the deflection as discussed below.

Graphing Results

From the main menu select Graph, then select Pile Response from the drop-down menu. The pile response is analyzed utilizing four separate graphs: Deflection, Moment, Shear Force, and Line Load. On the graph there is a tab for Graphic Control, which has no function with the program. Although it is still active and can be used to modify the overall look of the graph, it will tend to produce a graph that is not as usable. Once the graph has been manipulated with this function, it is not possible to return to the original graph. Do not fear: restarting the program will restore the graph to the default.

a. **Deflection**: This graph displays the deflection of the pile, in feet, along the y axis. Deflection is most critical when analyzed at a factor of safety of 1.0 (Figure 3-2). The amount of deflection allowed depends on the situation.
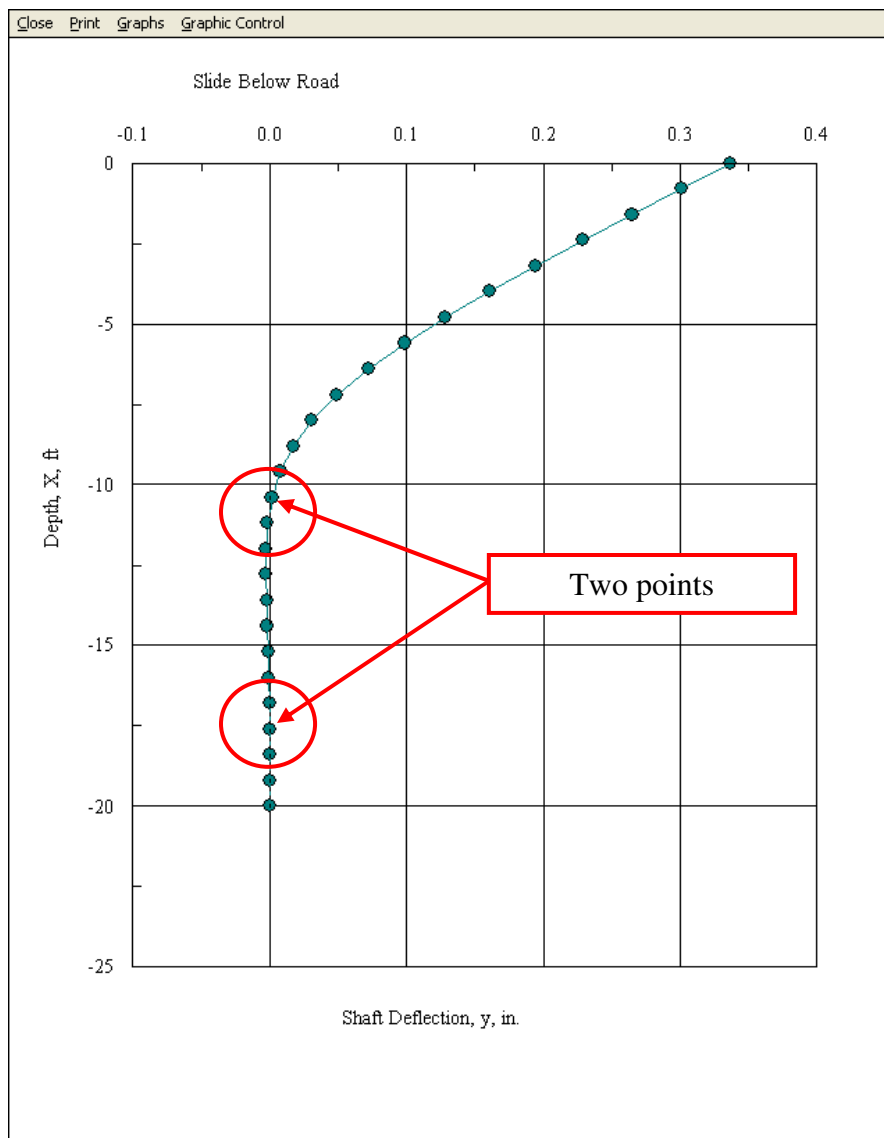
Figure 3-2. Pile deflection graph

b. **Bending Moment**: The location and magnitude of the bending moment can be visualized (Figure 3-3). As a check, the moment in the flexure formula (moment/section modulus = fiber stress) can be used to determine what section modulus to use if a different shape is desired.
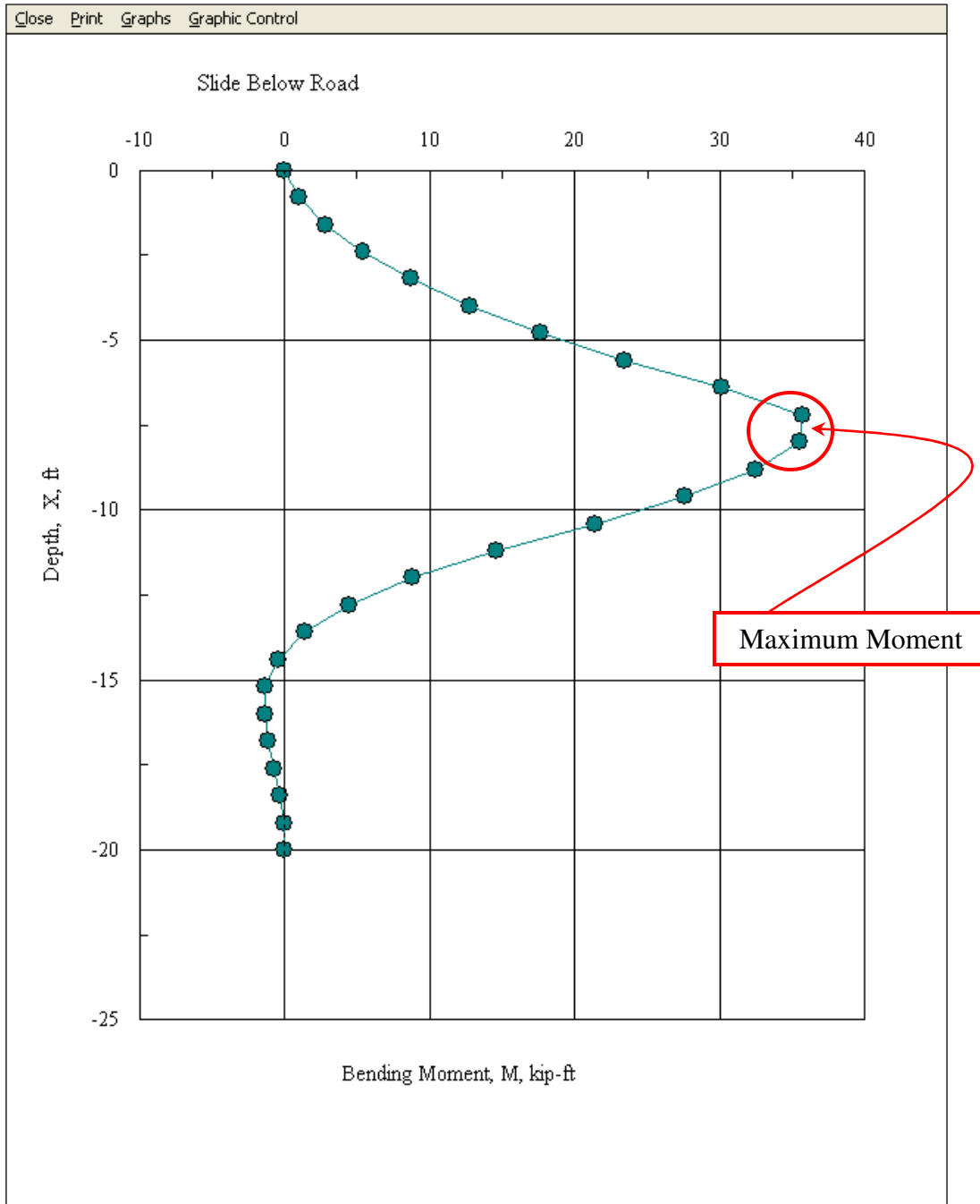
Figure 3-3. Pile bending moment

c. **Shear Force**: The shear is built up within the pile by the slipping mass then shed into the more resistive layer below the slip surface. Shear is usually not a critical design state for steel piles (Figure 3-4).
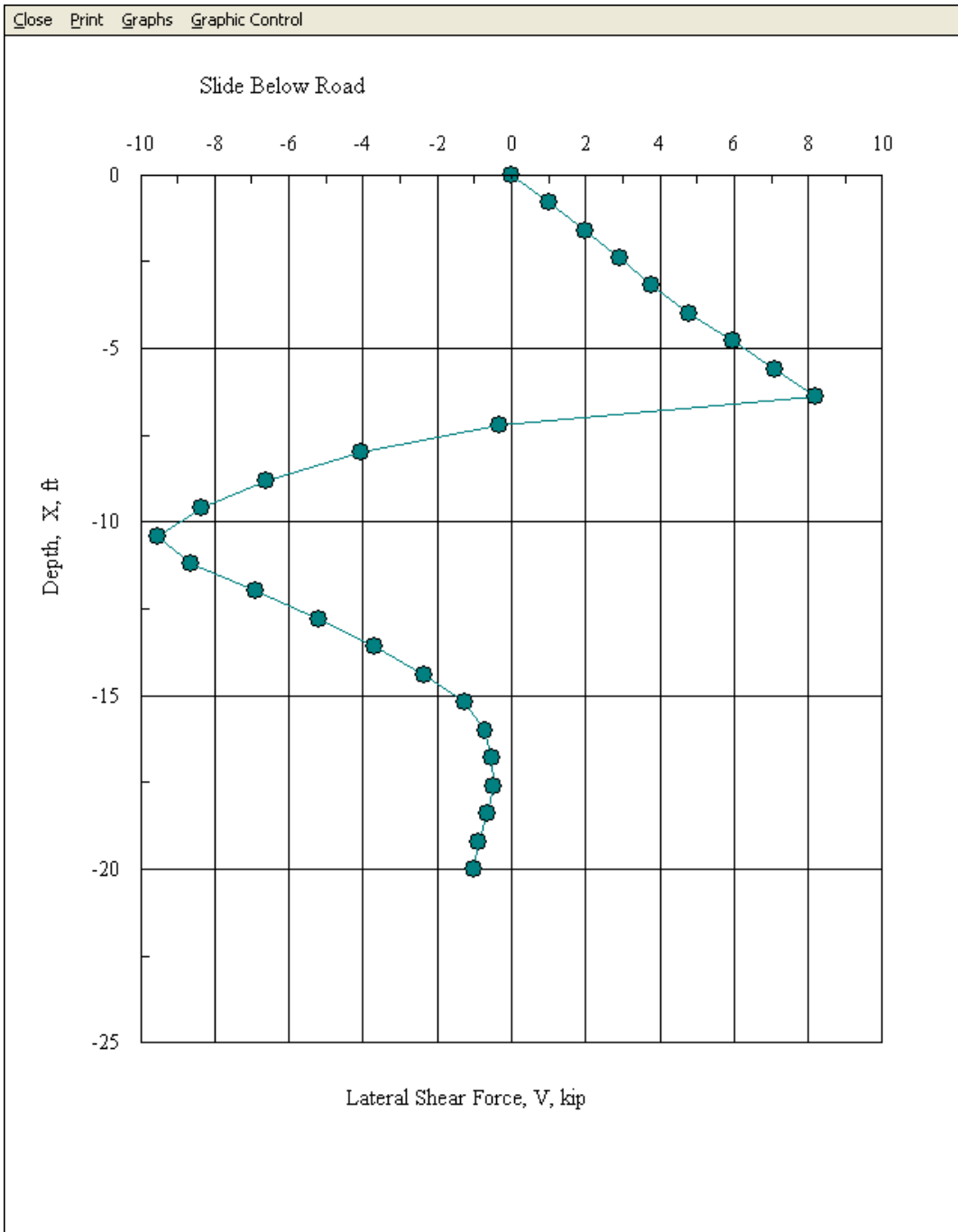
Figure 3-4. Pile shear force

d. **Line Load**: The line load is the load per vertical inch of the pile that the soil or rock exerts. To convert this load to stress, divide the force by the flange width. This is used to check the spike at the rock line to determine if the pressure exceeds the unconfined compressive strength of the rock mass (Figure 3-5).
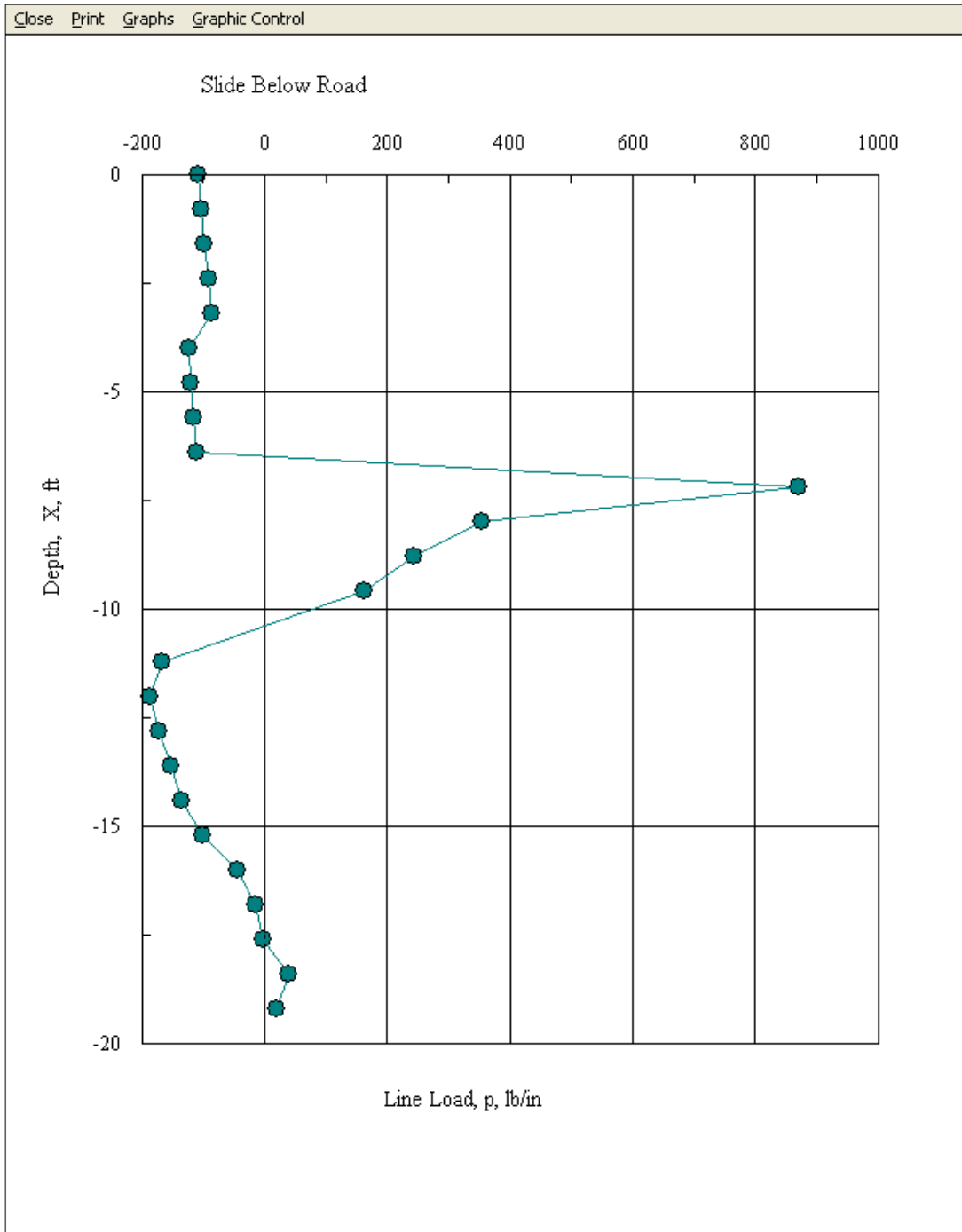
Figure 3.5. Soil-pile line load

Output Data Files

Once the required pile size has been determined by checking the pile performance at factors of safety of 1.0, 1.3, and 1.5 for bridge embankments, save the file and print any files required.

In addition to graphs and plots, the program generates two text files (Figures 3-6, 3-7, and 3-8). These files are output files generated and used as input files by other parts of the program. Care should be taken when examining these files, as changes will corrupt the original results. However, if needed, the user can obtain the exact deflection, location, and depth of the maximum moment from these files although, as with most things in Geotechnical Engineering, this level of accuracy is not really needed.

Figure 3-6. Output text files

```
Profile.txt - Notepad
File  Edit  Format  View  Help

Slide Below Road
 Number of Sections,        51
   Depth,ft    Deflect.,in.   Moment,Kip-ft    Shear,Kip    Slope,Rad    Soil Reaction,lb/in
   .00000E+00   .33699E+00    -.17118E-11     .00000E+00    .37620E-02   -.10754E+03
   .40000E+00   .31893E+00     .40139E+00     .51621E+00    .37592E-02   -.10525E+03
   .80000E+00   .30089E+00     .10097E+01     .10214E+01    .37524E-02   -.10280E+03
   .12000E+01   .28288E+00     .18206E+01     .15149E+01    .37401E-02   -.10020E+03
   .16000E+01   .26493E+00     .28280E+01     .19959E+01    .37210E-02   -.97451E+02
   .20000E+01   .24707E+00     .40281E+01     .24636E+01    .36938E-02   -.94550E+02
   .24000E+01   .22933E+00     .54154E+01     .29175E+01    .36572E-02   -.91501E+02
   .28000E+01   .21178E+00     .69840E+01     .33567E+01    .36100E-02   -.88307E+02
   .32000E+01   .19445E+00     .87284E+01     .37805E+01    .35511E-02   -.84969E+02
   .36000E+01   .17741E+00     .10642E+02     .41884E+01    .34792E-02   -.12586E+03
   .40000E+01   .16071E+00     .12719E+02     .47925E+01    .33933E-02   -.12373E+03
   .44000E+01   .14442E+00     .15038E+02     .53864E+01    .32917E-02   -.12155E+03
   .48000E+01   .12862E+00     .17593E+02     .59698E+01    .31728E-02   -.11933E+03
   .52000E+01   .11339E+00     .20382E+02     .65426E+01    .30351E-02   -.11706E+03
   .56000E+01   .98821E-01     .23400E+02     .71045E+01    .28770E-02   -.11476E+03
   .60000E+01   .85012E-01     .26642E+02     .76554E+01    .26970E-02   -.11240E+03
   .64000E+01   .72066E-01     .30105E+02     .81949E+01    .24936E-02   -.11001E+03
   .68000E+01   .60096E-01     .33783E+02     .38339E+01    .22654E-02    .10186E+04
   .72000E+01   .49222E-01     .35717E+02    -.34342E+00    .20241E-02    .87028E+03
   .76000E+01   .39507E-01     .35980E+02    -.23487E+01    .17810E-02    .41778E+03
   .80000E+01   .30958E-01     .35441E+02    -.40450E+01    .15416E-02    .35338E+03
   .84000E+01   .23558E-01     .34223E+02    -.54630E+01    .13104E-02    .29543E+03
   .88000E+01   .17268E-01     .32438E+02    -.66344E+01    .10913E-02    .24403E+03
   .92000E+01   .12030E-01     .30184E+02    -.75909E+01    .88735E-03    .19927E+03
   .96000E+01   .77706E-02     .27547E+02    -.83652E+01    .70124E-03    .16132E+03
   .10000E+02   .44046E-02     .24601E+02    -.89946E+01    .53505E-03    .13113E+03
   .10400E+02   .18364E-02     .21403E+02    -.95525E+01    .39045E-03    .11623E+03
   .10800E+02  -.37784E-04     .17981E+02    -.94693E+01    .26898E-03   -.17347E+02
   .11200E+02  -.13289E-02     .14593E+02    -.86622E+01    .17039E-03   -.16814E+03
   .11600E+02  -.21467E-02     .11528E+02    -.77748E+01    .92512E-04   -.18487E+03
   .12000E+02  -.25908E-02     .88172E+01    -.68827E+01    .32945E-04   -.18585E+03
   .12400E+02  -.27489E-02     .64635E+01    -.60159E+01   -.10722E-04   -.18060E+03
   .12800E+02  -.26975E-02     .44566E+01    -.51905E+01   -.40830E-04   -.17196E+03
   .13200E+02  -.25015E-02     .27798E+01    -.44126E+01   -.59610E-04   -.16206E+03
   .13600E+02  -.22154E-02     .14142E+01    -.36832E+01   -.69164E-04   -.15195E+03
   .14000E+02  -.18834E-02     .34034E+00    -.29994E+01   -.71463E-04   -.14247E+03
   .14400E+02  -.15404E-02    -.45999E+00    -.23551E+01   -.68356E-04   -.13422E+03
   .14800E+02  -.12122E-02    -.10026E+01    -.17435E+01   -.61582E-04   -.12743E+03
   .15200E+02  -.91665E-03    -.13006E+01    -.12560E+01   -.52795E-04   -.10156E+03
   .15600E+02  -.66324E-03    -.14036E+01    -.92617E+00   -.43313E-04   -.68707E+02
   .16000E+02  -.45533E-03    -.13746E+01    -.71383E+00   -.34027E-04   -.44237E+02
   .16400E+02  -.29200E-03    -.12607E+01    -.58579E+00   -.25510E-04   -.26673E+02
   .16800E+02  -.16956E-03    -.10956E+01    -.51572E+00   -.18108E-04   -.14599E+02
   .17200E+02  -.82638E-04    -.90246E+00    -.48345E+00   -.12011E-04   -.67227E+01
   .17600E+02  -.24985E-04    -.69640E+00    -.47422E+00   -.73064E-05   -.19227E+01
   .18000E+02   .10086E-04    -.48666E+00    -.47602E+00   -.40186E-05    .37438E+00
   .18400E+02   .29375E-04    -.27763E+00    -.66180E+00   -.21430E-05    .38705E+02
   .18800E+02   .39661E-04    -.14291E+00    -.78841E+00   -.11775E-05    .26378E+02
   .19200E+02   .45313E-04    -.58841E-01    -.88545E+00   -.77999E-06    .20216E+02
   .19600E+02   .49057E-04    -.13583E-01    -.96464E+00   -.68823E-06    .16498E+02
   .20000E+02   .52361E-04     .00000E+00    -.10326E+01   -.68823E-06    .14149E+02
```

Figure 3-7. Profile text file of data presented in the pile graphs

```
Single.txt - Notepad
File  Edit  Format  View  Help

 LONG PILE/SHAFT (L/T) =        4.204652
Slide Below Road
              *** PILE RESPONSE ***
      Yo,in      Po,kip      Mmax,kip-ft    Mmax Location,ft   Zero Deflect.,ft   Y.ground,in
       .1867      1.00          21.66            7.60               9.79              .18674
       .2625      1.00          28.55            7.60              10.49              .26247
       .3370      1.00          35.98            7.60              10.79              .33699
```

Figure 3-8. Output data indicating the pile type (short, intermediate, or long; i.e. rigid or flexible)

21

Section 4
Example Problem

Learning by Example

The following example is provided to show the user how to design a pile wall as a corrective measure. The user is encouraged to adjust the soil, rock, and water table parameters (layering and soil properties) to produce a variety of results. The user is also encouraged to experiment with the different slope-stability methods.

The program has been made as user friendly as practical; this includes trying to prevent common errors that the user may make. However, not all of these errors can be anticipated, and error messages that may arise are incomprehensible to the average user.

Notes on Factors of Safety

Although factors of safety (FS) are not used within the context of LRFD, they are in essence still used in limiting equilibrium stability analysis. Load factors and strength reduction factors are not used to reduce soil strength and increase the driving loads when using back-analysis to find the equilibrium with an FS = 1.0.

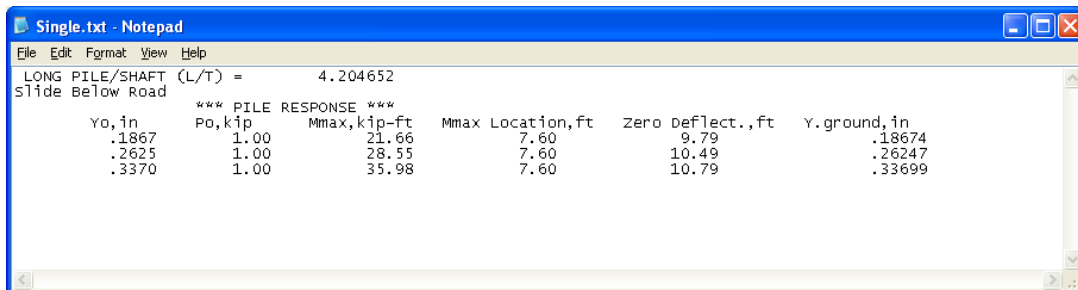   a. **Service Limit State**: In the analysis, an input of a load factor or SF of 1.0 is used to determine an acceptable deflection. If a higher FS is used, the deflection for serviceability becomes meaningless.

    b. **Strength Limit State**: The SF equivalent LRFD factors used by a number of dots for the design of ordinary soil slopes (cuts and embankments away from bridges) are 1.30 and 1.50 within the influence of a bridge.

Notes on Failure Surfaces

    a. **Failure Circle**: The failure circle must intersect the ground surface at two points (the end points of the circular arc); otherwise, an error message will appear. If the slide has a steep scarp or slope above the upper limit of the slip plane, the circle may intersect the ground surface *again* (for the third time). Hence, some superfluous lines above the slip plane must be eliminated. However, if a new circle is run to check the corrective design, *the eliminated lines may have to be added.*

    b. On rare occasions, a circle through the toe of the slope can intersect a line below (for the third time) to give an error. It is good to check your circles before you run the program.

Important Design Considerations

a. **Driving Forces**: The driving force to be resisted depends on the location of corrective measures within the slide and the slope configuration within the slide. For example, a piling correction near the top of the slide may only have to hold the top of the slide, not the entire slide. However, if we must fill on top of the slide (e.g. to rebuild the road surface), we need a piling wall (with lagging) to hold the top of the slide PLUS the new fill. We need to perform a new stability analysis on the slide <u>and fill</u> to obtain the force the piling must resist. To accomplish this, the soil surface profile will need to be modified to model the correction.

b. **Resisting Forces**:
   i. **Soil Strength**: Soil strength is defined by the parameters of the internal friction angle (ϕ) and the cohesion intercept (c). Each type of soil will, in general, have different values for ϕ and c. Furthermore, the same soil within and surrounding a slide mass will typically have different strengths.

      Where to use different strength parameters? Use ϕ_r along the slip plane (disturbed) during the original analysis. Within the slide mass and below the slip plane (undisturbed), use peak values. Be careful to not be too conservative in choosing strength parameters; doing so will require the ground water to be modeled higher to get the slide to fail.

   ii. **Ground Water:** The pore water force (U) values reduce the effective normal forces, thereby reducing resisting forces. The exact U values are rarely known since this requires extensive and usually long term piezometric water level measurements. Even when such measurements are made, they may not reflect values at the time of failure.

Example Problem

The number of soils used in the analysis will depend upon the information available. It is often easy to determine the number of soil zones from boring logs. For this example the soil parameters were derived from field observations and core borings they are depicted in Tables 4-1 and 4-2. The core boring indicated three main soil layers and a depth to water at the time of coring.

Table 4-1. Core boring table

Core Boring Results				
Soil Type	Blow Count (N)	Consistency	Moisture Content	Weathering
Silty Clay	10	Stiff	Slightly Moist	
Sandy Clay	6	Med Stiff	Moist	
Sandstone	NA	Hard	Dry	Slightly Weathered

Table 4-2. Soil strength parameters table

				Estimated Soil Strength Properties			
Soil #	Soil Type	Unit Weight	Saturated Unit Weight	Cohesion Intercept Disturbed	Friction Angle Residual	Cohesion Intercept Undisturbed	Friction Angle Peak
1	C-Phi	124	126	0	23	50	31
2	C-Phi	120	124	0	26	100	28
3	Rock	145	146	10000	36	10000	36

a. Input the soil data Tables 4-1 and 4-2.
b. Determining the soil boundary coordinates is best accomplished using coordinates derived from a professional survey. In this example the soil boundaries and water surface coordinates have been determined and plotted in Figure 4-1 and entered into Table 4-3.
c. The soil types and corresponding soil number are presented in Figure 4-2.
d. Input the total number of boundaries and the number of top boundaries and the soil layer boundary coordinates from Table 4-3.
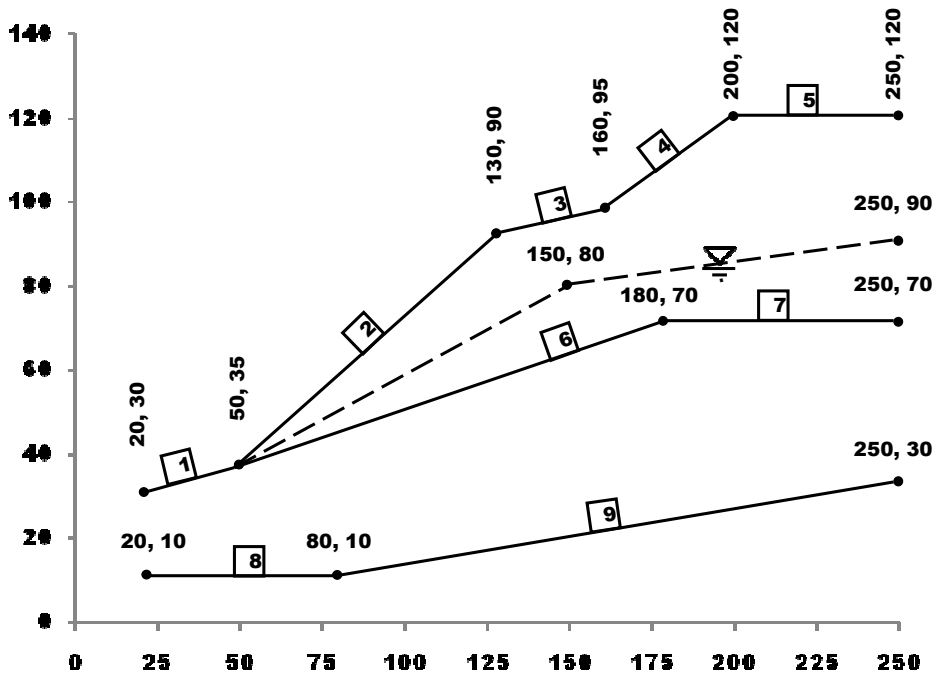
Figure 4-1. Surface boundary coordinates

24
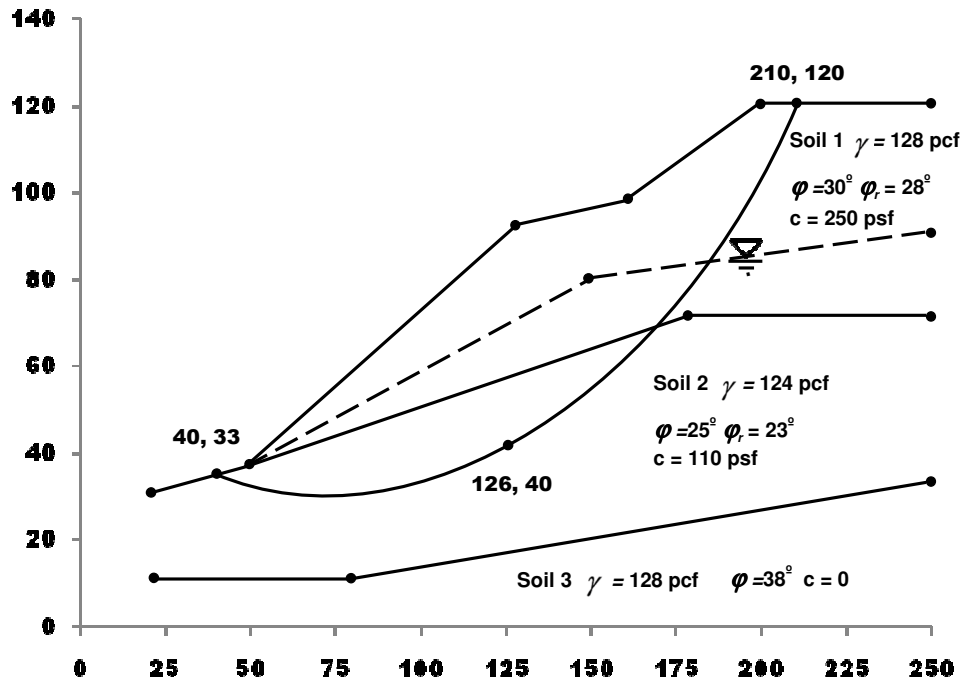
Figure 4-2. Soil types

e. Input the Water Surface coordinates from Table 4-3.

f. Input the Existing Failure Surface from Figure 4-2, utilizing the 3 points (Figure 4-3a). Plot the failure surface (Figure 4-3b); recall there are two methods for checking the failure surface. Adjust inputs as required, correcting any errors.

Points of Failure Surface	X -Coordinate ft	Y -Coordinate ft
Point No. 1	40	33
Point No. 2	126	40
Point No. 3	210	120

Close

Plot Failure Surface

Figure 4-3a. Three points on existing failure surface

25
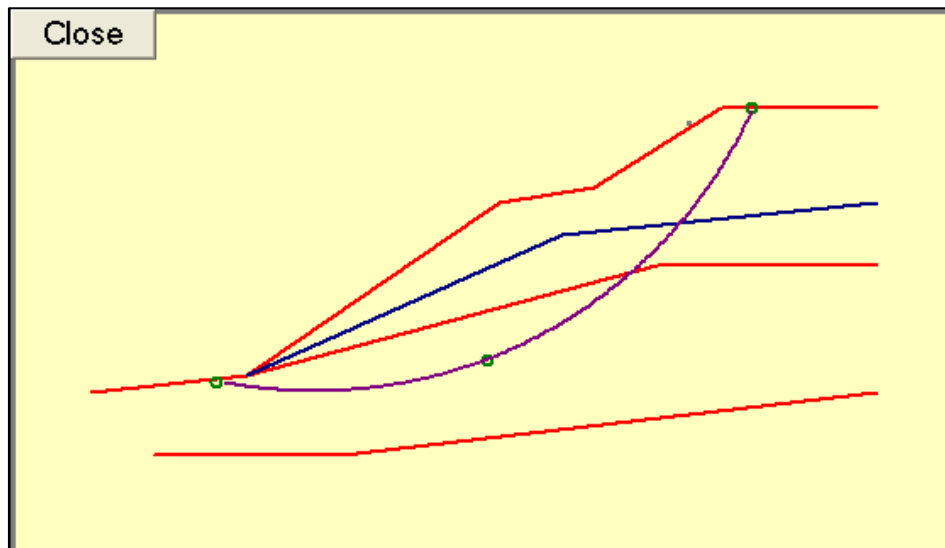
Figure 4-3b. Check the accuracy of the three points on the existing failure surface

g. After making any necessary adjustments, run the slope-stability analysis.
h. View the graph of the slope-stability analysis and check the factor of safety. The goal is to adjust the parameters to achieve a factor of safety of 1.0. At this point the graph should look similar to Figure 4-4.

In this example the initial input of soil parameters were assumed low to produce an FS of less than 1.0, for demonstration purposes. Adjust the soil parameters as required to obtain a rounded FS of 1.0. The Cohesion Intercept and Friction Angle have the greatest effect. However, disturbed soil has little to no cohesion, so it is highly recommended to enter 0 for cohesion. The friction angle is determined by the type of soil, which will have a close range of strength parameters. Try adjusting the friction angle and unit weight of the soil affected by the failure surface.

Table 4-3. Soil and water surface coordinate table

SOIL SURFACE COORDINATES					
Total Number of Boundaries = **9**			Total of Top Boundaries = **6**		
Boundary	X-Left	Y-Left	X-Right	Y-Right	Soil Num
1	20	30	50	35	1
2	50	35	130	90	1
3	130	90	160	95	1
4	160	95	200	120	1
5	200	120	250	120	1
6	50	35	180	70	2
7	180	70	250	70	2
8	20	10	80	10	3
9	80	10	250	30	3

WATER SURFACE COORDINATES										
No. of Pts	X(1)	Y(1)	X(2)	Y(2)	X(3)	Y(3)	X(4)	Y(4)	X(5)	Y(5)
3	50	35	150	80	250	90				

i. Adjust each item one at a time and check the graph until proficiency is gained at predicting the desired results.

The inputs in Table 4-4 will give the desired rounded FS of 1.0. Enter the inputs from the table below if an FS has not been achieved or the user inputs differ greatly from those listed in the table. Having similar inputs will be important to obtaining similar pile size for the rest of the exercise.

Table 4-4. Inputs that produce 1.0 factor of safety in example problem

Soil Strength Properties							
Soil #	Soil Type	Unit Weight	Saturated Unit Weight	Cohesion Intercept Disturbed	Friction Angle Residual	Cohesion Intercept Undisturbed	Friction Angle Peak
1	C-Phi	115	128	250	28	350	31
2	C-Phi	110	124	110	23	200	28
3	Sand	135	135	0	38	0	40

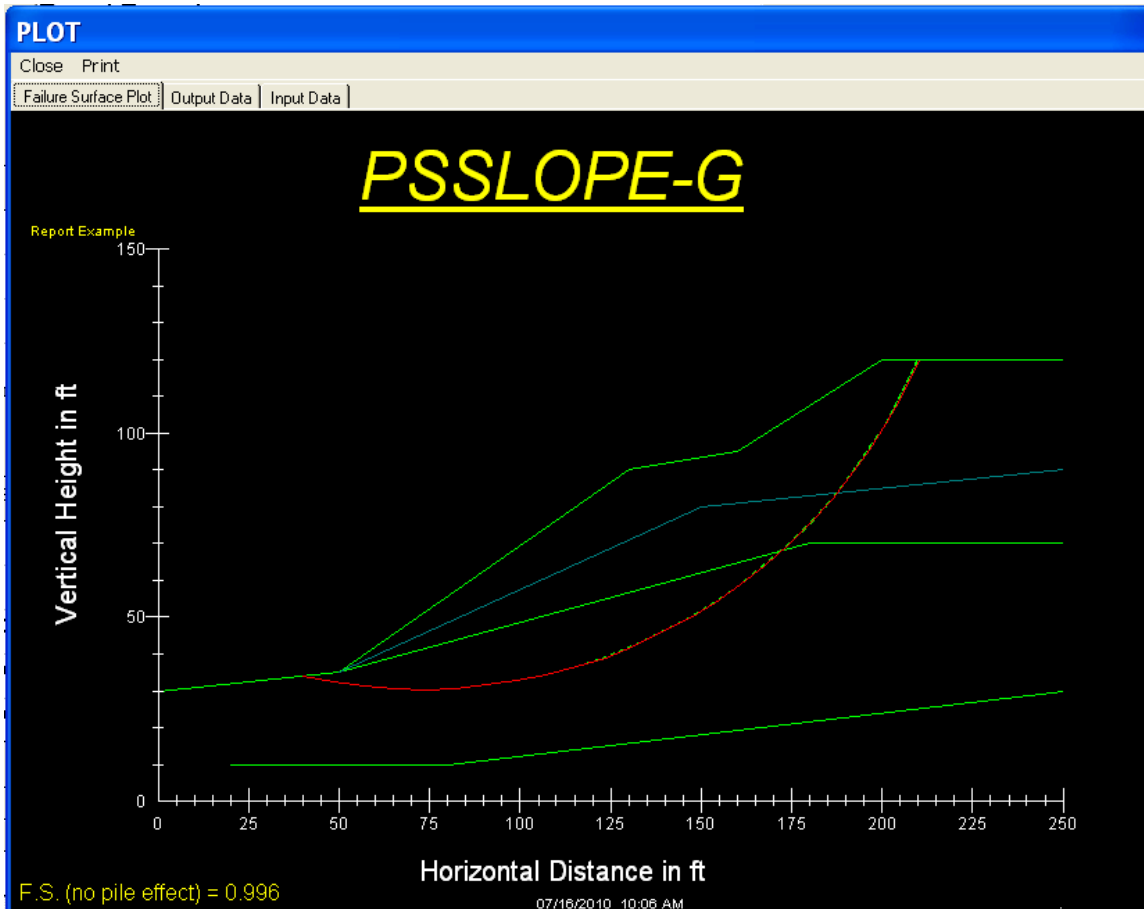The output graph should look similar to the graph in Figure 4-4.

Figure 4-4. Stability analysis graph

27

j. Once the soil parameters have been adjusted to produce a factor of safety of 1.0 (rounded), run the stability analysis for the slope and view the graph (Figure 4-4) for any errors. Ignore the factor of safety.

k. Input the undisturbed soil strength parameters from Table 4-4, if not already accomplished.

l. Input the pile-analysis information from Figure 4-5 and run Stability with Pile. The pile position into the slope can be checked after performing the slope-stability analysis and before the pile-stabilized slope analysis (Figure 4-6). It is a good practice to enter a larger pile size than you expect to use. However, for demonstration purposes the initial input will be smaller than the required size. The initial analysis should be done with the Desired FS of the Supported Portion of the Slope set to 1.0.

H-Pile	Lagging Depth	Total Length	Pile Spacings	Pile-Head	Pile-Head	Pile Rows	Pile Row
Section	ft	of the Pile, ft	ft	X-Coordinate, ft	Y-Coordinate, ft	⦿ One row	Spacing, ft
H-Pile	0	50	4	190	115	○ Two rows (Staggard)	0

Figure 4-5. Pile input data (one row pile)
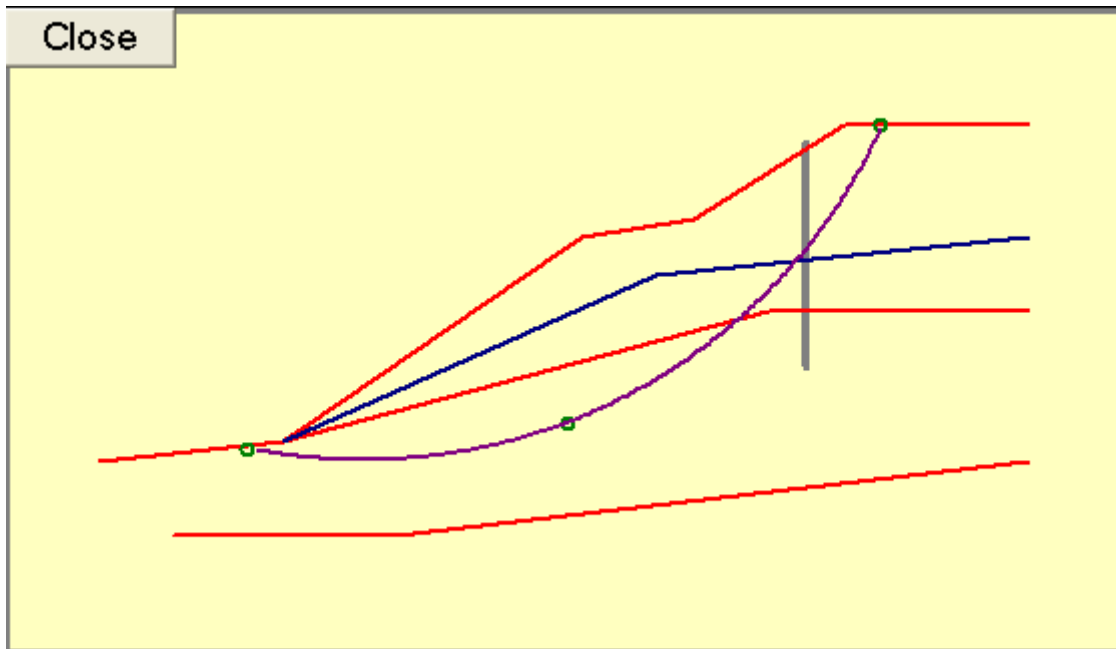
Figure 4-6a. Check pile location with existing failure surface
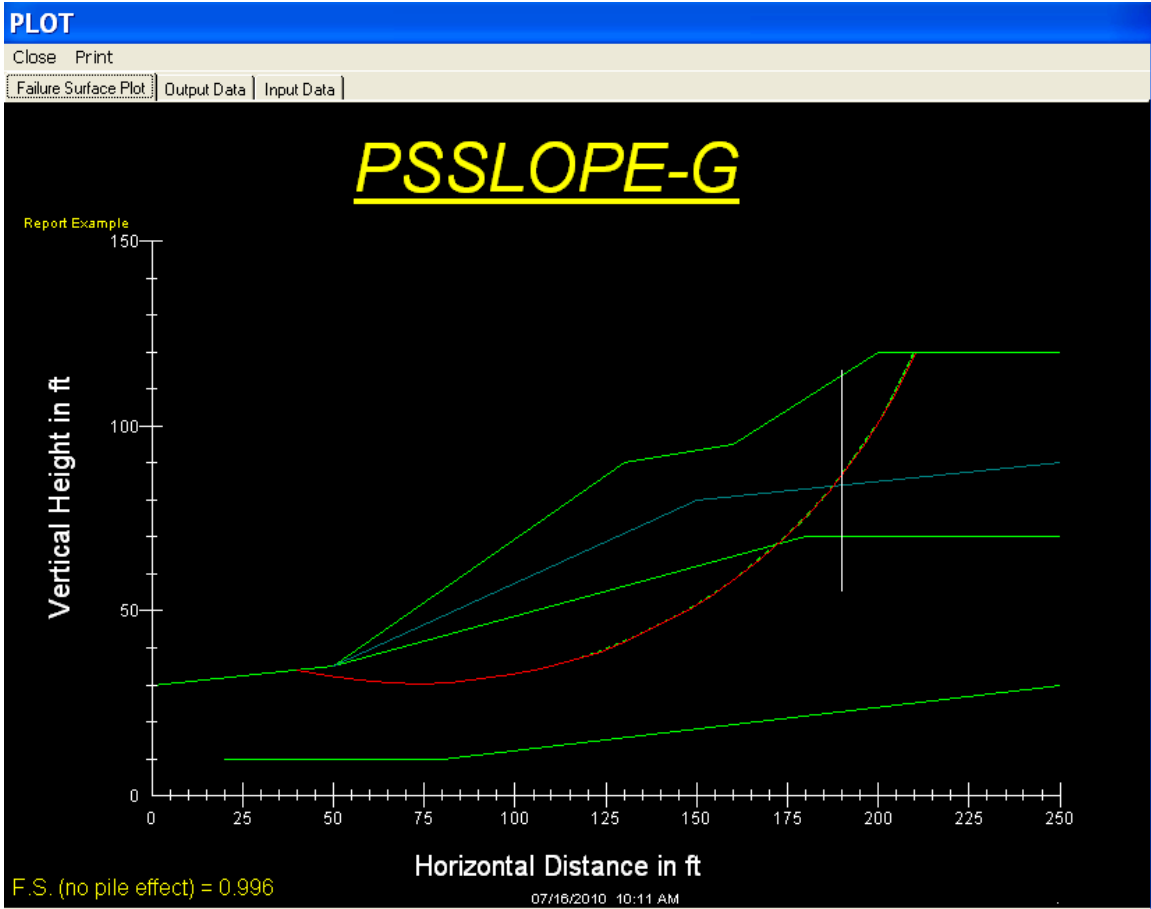
Figure 4-6b. Check pile location within the existing failure surface after slope-stability analysis

If the selected pile is too short to maintain stability, the program generated the warning in Figure 4-7.
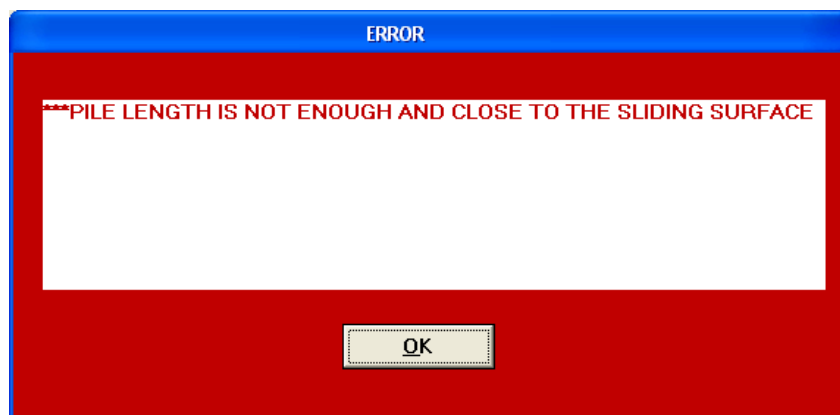
Figure 4-7. Pile length error box

Click OK. The program will generate another error message: "Check data for zero value" (Figure 4-8). Click OK again; this is normal because the short pile length caused a division by zero error.

29
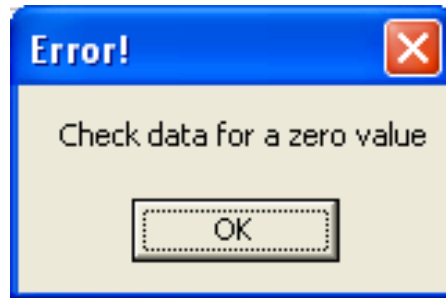
Figure 4-8. Error message

n. Adjust the pile length to 50 feet and run the slope stability and slope with piles programs again. The Pile Performance Ratio and FS of the Unsupported Portion of Slope are now displayed to the left of the input table. Check the stability graph and note that the pile wall was not used in the calculations of the pre-stabilization slope-stability analysis but is present on the graph.

o. Close the graph and view the pile response (deflection, moment, and shear graphs) (Figure 4-9).
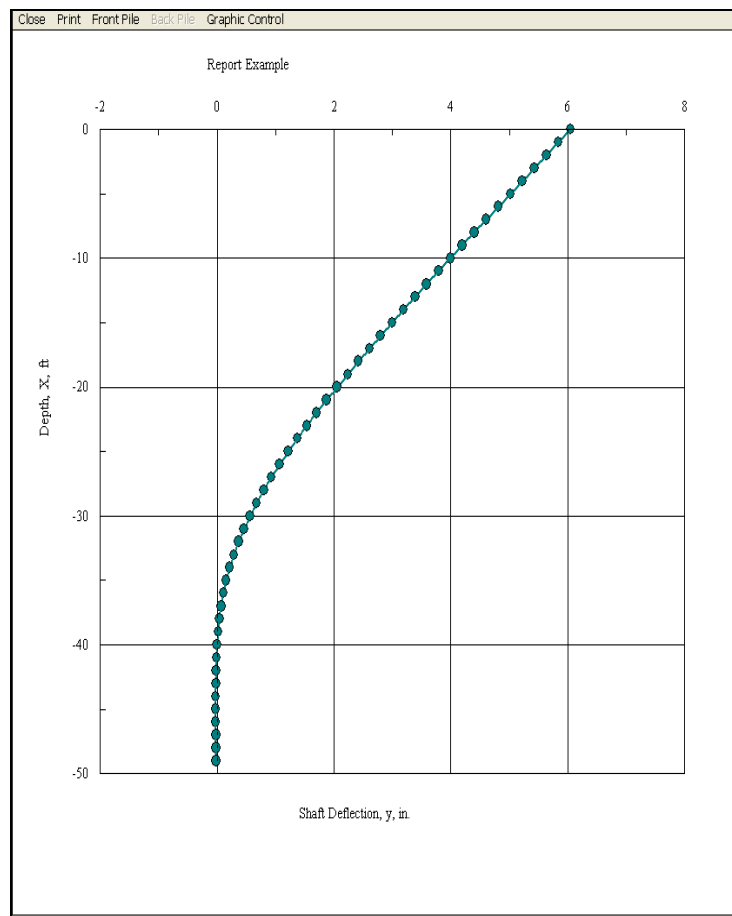
Figure 4-9a. Graph of pile deflection

30

The pile has two points on the zero line (nodes); this indicates that under these conditions the pile has fixity and the length is long enough. The deflection is almost 6 inches at the pile head; this could be excessive for an FS of 1.0. Increase the pile size and run the analyses again.

The FS of the Unsupported Portion of Slope is less than 1.0. It is anticipated the slope below the pile will continue to move, o place the lagging deep enough to account for the loss of material. If structure or road is below the slip, then the unsupported portion of the slope may need to be addressed.
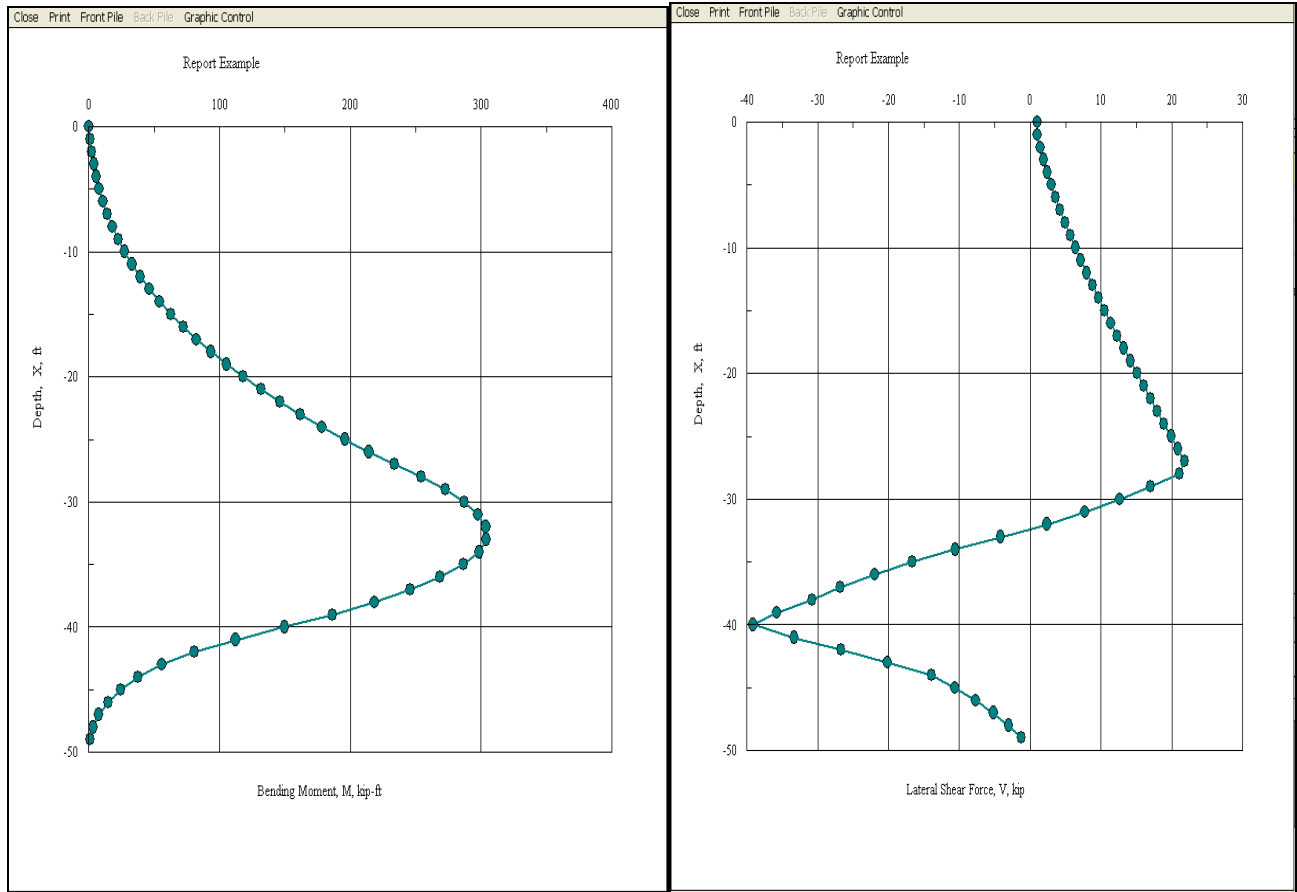
Figure 4-9b. Graphs of pile moment and shear

The same slope, shown in Figure 4-4, is stabilized by using **2 rows of piles** that are 8 ft apart (Figure 4-10). Figure 4-11 describes the location of the front and back piles along the slope side. The response of the piles in the front and back rows are presented in Figure 4-12.

H-Pile	Lagging Depth	Total Length	Pile Spacings	Pile-Head	Pile-Head	Pile Rows	Pile Row
Section	ft	of the Pile, ft	ft	X-Coordinate, ft	Y-Coordinate, ft	○ One row	Spacing, ft
H-Pile	0	50	4	190	115	⦿ Two rows (Staggard)	8

Figure 4-10. Pile input data (2 rows of piles)

31
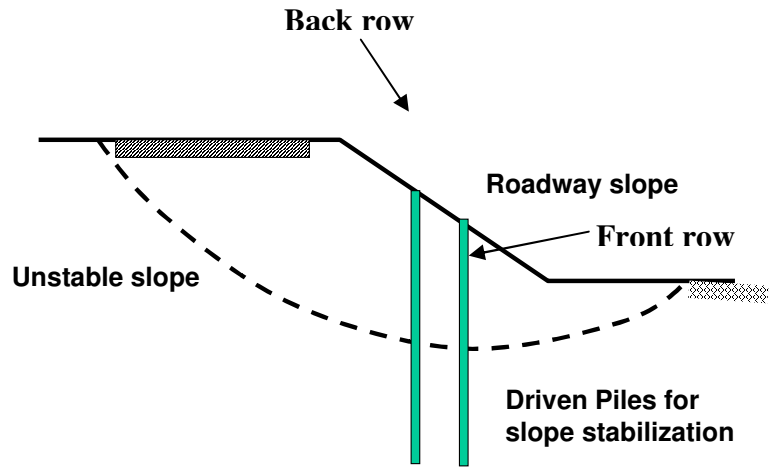
Figure 4-11. Pile description along the slope side
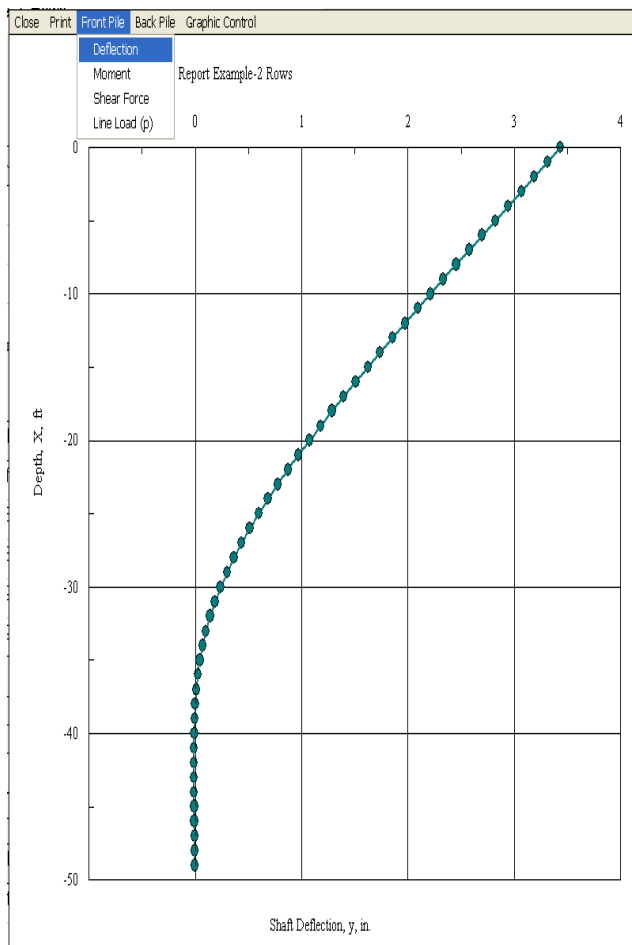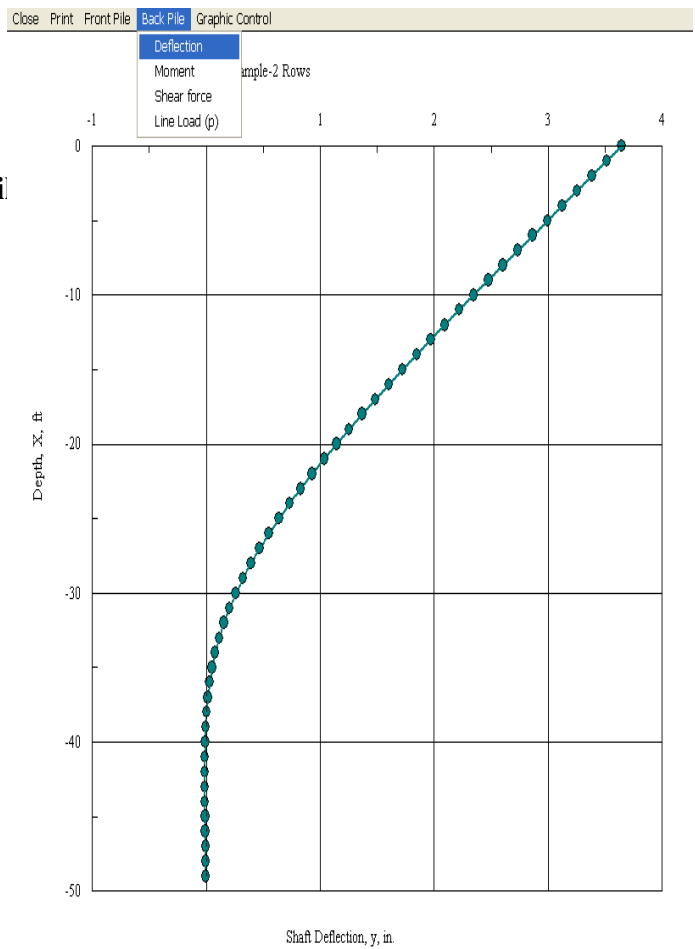
Figure 4-12a. Front and back pile deflections
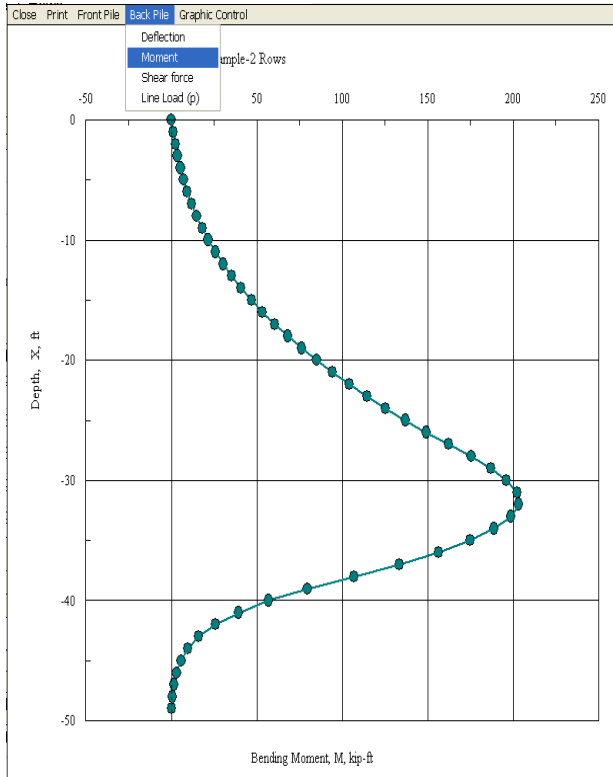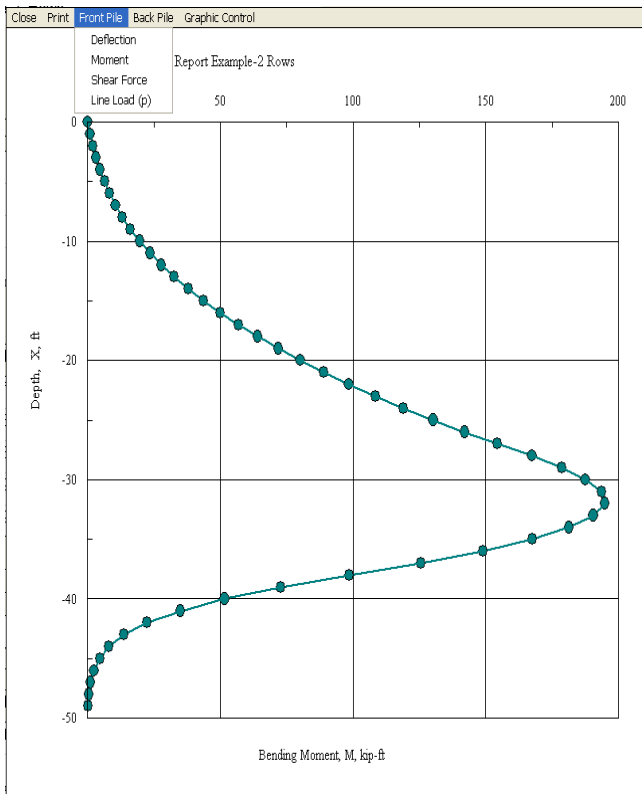
Figure 4-12b. Front and back pile moment
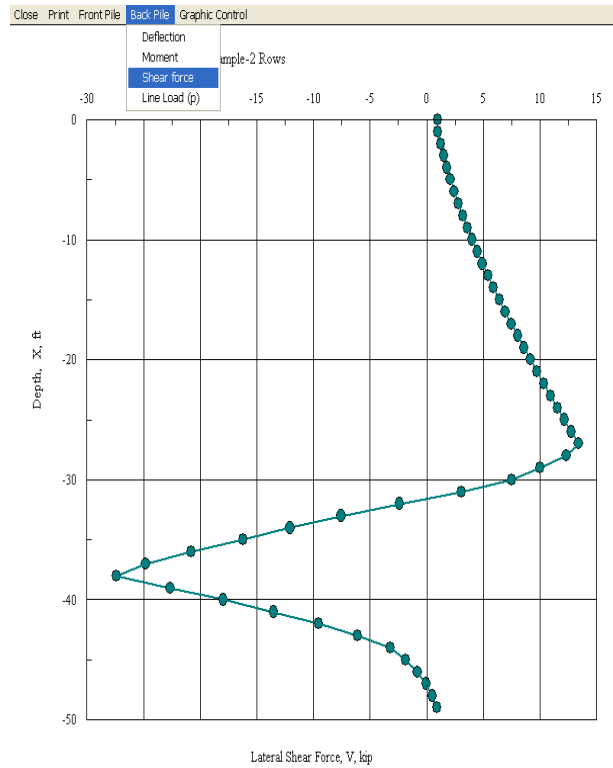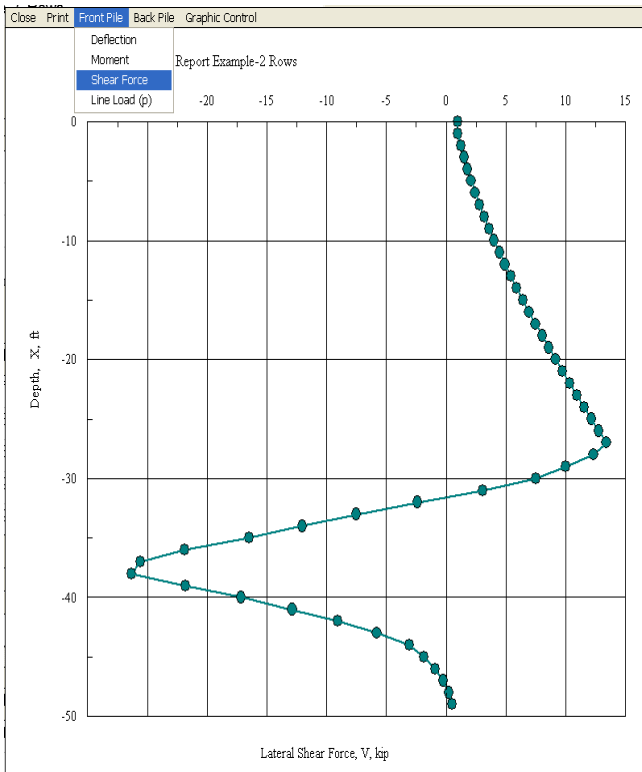
Figure 4-12c. Front and back pile shear force

Section 5
Case History and Validation

Reinforced Concrete Piles Used to Stabilize a Railway Embankment

Instrumented discrete reinforced concrete piles were used to stabilize a 26-ft high railway embankment of Weald Clay at Hildenborough, Kent, UK (Smethurst and Powerie 2007) (Figure 5-1). Remediation of the embankment was carried out to solve long-term serviceability problems, including excessive side slope displacements and track settlements. Stability calculations carried out after an initial site investigation showed the north slopes of the embankment to be close to failure. An 11.5-ft high rockfill berm was constructed at the toe of the embankment, and 200 piles were installed 7.8 ft apart along two lengths of the embankment to increase the factor of safety of the <u>whole</u> slope to the required value of 1.3. Smethurst and Powerie (2007) estimated the soil driving (shear) force required to achieve the desired factor of safety and transferred by the pile to be 13.3 kips. The soil strength parameters used in design, which are based on data from the site investigation and associated triaxial tests, are given in Table 5-1.

Table 5-1. Design soil parameters

Soil type	Unit weight, γ : lb/ft^3	Friction angle, ϕ' : degrees	Effective cohesion, c' : lb/ft^3
Weald Clay embankment fill	121	25	20.9
Softened Weald Clay embankment fill	121	19	20.9
Weathered Weald Clay	121	25	20.9
Weald Clay	127	30	104.4
Rockfill	121	35	0

Instrumented Embankment Section

The piles at the instrumented section are 33 ft long. The 1.97-ft diameter bored concrete piles were constructed at a spacing of 7.8 ft. Each pile contains six #8 reinforcement bars over their full length and six #10 bars over the bottom 23 ft, giving an estimated ultimate bending moment capacity of 22.13×10^5 lb-in over the top 10 ft and 46×10^5 lb-in over the bottom part of the pile.

After pile construction, the granular rockfill material was regraded into a two-stage slope (Figure 5-2). The final regraded profile included a small horizontal platform downslope of piles. Figure 5-2 shows the embankment profile geometry after the construction platform had been regarded and the suggested slip surface is identified.

Strain gauges were installed in three adjacent piles to measure the bending moments induced in the pile by slope movements. Inclinometer tubes were installed both inside the strain-gauged

piles and in the slope midway between each pair of instrumented piles to measure any difference in the movement of the piles and movement of the soil midway between the piles.

The strain gauges were data logged to obtain a continuous record of their output. Pile C also contains twelve Gage Technique vibrating-wire concrete embedment strain gauges, installed to compare their performance with those attached to the reinforcement cage. The embedment gauges, which were supported during pile construction by steel holding bars spanning between adjacent pile reinforcement bars, measure the strain within the concrete.

Figure 5-1. Instrumented section of embankment at Hildenborough after berm had been regraded to create a two-stage slope (Smethurst and Powerie 2007)
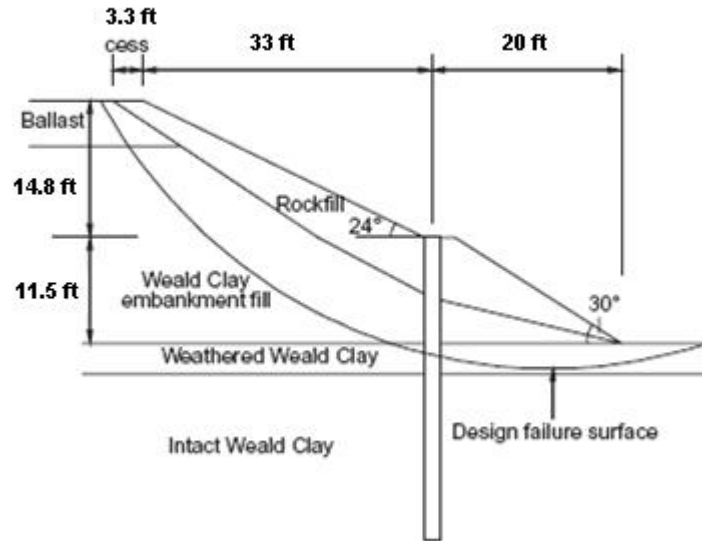
Figure 5-2. Embankment profile after the construction platform had been regraded (Smethurst and Powerie 2007)

Pile and Soil Displacements

Datum readings were taken on day three for the inclinometer tubes installed in the piles and day five for the tubes in the slope midway between the piles. Further sets of inclinometer readings

were taken for the four years after pile installation. The inclinometer data are analyzed assuming that the bases of the piles have not displaced laterally. Displacement data for the soil and piles were obtained from the inclinometer tubes in the slope midway between the piles and the inclinometer tubes in Piles A, B and C respectively.

The average pile and soil displacements for day 42—shortly after the rockfill on the slope surface had been regarded—and day 1345 are shown in Figure 5-3. A movement of about 0.27 in over the top 13 ft of the slope on day 42 increased to an inch by day 1345. The significant increase in displacement at about 13 ft depth corresponds to the location of the critical failure surface identified in design and the depth of the slope failures recorded on adjacent sections of the embankment before remediation. At day 42, the piles had moved 0.24–0.31 inches at the head, similar to the soil midway between the piles. By day 1345 the pile movements had increased, with total pile-head movements of about 1.46 inches.
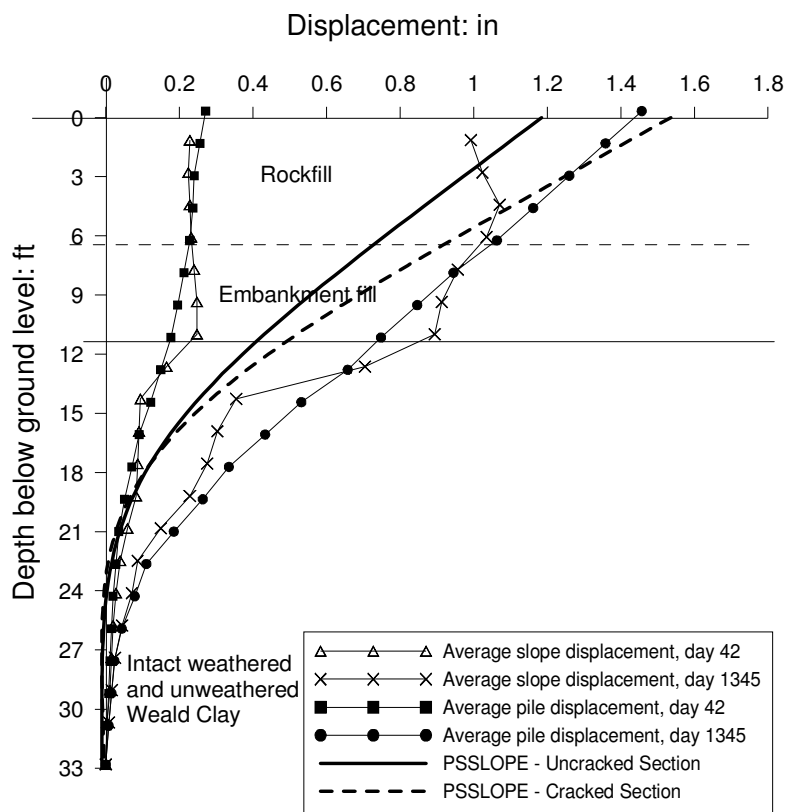
Figure 5-3. Averaged measured pile and soil displacements (after Smethurst and Powerie, 2007)

By day 1345, the relative soil/pile displacements are reasonably clear: a depth between 6.5 ft and 13 ft, slope displacements up to 0.16 inches larger, and pile displacements up to 0.4 inches further than the soil between 13 ft and 26 ft and above 6.5 ft depth.

Measurements and Calculations of Bending Moment

Standard engineering beam theory is used to convert the longitudinal strains ε_1 and ε_2 measured by each pair of strain gauges into bending moment M:

$$M = \frac{EI(\varepsilon_1 - \varepsilon_2)}{y},$$

where y is the distance between the gauges in each pair. Uncracked behavior was assumed in the analysis of field measurements. Thus the composite flexural rigidity, *EI*, was calculated as 65.2×10^9 lb-in^2 for the lower 23 ft of the pile and 59.6×10^9 lb-in^2 for the top 10 ft, both using $E = 3.626 \times 10^6$ Ib/in^2 for uncracked concrete. EI of 59.6×10^9 lb-in^2 is taken to be the EI of the whole pile in linear analysis. EI = 40 x 10^9 lb-in^2 is considered the bending stiffness of the partially cracked section.

Analysis of the bending strain focuses on Pile C because there are two sets of gauges in this pile and there have been fewer gauge failures. Figure 5-4 shows the distributions of bending moment with depth from the two sets of gauges in Pile C for day 1345. Positive bending moments correspond to tension on the upslope side of the pile.

Comparison of the results from each of the sets of gauges shows variation in the measured bending moments. While the distributions are broadly the same shape, in that there are negative moments at the top of the pile and a positive moment in the middle, the exact depth and magnitude of the peak moments vary. Having a negative moment in the upper portion of the pile against slipping mass of soil indicates a pile displacement larger than the rock-fill layer displacement at the upper portion of the pile (Figure 5-4).
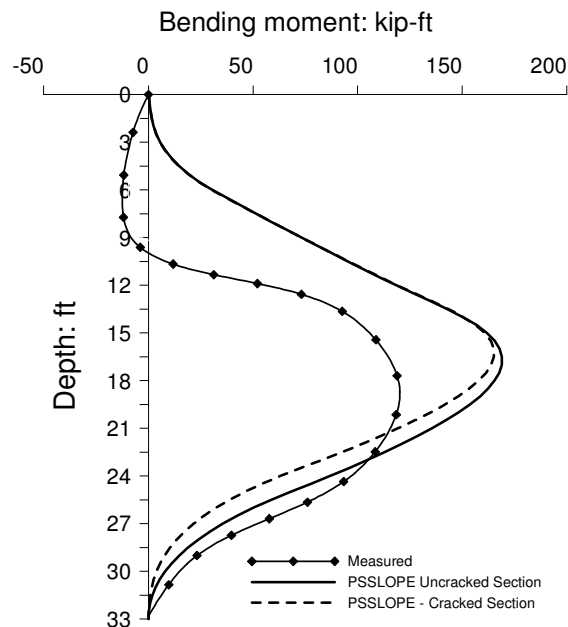
Figure 5-4. Measured bending moment from pile C embedded strain gauges (after Smethurst and Powerie 2007)

Slope Stabilization Using PSSLOPE-G (Input/Output Data Analysis)

The Modified Bishop method is applied in the PSSLOPE-G computer program to study the stability of the given slope without piles (Figure 5-5). Figure 5-6 shows the location of the pile into the slope as utilized in PSSLOPE-G. Smethurst and Powerie (2007) reported a slope factor of safety (no piles) close to one for the failure surface shown in Figure 5-2. No specific slope factor of safety value was given. Soil parameters employed in the PSSLOPE-G analysis are presented in Table 5-2. The PSSLOPE-G analysis provides a factor of safety of 1.176 for the same slip surface and soil profile (Figure 5-5 and Table 5-3). It should be noted that the slope factor of safety is sensitive to slight changes in the slip surface coordinates. Pile properties input data is presented in Table 5-4. EI values for cracked and partially uncracked section are used in the analysis (Table 5-5).

Figures 5-3 and 5-4 show the PSSLOPE-G pile lateral response in comparison with the measured data. The PSSLOPE-G results are based on 15.5 kips of shear force transferred by the pile, which is larger than the shear force (13.3 kips) anticipated by Smethurst and Powerie (2007). In addition, the negative moment measured in the upper portion of the pile affects and reduces the lower peak of the positive moment (Figure 5-4). This could be referred to the top rock-fill layer displacement, which is less than the adjacent pile deflection. This explains the larger moments obtained by the PSSLOPE-G analysis. Again, the current PSSLOPE-G program assumes soil displacement above the slip surface to be larger than or equal to the pile displacement. Therefore, the installed pile is always subjected to driving force from the sliding soil mass.
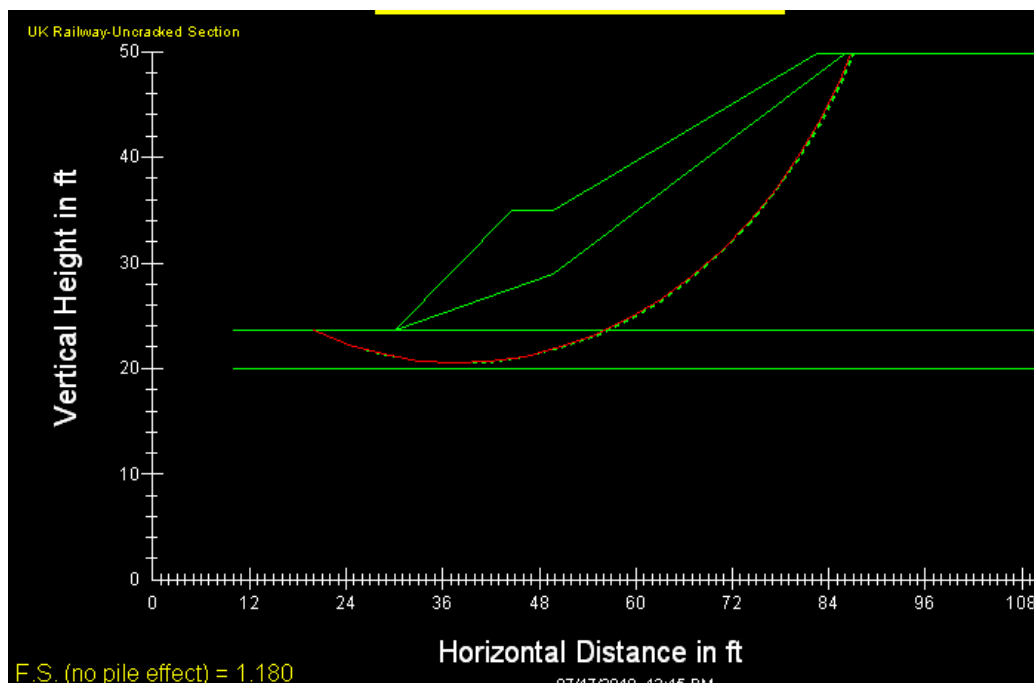
Figure 5-5. Embankment profile and slip surface as predicted in PSSLOPE-G

38
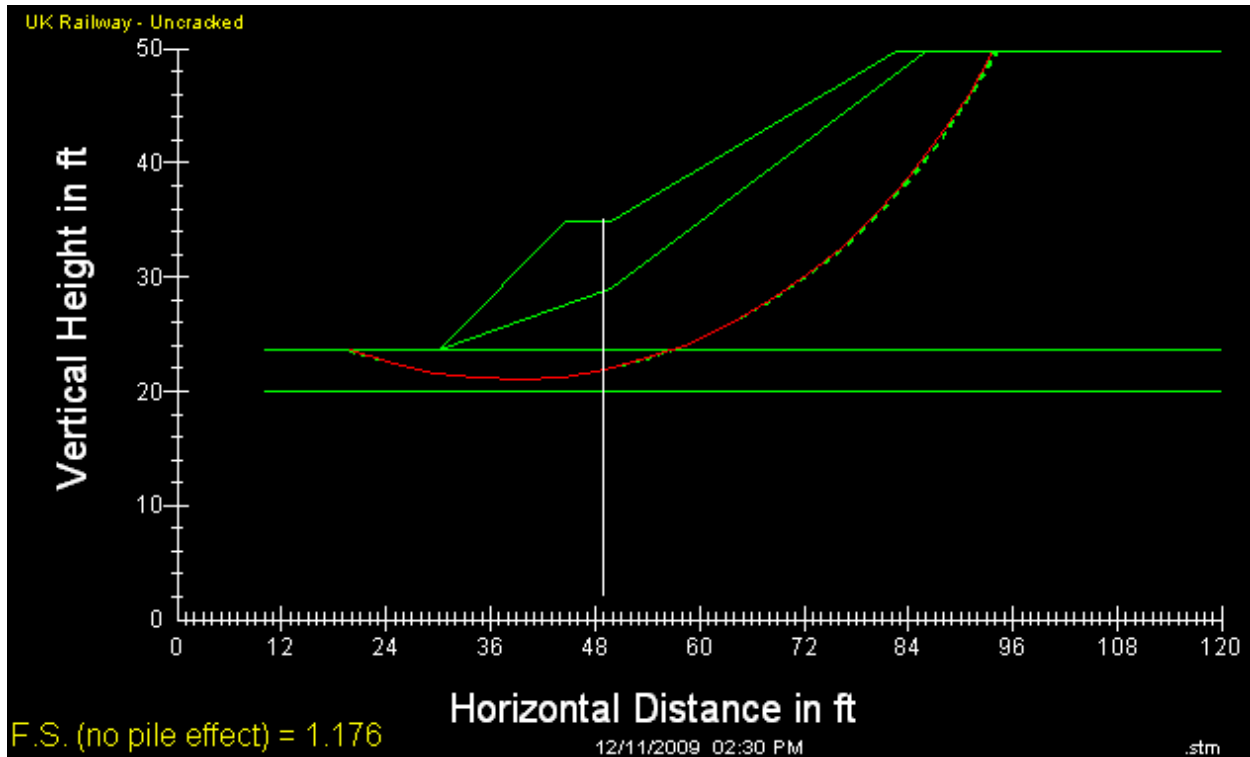
Figure 5-6. Embankment profile and slip surface as used in PSSLOPE-G

Similar to LPILE nonlinear analysis, the pile EI is reduced to 40×10^9 lb-in^2 to account for the pile section cracks (EI reduction) (Table 5-4). However, the use of constant reduced EI for cracked section could be argued as a compromise because of the varying cracked section EI along the pile which is a function of the induced bending moment.

Table 5-2. PSSLOPE-G input soil properties

Soil	Soil	Unit Wt.	Saturated Unit Wt.	Cohesion Intercept	Friction Angle	Blowcounts	RMR	Cohesion Intercept	Friction Angle
Number	Type	pcf	pcf	(Disturbed) psf	(Residual) deg	N	(Rock)	(Undisturbed) psf	(Peak) deg
1	Sand	121	121	0	35		0	0	35
2	C-Phi	121	121	20.9	19		0	20.9	19
3	C-Phi	121	121	20.9	25		0	20.9	25
4	C-Phi	127	127	104.4	30		0	104.4	30

Table 5-3. PSSLOPE-G input slip surface coordinates

Points of Failure Surface	X -Coordinate ft	Y -Coordinate ft
Point No. 1	20	23.5
Point No. 2	40	21.5
Point No. 3	94	49.8

Close

Plot Failure Surface

Table 5-4. PSSLOPE-G input pile properties

H-Pile	Lagging Depth	Total Length	Pile Spacings	Pile-Head	Pile-Head	Pile Rows		Pile Row
Section	ft	of the Pile, ft	ft	X-Coordinate, ft	Y-Coordinate, ft	⊙ One row		Spacing, ft
Concrete Pile	0	0	7.8	49	35	○ Two rows (Staggard)		0

Table 5-5a. Uncracked pile section

Properties of Steel Pipe-Pile Section				Close
Pile Diameter, in.	Shell Thick., in.	EI, lb-in2	Unfactored Mp, lb-in	
23.6	0.5	59.60E+0	46.90E+05	

Table 5-5b. Cracked pile section

Properties of Steel Pipe-Pile Section				Close
Pile Diameter, in.	Shell Thick., in.	EI, lb-in2	Unfactored Mp, lb-in	
23.6	0.5	40.00E+0	46.90E+05	

Section 6
Methodology of Pile-Stabilized Slopes

Introduction

Landslides (slope failure) are critical and likely result from poor land management or the seasonal change in the soil moisture conditions. Driven piles, drilled shafts, or micropiles can be installed to reduce the likelihood of slope failure or landslides (Figure 6-1). At present, simplified methods based on crude assumptions are used to design the driven piles/drilled shafts/micropiles needed to stabilize slopes of bridge embankments or to reduce the potential for landslides. The major challenge lies in the evaluation of lateral loads (pressure) acting on the piles/pile groups by the moving soil (Figure 6-2). The interaction among piles including the lateral effective range of pile resistance is complex and depends on soil and pile properties and the level of soil-induced driving force. The design manual by Naval Facilities Engineering (NAVFAC 1982) recommends an empirical value for the driving force of the soil on the piles based on the full passive resistance of soil. There may be considerable error in this assumption.
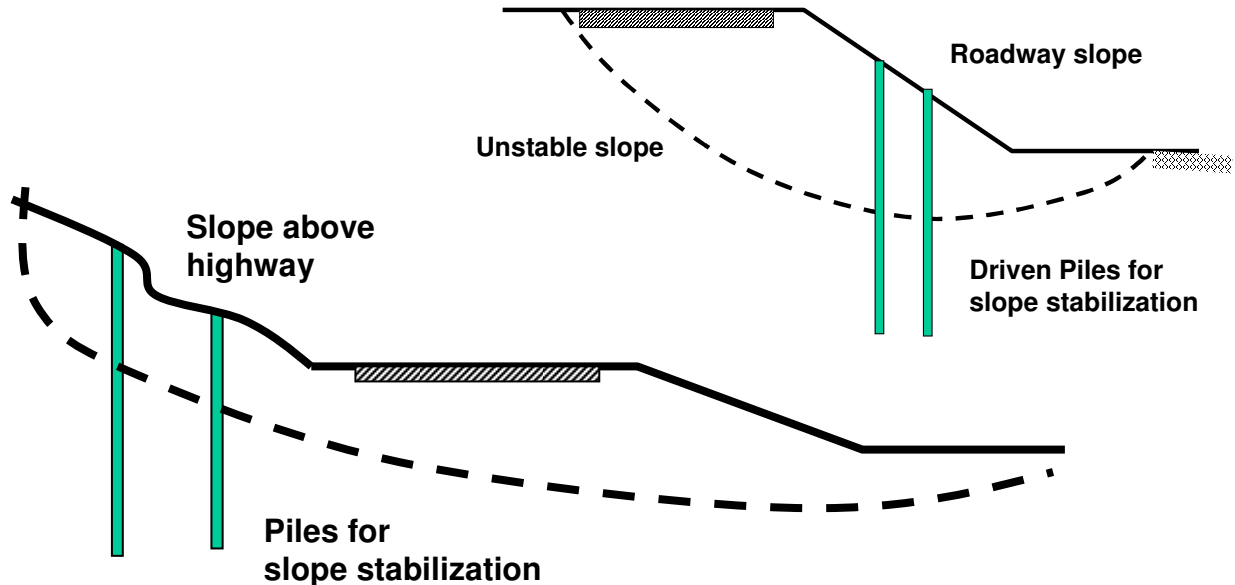
Figure 6-1. Different types of pile-stabilized slopes

The problem of landslides and the use of piles to improve the stability of such slopes require better characterization of the integrated effect of laterally loaded pile behavior, pile-structure-interaction, and nonlinear behavior of pile materials (steel or concrete) on the resulting slope

stability condition. The lateral driving load (P_D) caused by the sliding soil mass is assumed to act on the slipping surface (Figure 6-3), which is not correct. In reality, the driving force of the soil mass acts along the entire length of the portion of the pile above the failure surface to be transmitted to the lower (stable) soil layers, as shown in Figure 6-4. Such a scenario requires representative modeling for the soil-pile interaction above the failure surface that reflects and describes actual distribution for the soil driving force along that particular portion of the pile.
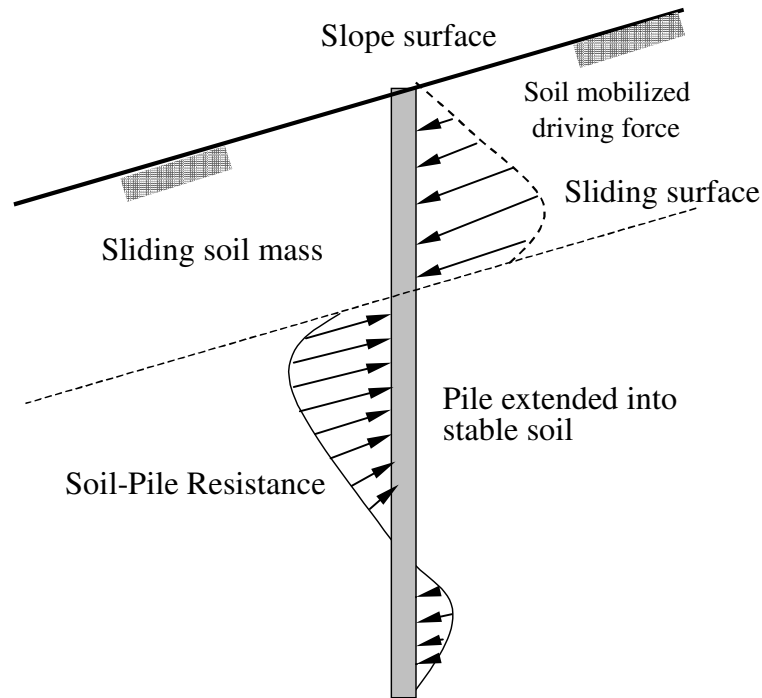
Figure 6-2. Driving force induced by soil mass above sliding surface

One approach has been to calculate the soil passive resistance (driving force) based on Broms' method (1964) as characterized in DM 7-2 (NAVFAC 1982) in the program FLAC. Another alternative is to use the ultimate soil reaction from the traditional (Matlock and Reese) p-y curve. Neither of these ultimate resistances was envisioned for sloping ground, and neither consider group interference effects in a fundamental way, certainly not for sloping ground conditions. Since the traditional (Matlock-Reese) p-y curves were developed for long piles beneath level ground with the concentrated lateral load at the pile head, the use of these curves in the soil mass above the failure surface for the envisioned failure mechanism is not appropriate. In addition, such analysis implies that gravity acts in an upward direction in the soil mass above the sliding plane. In addition, flow-around failure of soil around the pile is a significant phenomenon that should be considered in the current practice. It should be noted that the flow-around failure governs the amount of soil mass driving force applied on the pile, along with the pile spacing on the slope.
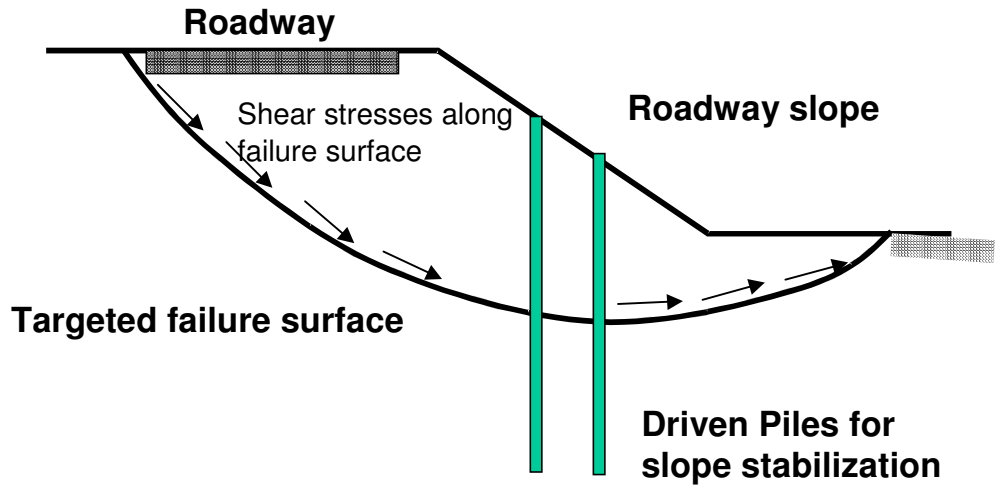
Figure 6-3. Flow of shear stresses along anticipated sliding surface
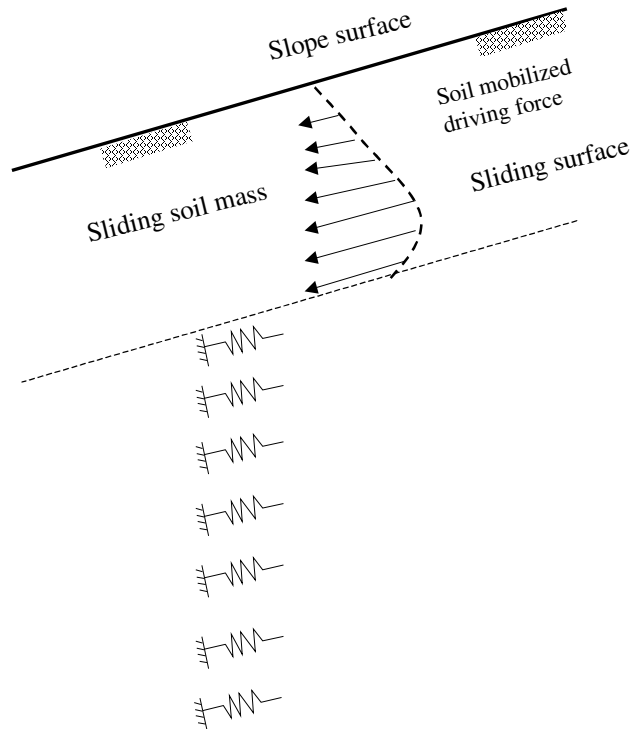
Figure 6-4. Proposed modeling for soil-pile analysis in pile-stabilized slopes

The strain wedge (SW) model technique developed by Norris (1986) and Ashour, *et al.* (1998) for laterally loaded piles based on soil-structure interaction is modified to evaluate the mobilized non-uniformly distributed soil driving force (F_D) along the length of the pile located above the anticipated failure surface (Figure 6-4). However, the force F_D is governed by the soil-pile interaction (i.e. soil and pile properties) (Ashour and Norris 2000) and the developing flow

43

around failure. The SW model approach has the capability of capturing the developing flow around response based on soil-pile interaction (Figure 6-5).

Flow-Around Soil with Pile
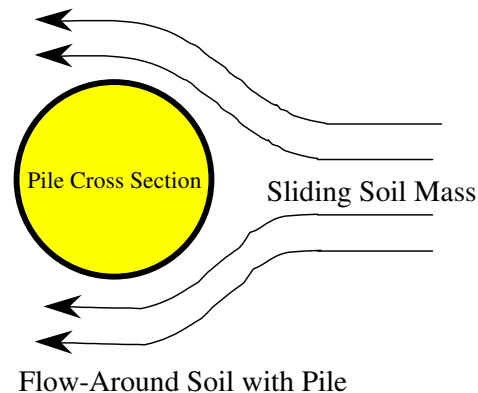
Figure 6-5. Developing flow-around failure of soil

Compared to the traditional p-y curves, the SW model approach can build its own p-y curves in soil (sand, clay, and C-φ soil) and rock based on soil-structure interaction. The p-y curve provided by the SW model accounts for soil and pile properties and soil continuity that the traditional p-y curve lacks. This has been proven via more than fifty full- and model-scaled tests (Ashour, *et al.* 1996). As a result, the stabilizing pile can be modeled and analyzed based on a realistic mechanism.

The full stress-strain relationships for soils within the slide mass (sand, clay, C-φ soil, and rock) is assessed to evaluate the compatible deformation and deflection of the slide mass and pile respectively for the associated factor of safety. As shown in Figure 6-4, the soil-pile model will be subjected to lateral driving load (above the failure surface) and the lateral resistance from soil (below the failure surface). Shear force and bending moment along the pile are calculated. Thereafter, the factor of safety of the pile-stabilized slope will be re-evaluated.

The number of piles required for slope stabilization is calculated based on pile spacing and the interaction among the piles. The research work developed by Ashour, *et al.* (2004) is used to estimate the interaction among piles installed into the slope in the zones above and below the anticipated sliding surface (Figure 6-4).

The factor of safety of the pile-stabilized slope can be re-evaluated based on the distributed lateral force (F_D) induced by soil mass and carried by the pile down to the stable soil below the slide surface. However, as addressed in this research work, the use of tie-backs with pile-stabilized slopes significantly improves the slope factor of safety.

The Theoretical Basis of Strain Wedge Model Characterization

The strain wedge (SW) model is an approach that has been developed to predict the response of a flexible pile under lateral loading (Norris 1986; Ashour, *et al.* 1996; and Ashour, *et al.* 1998). The main concept associated with the SW model is that traditional one-dimensional Beam on Elastic Foundation (BEF) pile response parameters can be characterized in terms of

44

three-dimensional soil-pile interaction behavior (Figure 6-6). The SW model was initially established to analyze a free head pile embedded in one type of uniform soil (sand or clay). However, the SW model has been improved and modified through additional research to accommodate a laterally loaded pile embedded in multiple soil layers (sand, clay, c-φ soils, and weathered rock). The main objective behind the development of the SW model is to solve the BEF problem of a laterally loaded pile based on the envisioned soil-pile interaction and its dependence on both soil and pile properties.
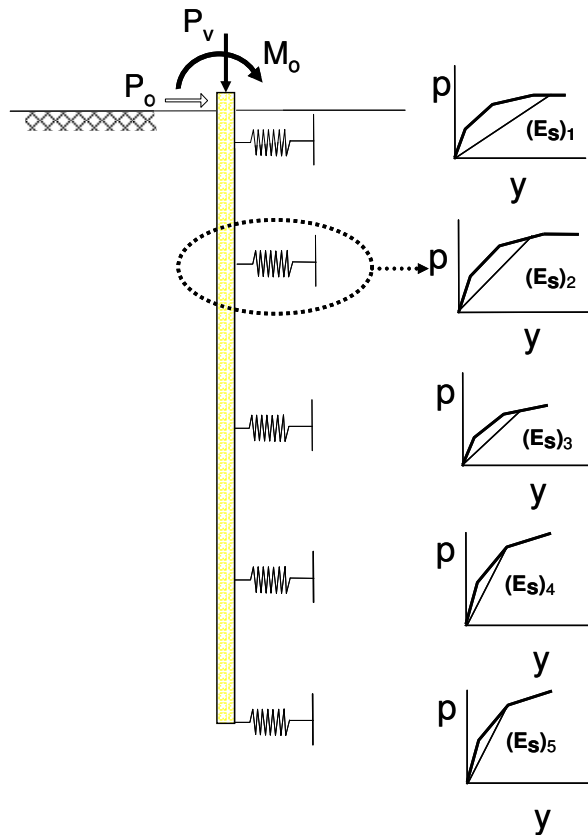
Figure 6-6. Beam on elastic foundation modeling of the laterally loaded pile

The SW model parameters are related to an envisioned three-dimensional passive wedge of soil developing in front of the pile. The basic purpose of the SW model is to relate stress-strain-strength behavior of the soil in the wedge to one-dimensional BEF parameters. The SW model is, therefore, able to provide a theoretical link between the more complex three-dimensional soil-pile interaction and the simpler one-dimensional BEF characterization. The previously noted correlation between the SW model response and BEF characterization reflects the following interdependence:

- The horizontal soil strain (ε) in the developing passive wedge in front of the pile to the deflection pattern (y versus depth, x) of the pile.
- The horizontal soil stress change ($\Delta\sigma_h$) in the developing passive wedge to the soil-pile reaction (p) associated with BEF behavior.

- The nonlinear variation in the Young's modulus ($E = \Delta\sigma_h/\varepsilon$) of the soil to the nonlinear variation in the modulus of soil subgrade reaction ($E_s = p/y$) associated with BEF characterization.

These analytical relations reflect soil-pile interaction response characterized by the SW model illustrated later in this report. The reason for linking the SW model to BEF analysis is to allow the appropriate selection of BEF parameters to solve the following fourth-order ordinary differential equation to proceed.

$$EI\left(\frac{d^4 y}{d^4 x}\right) + E_s(x)\,y + P_x\left(\frac{d^2 y}{d^2 x}\right) = 0 \tag{6-1}$$

Matlock and Reese (1961) obtained the closed form solution of the basic form of this equation for uniform soil. To appreciate the SW model's enhancement of BEF analysis, one should first consider the governing analytical formulations related to the passive wedge in front of the pile and the soil's stress-strain formulations, and the related soil-pile interaction.

Soil Passive Wedge Configuration

The SW model represents the mobilized passive wedge in front of the pile, which is characterized by the base angles, φ_m and β_m; the current passive wedge depth h; and the spread of the wedge fan angle, φ_m (the mobilized friction angle of soil). The horizontal stress change at the passive wedge face, $\Delta\sigma_h$, and side shear, τ, as shown in Figure 6-7. An assumption of the SW model is that the deflection pattern of the pile is initially taken to be linear over the controlling depth of the soil near the pile top, resulting in a linearized deflection angle, δ, as seen in Figure 6-8 for uniform soil.

The SW model makes the analysis simpler because forces (F_1) on the opposite faces cancel, but the real zone of stress is like the dashed outline shown in Figure 6-9b, which includes side shear influence (τ) on the shape of the strained zone. However, the τ perpendicular to the face of the pile is still considered in the SW model analysis. As seen in Figure 6-9c, the horizontal equilibrium in the SW wedge model is based on the concepts of the conventional triaxial test. The soil at the face of the passive wedge is represented by a soil sample in the conventional triaxial test, where $\overline{\sigma}_{vo}$ (i.e. K = 1) and the horizontal stress change, $\Delta\sigma_h$, (from pile loading) are the confining and deviatoric stresses in the triaxial test respectively.
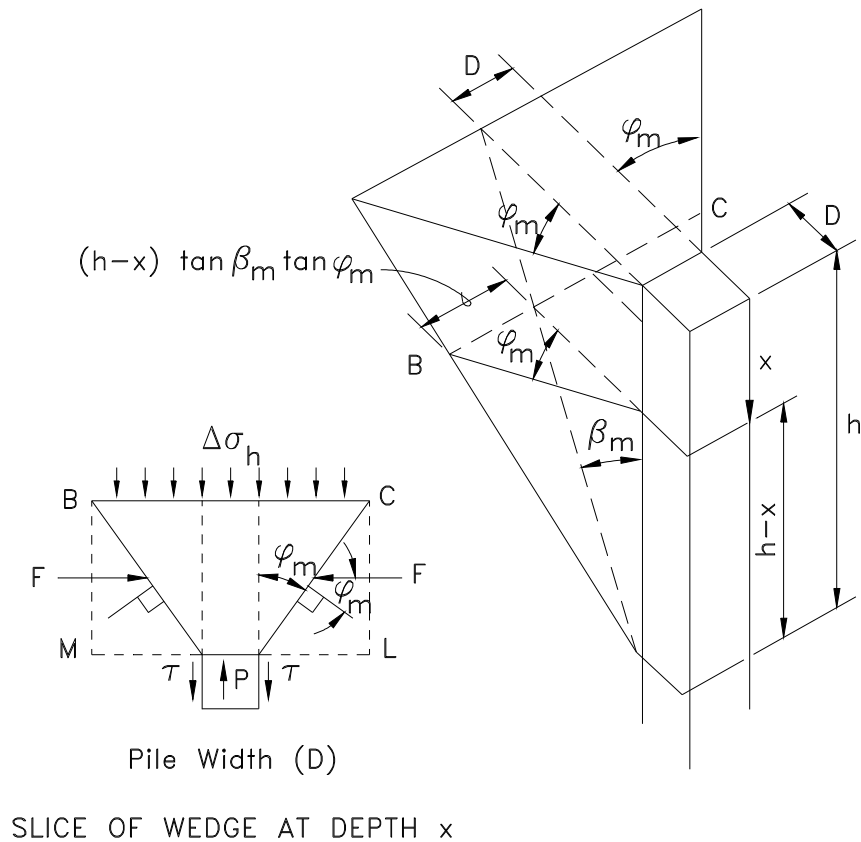
Figure 6-7. The basic strain wedge in uniform soil

The relationship between the actual (closed-form solution) and linearized deflection patterns of long pile has been established by Norris (1986) ($h/X_o = 0.69$). As seen in Figure 6-10, the relationship (h/X_o) between the actual and linearized deflection for the short pile is equal to 1 and varies for the intermediate piles from 0.69 at ($L/T = 4$) to 1 at ($L/T = 2$). L is the embedded length of the pile and T is the initial relative pile stiffness.

It should be noted that the idea of the change in the full passive wedge (mobilized passive wedge at different levels of deflection) employed in the SW model has been established by Rowe (1956) and shown experimentally by Hughes and Goldsmith (1978).

Changes in the shape and depth of the upper passive wedge, along with changes in the state of loading and pile deflection, occur with change in the uniform strain (ε) in the developing passive wedge. As seen in Figure 6-10, two mobilized (top to tip) passive wedges are developed in soil in front of the short pile. Because of the pile straight-line deflection pattern with a deflection angle δ, the uniform soil strain (ε) will be the same in both (i.e. upper and lower) passive wedges.

47
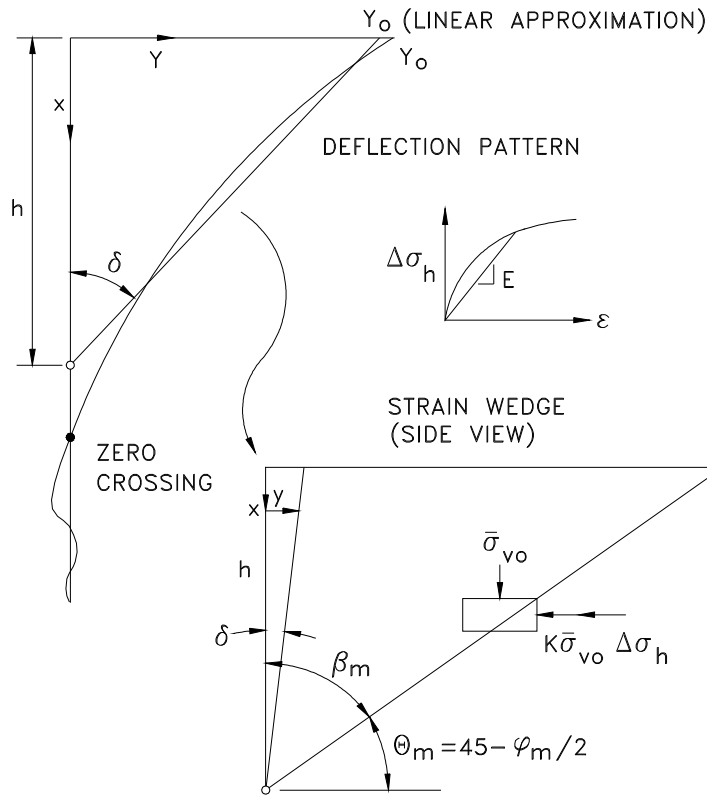
Figure 6-8. Deflection pattern of a laterally loaded long pile/shaft and the associated strain wedge in uniform soil

As shown in Figure 6-10, the deflection pattern is no longer a straight line for the intermediate pile, and the lower passive wedge has a curved shape that is similar to the deflection pattern. Accordingly, the soil strain (ε_x) at depth x below the zero crossing will not be uniform and will be evaluated in an iterative method based on the associated deflection at that depth (Figure 6-10).

The non-uniform soil strain (ε_x) in the lower passive soil wedge (Figure 6-10c) becomes much smaller compared to the strain in the upper soil wedge when the pile deflection approaches the deflection pattern of the long pile. Since the lateral deflection of the long pile/pile below the zero crossing is always small, the associated soil strain and developing passive wedge will be small as well. Consequently, the developing upper passive soil wedge (and uniform strain therein) dominates the lateral response of the long pile/pile, hence the adopted name "strain wedge" (SW).

48

Figure 6-9. Characterization and equilibrium of the SW model

As seen in Figures 6-7 and 6-8, the configuration of the wedge at any instant of load—and therefore base angle, β; mobilized friction angle, φ_m; and wedge depth, h—is given by the following equation:

$$\Theta_m = 45 - \frac{\varphi_m}{2} \tag{6-2}$$

$$\beta_m = 45 + \frac{\varphi_m}{2} \tag{6-3}$$

49

The width, $\overline{BC}$, of the wedge face at any depth is

$$\overline{BC} = D + (\, h - x) \, 2 \tan \beta_m \tan \varphi_m \, , \tag{6-4}$$

where x denotes the depth below the top of the studied passive wedge and D symbolizes the width of the pile cross-section. It should be noted that the SW model is based upon an effective stress analysis of both sand and clay soils. As a result, the mobilized fanning angle, φ_m, is not zero in clay soil as assumed by Reese (1958, 1983). The above equations are applied to the upper and lower passive wedges in the case of short and intermediate piles where x for any point on the lower passive wedge (Figure 6-10) is measured downward from the zero crossing and replaces the term (h - x) in Equation 6-4. Therefore,

$$\varepsilon_x = \varepsilon \, (y_x \, / \, x) \, / \, \delta \quad = \quad \varepsilon \, (\frac{\delta_x}{\delta}) \, , \tag{6-5}$$

where ε and δ are the uniform soil strain and linearized pile deflection angle of the upper passive wedge respectively. y_x and δ_x are the pile deflection and secant deflection angle at depth x below the zero crossing (Figure 6-10).

Strain Wedge Model in Layered Soil

The SW model can handle the problem of multiple layers of different soil types. The approach employed, which is called the multi-sublayer technique, is based on dividing the soil profile and the loaded pile into sublayers and segments of constant thickness respectively, as shown in Figure 6-11. Each sublayer of soil is considered to behave as a uniform soil and have its own properties according to the sublayer location and soil type. In addition, the multi-sublayer technique depends on the deflection pattern of the embedded pile being continuous regardless of the variation of soil types. Therefore, the face of the passive wedge shown in Figure 6-11 will be broken lines (not straight line). The depth, h, of the deflected portion of the pile is controlled by the stability analysis of the pile under the conditions of soil-pile interaction. The effects of the soil and pile properties are associated with the soil reaction along the pile by the Young's modulus of the soil, the stress level in the soil, the pile deflection, and the modulus of subgrade reaction between the pile segment and each soil sublayer. To account for the interaction between the soil and the pile, the deflected part of the pile is considered to respond as a continuous beam loaded with different short segments of uniform load and supported by nonlinear elastic supports along soil sublayers, as shown in Figure 6-12. At the same time, the point of zero deflection (X_o in Figure 6-12) for a pile in a particular layered soil varies according to the applied load and the soil strain level.
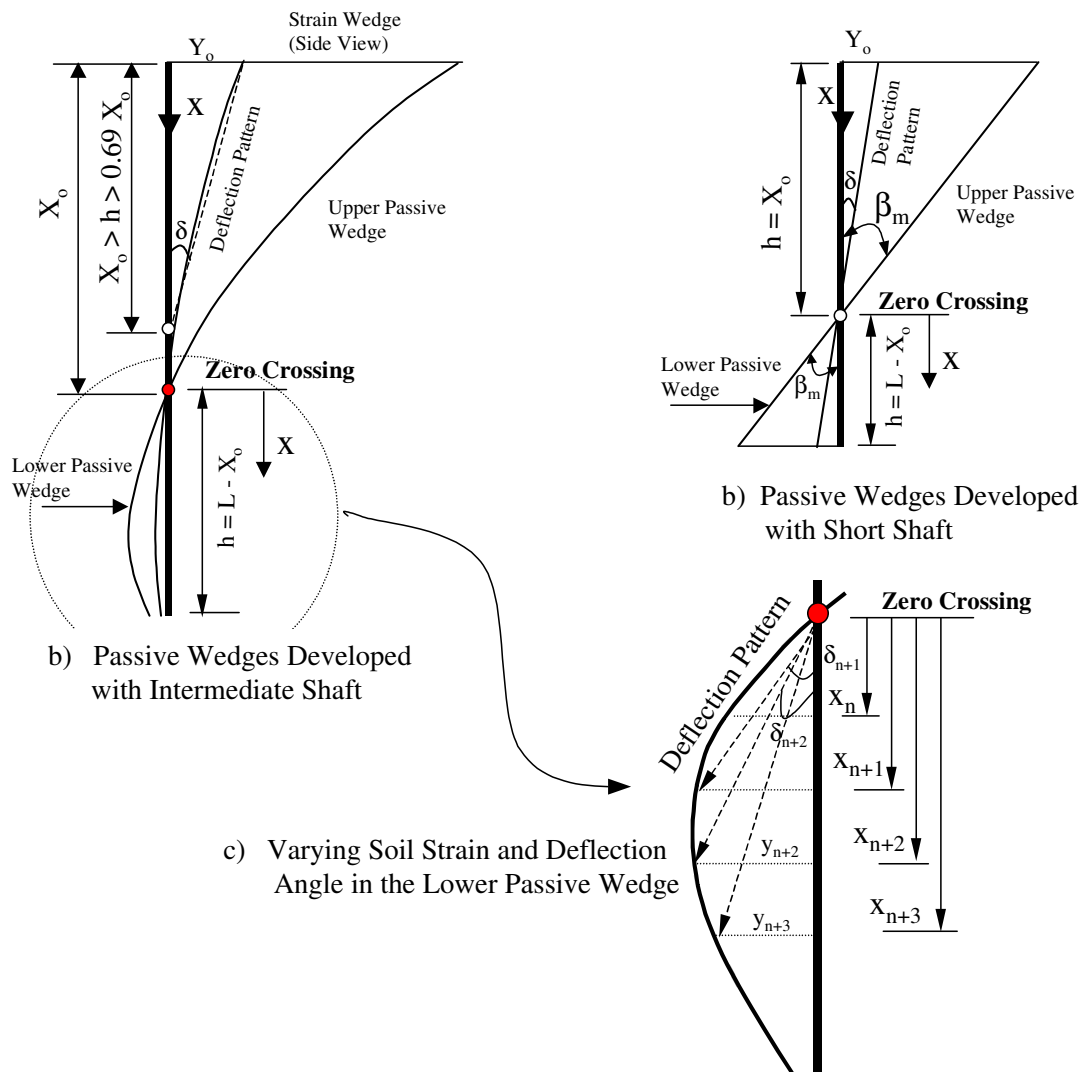
Figure 6-10. Developed passive wedges with short and intermediate piles

The SW model in layered soil provides a means for distinguishing layers of different soil types as well as sublayers within each layer where conditions (ε_{50}, SL, φ_m) vary even though the soil and its properties (γ, e or D_r, φ , etc.) remain the same. In fact, there may be a continuous change over a given sublayer, but the values of stress level (SL) and mobilized friction angle (φ_m) at the middle of each sublayer of height, H_i, are treated as the values for the entire sublayer.

An iterative process is performed to satisfy the equilibrium between the mobilized geometry of the passive wedge of the layered soil and the deflected pattern of the pile for any level of loading (as presented by the flowchart in Figure 6-22).
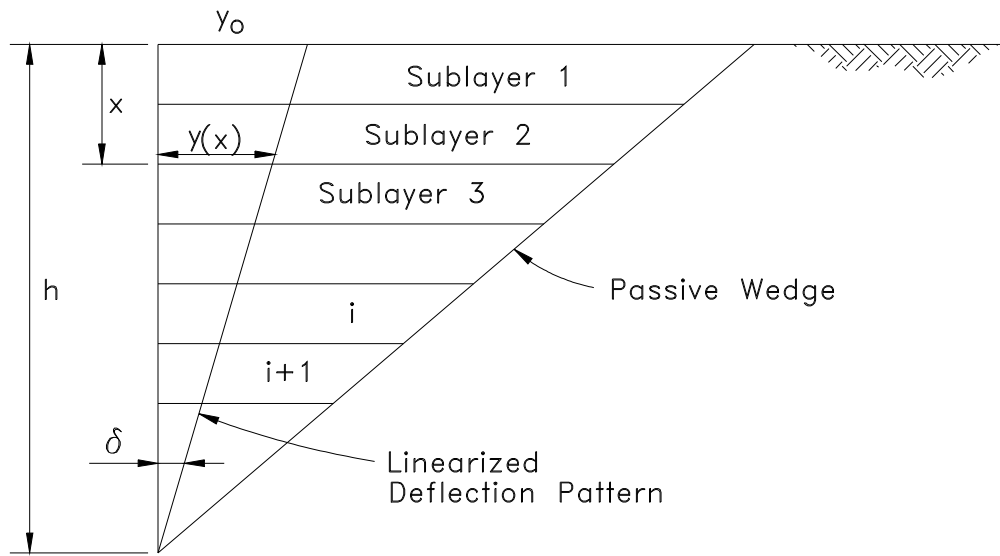
Figure 6-11. The linearized deflection pattern of a pile/pile embedded in soil using the multi-sublayer strain wedge model
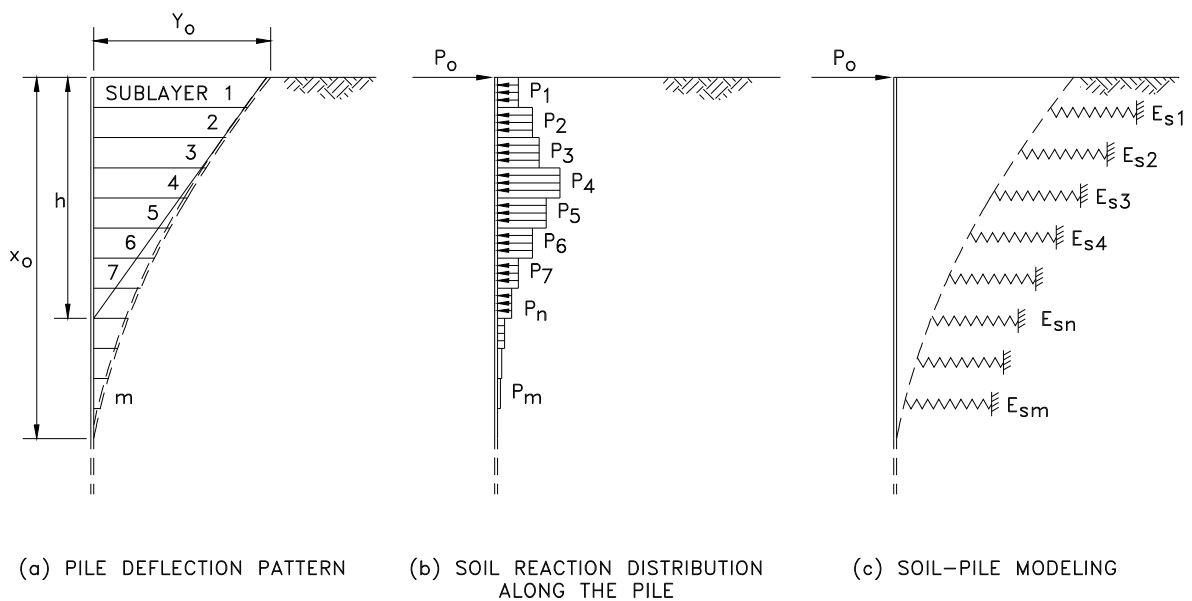
(a) PILE DEFLECTION PATTERN

(b) SOIL REACTION DISTRIBUTION ALONG THE PILE

(c) SOIL-PILE MODELING

Figure 6-12. Soil-pile interaction in the multi-sublayer technique *Soil Stress-Strain Relationship*

The horizontal strain (ε) in the soil in the passive wedge in front of the pile is the predominant parameter in the SW model, hence the name "strain wedge." Consequently, the horizontal stress change ($\Delta\sigma_h$) is constant across the width of the rectangle BCLM (of face width BC of the passive wedge), as shown in Figure 6-7. The stress-strain relationship is defined based on the results of the isotropically consolidated drained (sand) or undrained (clay) triaxial test. These properties are summarized as follows:

52

- The major principle stress change ($\Delta\sigma_h$) in the wedge is in the direction of pile movement, and it is equivalent to the deviatoric stress in the triaxial test as shown in Figure 6-9 (assuming that the horizontal direction in the field is taken as the axial direction in the triaxial test).
- The vertical stress change ($\Delta\sigma_v$) and the perpendicular horizontal stress change ($\Delta\sigma_{ph}$) equal zero, corresponding to the standard triaxial compression test where deviatoric stress is increased while confining pressure remains constant.
- The initial horizontal effective stress is taken as

$$\overline{\sigma}_{ho} = K\,\overline{\sigma}_{vo} = \overline{\sigma}_{vo},$$

where K=1 due to pile installation effects. Therefore, the isotropic confining pressure in the triaxial test is taken as the vertical effective stress ($\overline{\sigma}_{vo}$) at the associated depth.
- The horizontal stress change in the direction of pile movement is related to the current level of horizontal strain (ε) and the associated Young's modulus in the soil, as are the deviatoric stress and the axial strain, to the secant Young's modulus ($E = \Delta\sigma_h/\varepsilon$) in the triaxial test.
- Both the vertical strain (ε_v) and the horizontal strain perpendicular to pile movement (ε_{ph}) are equal and are given as

$$\varepsilon_v = \varepsilon_{ph} = -\nu\,\varepsilon \qquad \text{where } \nu \text{ is the Poisson's ratio of the soil.}$$

The corresponding stress level (SL) in sand (see Figure 6-13) is

$$SL = \frac{\Delta\sigma_h}{\Delta\sigma_{hf}} = \frac{\tan^2\left(45 + \varphi_m/2\right) - 1}{\tan^2\left(45 + \varphi/2\right) - 1}, \tag{6-6}$$

where the horizontal stress change at failure (or the deviatoric stress at failure in the triaxial test) is

$$\Delta\sigma_{hf} = \overline{\sigma}_{vo}\left[\tan^2\left(45 + \frac{\varphi}{2}\right) - 1\right] \tag{6-7}$$

In clay,

$$SL = \frac{\Delta\sigma_h}{\Delta\sigma_{hf}} \; ; \qquad \Delta\sigma_{hf} = 2\,S_u, \tag{6-8}$$

where S_u represents the undrained shear strength, which may vary with depth. Determination of the values of SL and φ_m in clay requires the involvement of an effective stress analysis which is presented later in this chapter.

The relationships above show clearly that the passive wedge response and configuration change with the change of the mobilized friction angle (φ_m) or stress level (SL) in the soil. Such behavior provides the flexibility and the accuracy for the strain wedge model to accommodate both small and large strain cases. The above equations are applied for each soil sublayer along the pile to evaluate the varying stress level in the soil and the geometry of the passive wedges.
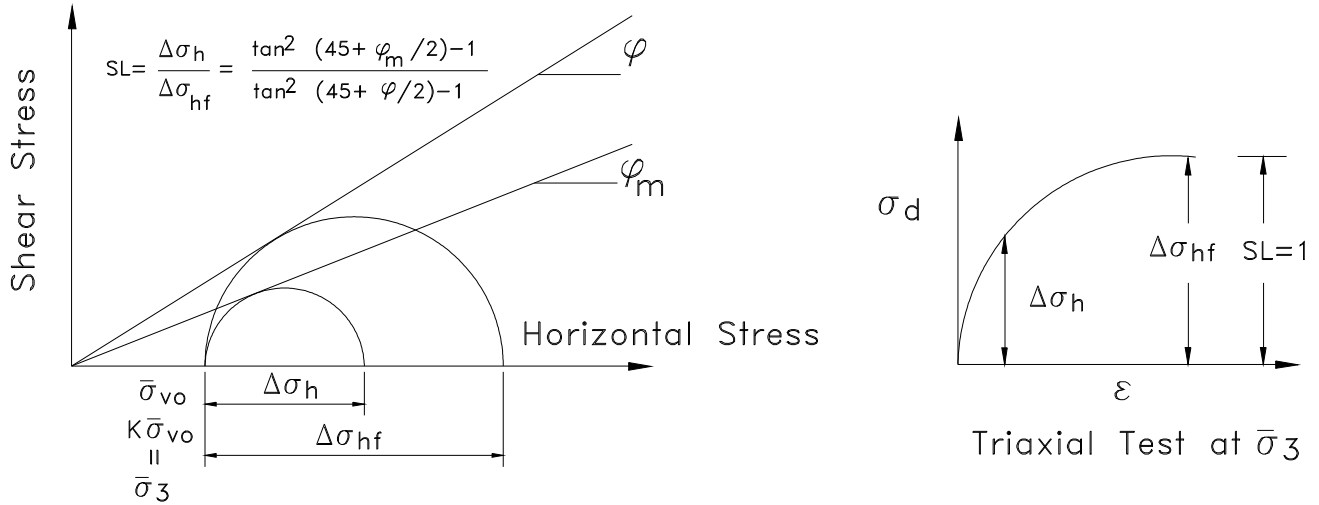
Figure 6-13. Relationship between horizontal stress change, stress level, and mobilized friction angle

Weathered (Weak) Rock Stress-Strain Relationship

The basic step in the SW model analysis is to assess the stress-strain response of the geotechnical material, whether it is sand, clay, c-φ soil, or rock. Based on the concepts of the triaxial test (Figure 6-14), rock response is a function of the uniaxial compressive strength of rock mass (q_u), the confining pressure (i.e. vertical effective stress σ_{vo} adjacent to the shaft), and the internal angle of friction (φ). Therefore, the mobilized stress-strain relationship of rock can be analytically assessed as described by Figures 6-14 and 6-15 and the following equations (Ashour, *et al.* 2001). In the SW model analysis, weathered rock mass is treated as a C-φ soil that has an unconfined strength of q_u and an effective angle of internal friction φ:

$$q_u = 2C_i \tan\left(45 + \frac{\varphi}{2}\right) \qquad (6\text{-}9)$$

Therefore, the horizontal stress change to failure at the face of the strain wedge at depth x becomes

$$\Delta\sigma_{hf} = q_u + \overline{\sigma}_{vo}\left[\tan^2\left(45 + \frac{\varphi}{2}\right) - 1\right]$$

54

$$(6\text{-}10)$$
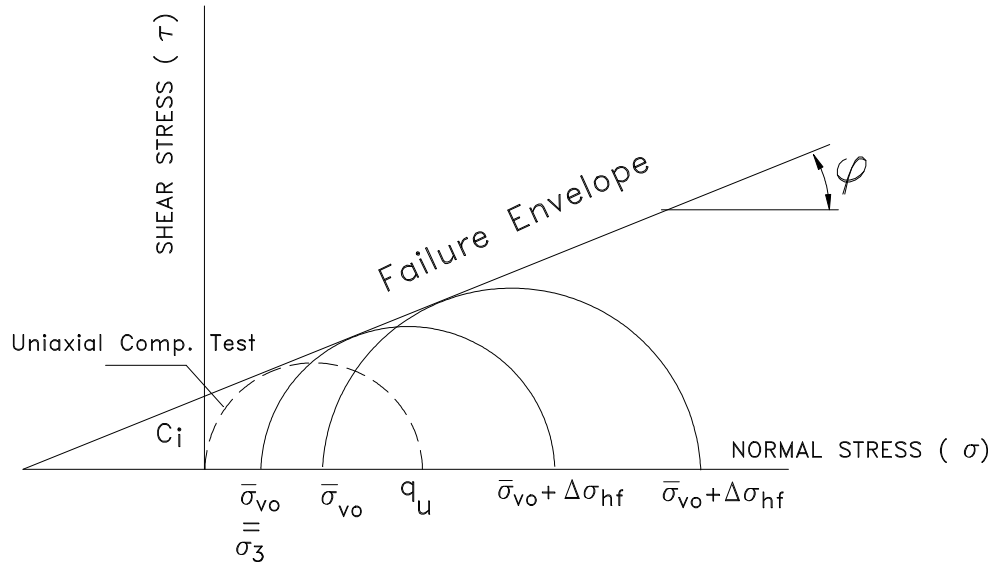
Figure 6-14. Mohr-Coulomb failure criteria from the triaxial test (weathered rock)

This is the deviator stress at failure in a triaxial test at confining pressure $\sigma_3 = \overline{\sigma}_{vo}$. The corresponding stress level (SL) at any level of loading is expressed as

$$SL = \frac{\Delta\sigma_h}{\Delta\sigma_{hf}} \qquad (6\text{-}11)$$

where

$$\Delta\sigma_h = \left(q_u\right)_m + \overline{\sigma}_{vo}\left[\tan^2\left(45 + \frac{\varphi_m}{2}\right) - 1\right] \qquad (6\text{-}12)$$

$(q_u)_m$ is the mobilized unconfined compressive strength which varies with the stress level (SL).

$$\left(q_u\right)_m = 2\left(C_i\right)_m \tan\left(45 + \frac{\varphi_m}{2}\right) \qquad (6\text{-}13)$$

$$\frac{\left(C_i\right)_m}{C_i} = \frac{\tan\varphi_m}{\tan\varphi} \qquad (6\text{-}14)$$

where C and C_m are the cohesion intercepts for ultimate and mobilized resistance respectively.

55
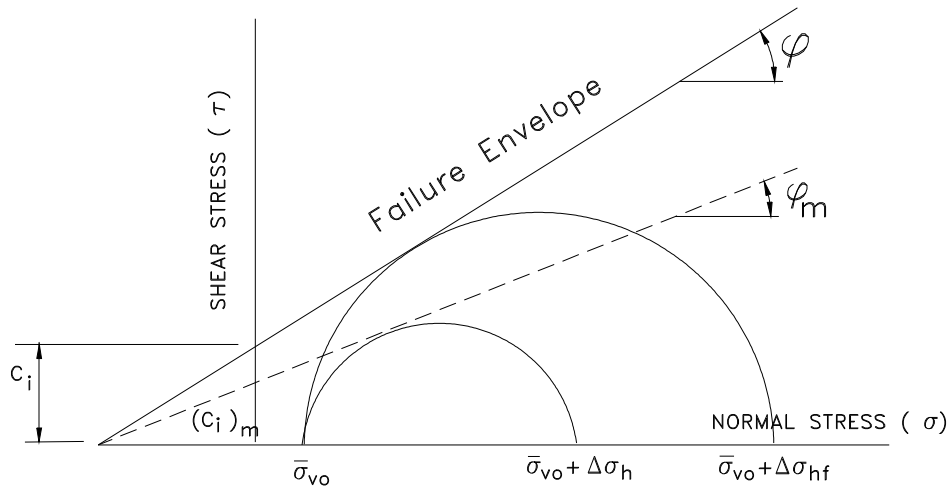
Figure 6-15. Relationship between failure and mobilized stresses in weak rock mass soil property characterization in the strain wedge model

One of the main advantages of the SW model approach is the simplicity of the required soil properties necessary to analyze the problem of a laterally loaded pile. The properties required represent the basic and the most common properties of soil, such as the effective unit weight and the angle of internal friction or undrained strength.

The soil profile is divided into one or two foot sublayers, and each sublayer is treated as an independent entity with its own properties. In this fashion, the variation in soil properties or response (such as ε_{50} and φ in the case of sand or S_u and $\bar{\varphi}$ in the case of clay) at each sublayer of soil can be explored. It is obvious that soil properties should not be averaged at the midheight of the passive wedge in front of the pile for a uniform soil profile (as in the earlier work of Norris 1986) or averaged for all sublayers of a single uniform soil layer of a multiple layer soil profile.

Properties Employed for Sand Soil

- Effective unit weight (total above water table, buoyant below), $\bar{\gamma}$
- Void ratio, e, or relative density, D_r
- Angle of internal friction, φ
- Soil strain at 50% stress level, ε_{50}

While standard subsurface exploration techniques and available correlations may be used to evaluate or estimate γ, e or D_r, and φ, some guidance may be required to assess ε_{50}.

56
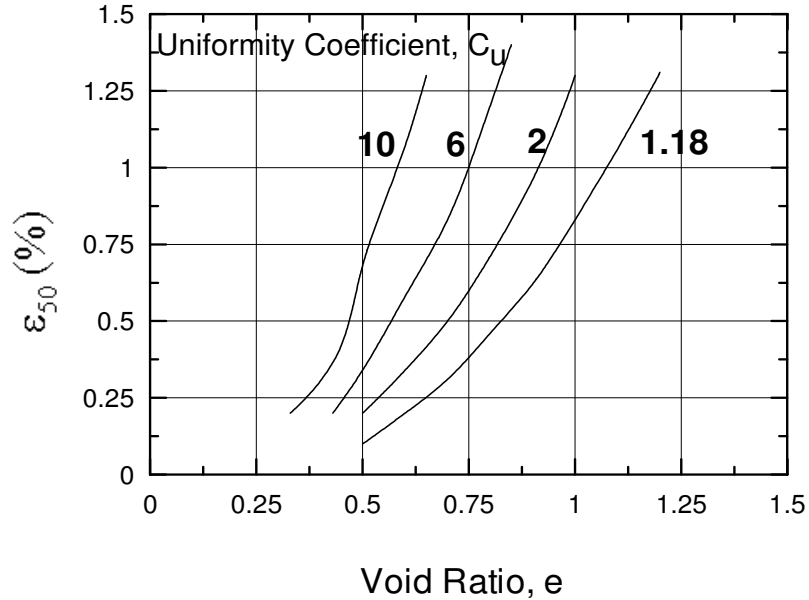
Figure 6-16. Relationship between ε_{50}, uniformity coefficient (C_u) and void ratio (e) (Norris 1986)

The ε_{50} represents the axial strain (ε_1) at a stress level equal to 50 percent in the ε_1-SL relationship that would result from a standard drained (CD) triaxial test. The confining (consolidation) pressure for such tests should reflect the effective overburden pressure (σ_{vo}) at the depth (x) of interest. The ε_{50} changes from one sand to another and also changes with density state. To obtain ε_{50} for a particular sand, one can use the group of curves shown in Figure 6-16 (Norris 1986), which show a variation based upon the uniformity coefficient, C_u, and void ratio, e. These curves have been assessed from sand samples tested with "frictionless" ends in CD tests at a confining pressure equal to 42.5 kPa (Norris 1977). Since the confining pressure changes with soil depth, ε_{50}, as obtained from Figure 6-16, should be modified to match the existing pressure as follows:

$$\left(\varepsilon_{50} \right)_i = \left(\varepsilon_{50} \right)_{42.5} \left(\frac{\left(\overline{\sigma}_{vo} \right)_i}{42.5} \right)^{0.2} ,$$
(6-28)

where $\overline{\sigma}_{vo}$ should be in kPa.

57
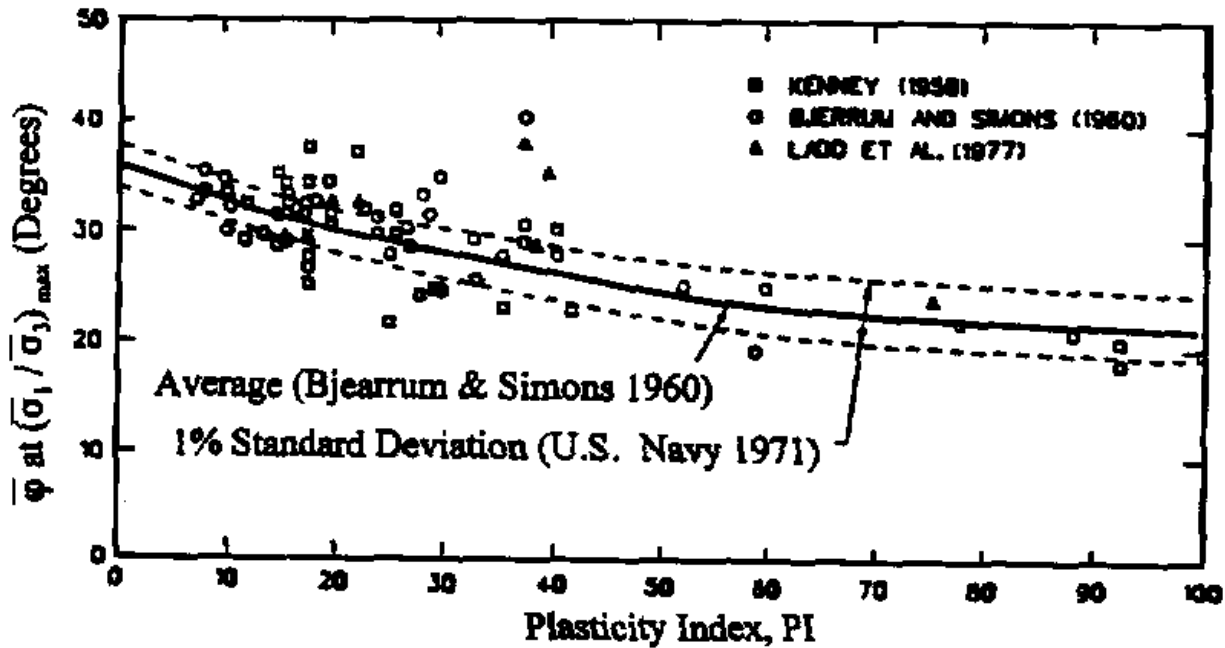
Figure 6-17. Relationship between plasticity index (pi) and effective stress friction angle (φ) (US Army Corps of Engineers 1996)

Properties Employed for Clay

- Effective unit weight, $\overline{\gamma}$
- Plasticity index, PI
- Effective angle of friction, $\overline{\varphi}$
- Undrained shear strength, S_u
- Soil strain at 50% stress level, ε_{50}

Plasticity index, PI, and undrained shear strength, S_u, are considered the governing properties because the effective angle of internal friction, $\overline{\varphi}$, can be estimated from the PI based on Figure 6-17. The ε_{50} from an undrained triaxial test (UU at depth x or CU with $\sigma_3 = \overline{\sigma}_{vo}$) can be estimated based on S_u as indicated in Figure 6-18.

58
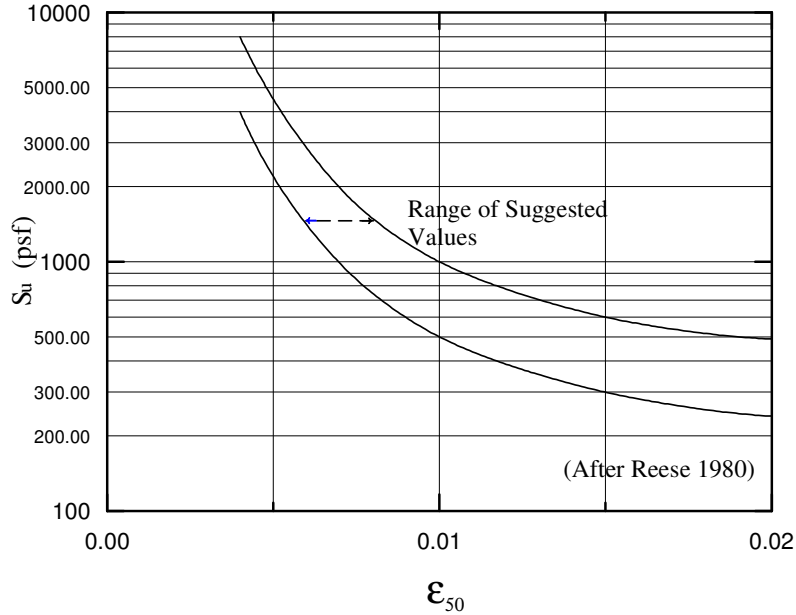
Figure 6-18. Relationship between ε_{50} and undrained shear strength, s_u (Evans and Duncan 1982)

Soil-Pile Interaction in the Strain Wedge Model

The strain wedge model relies on calculating the modulus of subgrade reaction, E_s, which reflects the soil-pile interaction at any level of soil strain during pile loading. E_s also represents the secant slope at any point on the p-y curve, i.e.

$$E_s = \frac{p}{y}$$ (6-39)

Note that p represents the force per unit length of the pile or the BEF soil-pile reaction and y symbolizes the pile deflection at that soil depth. In the SW model, E_s is related to the soil's Young's modulus, E, by two linking parameters: A and ψ_s. It should be mentioned that the SW model establishes its own E_s from the Young's modulus of the strained soil, and therefore one can assess the p-y curve using the strain wedge model analysis. Therefore, E_s should first be calculated using the strain wedge model analysis to identify the p and y values.

Corresponding to the horizontal slice (a soil sublayer) of the passive wedge at depth x (see Figures 6-7 and 6-9), the horizontal equilibrium of horizontal and shear stresses is expressed as

$$p_i = \left(\Delta \sigma_h \right)_i \overline{BC_i} \, S_1 + 2 \, \tau_i \, D \, S_2 ,$$ (6-15)

where S_1 and S_2 equal 0.75 and 0.5 respectively for a circular pile cross section and equal 1.0 each for a square pile (Briaud, *et al.* 1984). Alternatively, one can write the above equation as follows:

59

$$A_i = \frac{p_i / D}{\left(\Delta \sigma_h\right)_i} = \frac{\overline{BC_i}\, S_1}{D} + \frac{2\, \tau_i\, S_2}{\left(\Delta \sigma_h\right)_i} \qquad (6\text{-}16)$$

Here the parameter A is a function of pile and wedge dimensions, applied stresses, and soil properties (Ashour and Norris 2000). However, given that $\Delta \sigma_h = E\varepsilon$,

$$p_i = A_i\, D\, (\Delta \sigma_h)_i = A_i\, D\, E_i\, \varepsilon \qquad (6\text{-}17)$$

It should be mentioned that the SW model develops its own set of non-unique p-y curves that are functions of both soil and pile properties, including soil continuity (layering) as presented by Ashour*, et al.* (1996). For the lower passive wedge, $(h - x_i)$ will be replaced by x_i, which is measured downward from the point of zero crossing (Figure 6-10).

Pile Head Deflection

As mentioned previously, the deflection pattern of the pile in the SW model is continuous and linear. Based on this concept, pile deflection can be assessed using a simplified technique that estimates the linearized pile deflection, especially y_o at the pile head. By using the multi-sublayer technique, the deflection of the pile can be calculated starting with the base of the mobilized passive wedge and moving upward along the pile, accumulating the deflection values at each sublayer as shown in the following relationships and Figure 6-19.

$$y_i = H_i\, \delta_i = H_i\, \frac{\varepsilon}{\Psi_s} \qquad (6\text{-}18)$$

$$y_o = \Sigma\, y_i \qquad i = 1\, to\, n \qquad (6\text{-}19)$$

where the ψ_s value changes according to the soil type (sand or clay) (Ashour*, et al.* 1998), H_i indicates the thickness of sublayer I, and n symbolizes the current number of sublayers in the mobilized passive wedge.

The main point of interest is the pile head deflection, which is a function of not only the soil strain but also of the depth of the compound passive wedge that varies with soil and pile properties and the level of soil strain.

Sloping Ground in the SW Model

The SW model technique incorporates the effect of sloping ground on the pile lateral response according to the slope geometry and the growing stresses in the resisting soil. As discussed in this chapter, the shape and geometry of the mobilized passive wedge of soil vary with the level of loading and associated stress/strain. Therefore, as seen in Figure 6-19, the growth of the passive wedge will be limited by the boundary and location of sloping ground surface that terminates the increase of soil horizontal resistance at specific level. The multi-sublayer technique employed in the SW model analysis that divides the soil layers into sublayers identifies the horizontal extension of each soil sublayer until the soil wedge at that particular depth reaches the slope open face (Figure 6-20).
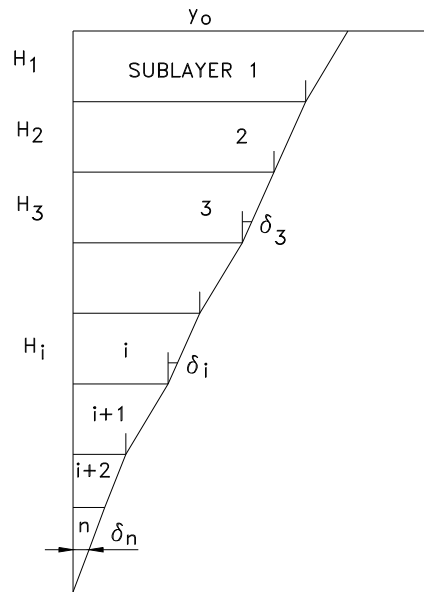
Figure 6-19. Assembling of pile head deflection using the multi-sublayer technique
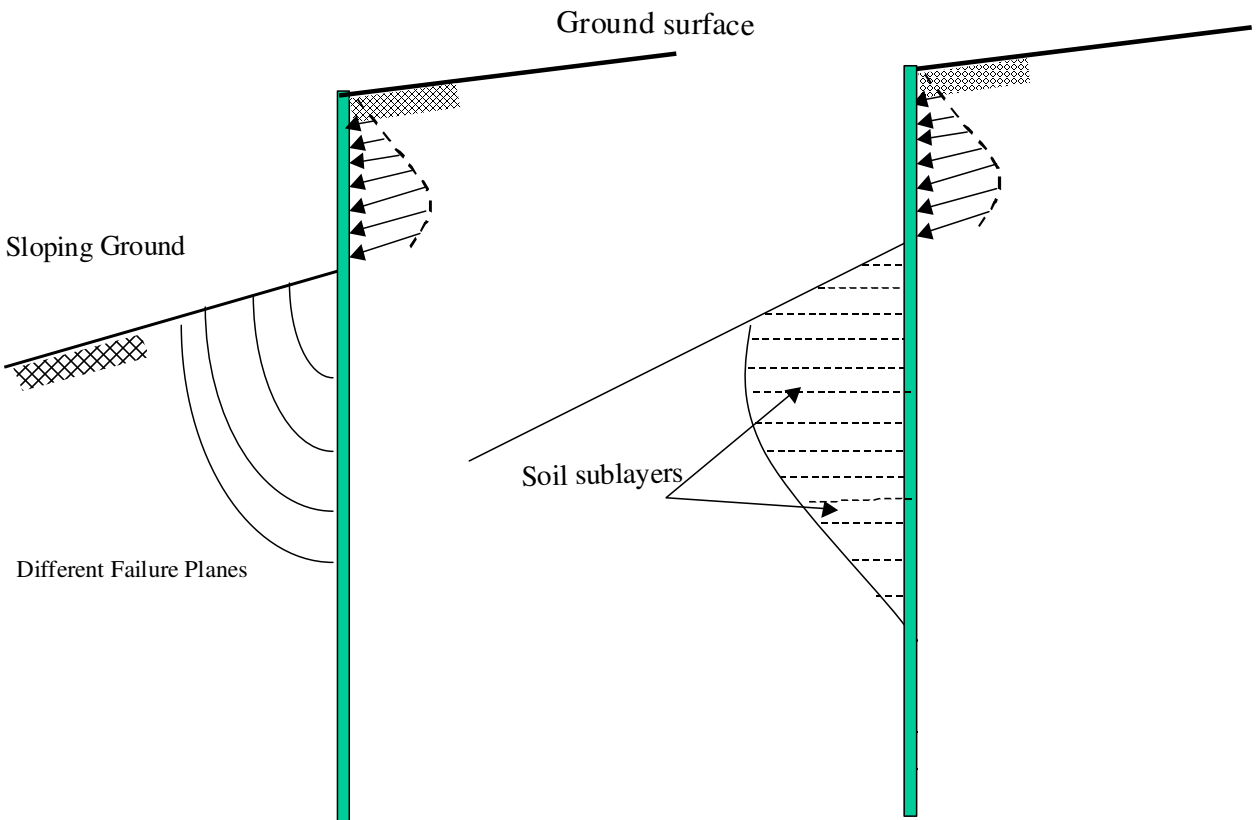
Figure 6-20. Mobilized soil passive with sloping ground as employed in the SW model

61

Pile Stability and Soil Pressure (Driving Force) above the Slip Surface

The SW model concepts presented in this chapter are employed to determine the distribution of the mobilized driving force above the slip surface. The value and distribution of the soil driving force are calculated in incremental fashion to maintain the pile stability under the driving force above the slip surface and associated resistance forces below the slip surface. Under such a sophisticated scenario soil strain developing in the stable soil below the slip surface is controlled by the soil mass displacement (i.e. soil strain) developing into the soil layers above the slip surface (Figure 6-21). This is the key mechanism utilized in the proposed research and the accompanying PSSLOPE-G software. The interaction between the pile and surrounding soils above and below the slip surface highlights the advantage of the established mechanism versus current practice that requires the assumption of either pile-head displacement along with the employment of the traditional p-y curves or the distribution of driving force. The SW model analysis above the slip surface also evaluates the ultimate driving forces that can be transferred via the pile to the sable soil below the slip surface. This depends on soil and pile properties and the interaction between the pile and surrounding soils before the stress in displaced soil reaches its ultimate strength or soil flow-around failure takes place at that depth.

Figure 6-21. Basic soil-pile modeling of pile-stabilized slopes using the SW model

INPUT DATA
Soil Properties (Fig. 2.3), Slope Profile (Fig. 2.4)
Type of Slope Failure (Figs. 2.5, 2.7 or 3.12)
Pile Properties (Fig. 3.1) and Desired Safety Factor

Simple Wedge

Exsiting or Potential
Failure Surface

Perform wedge stability analysis
with no piles

Perform slope stability analysis
(modified Bishop) with no piles

Calculate the driving force (F_D) along the slope
surface needed to acheive the desired safety factor
for the upslope (supported) part of the slope side

Divide soil layers into thin soil sublayers (i) with thichness H_i
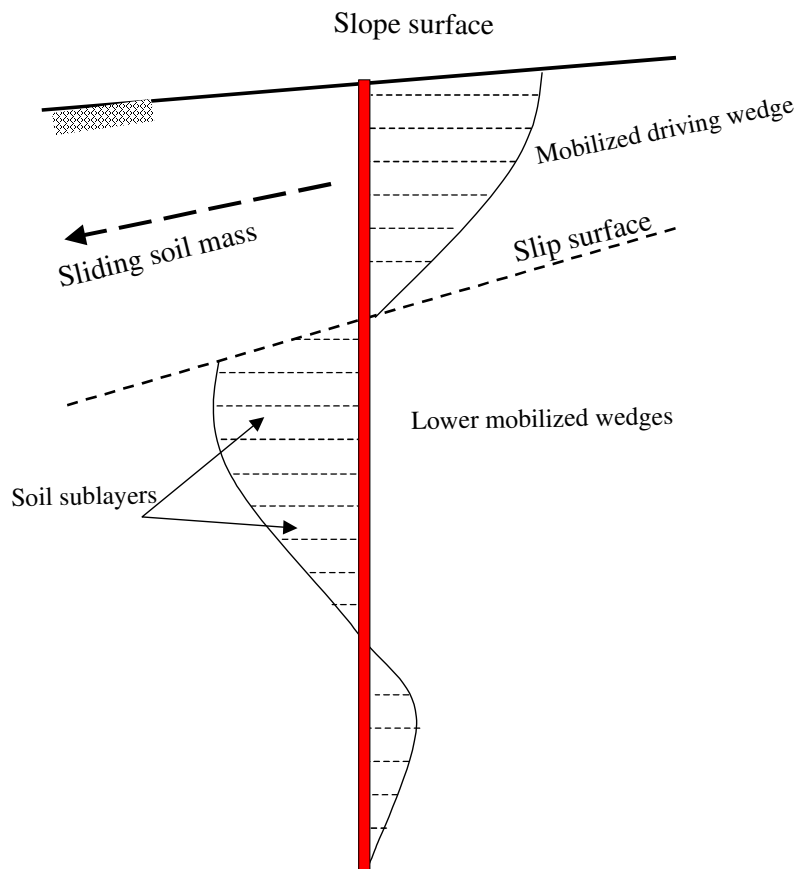
Calculate $\bar{\sigma}_{3c} = \bar{\sigma}_{vo}$ for each sublayer

Assume an initial small soil strain ε_u in soil above the slip surface

Assume a very small soil strain in soil layers below the slip surface

Just for the first trial use the soil profile to calculate
the pile type (L/T) (Fig.6.10)

Apply the SW model concepts/Eqs presented in this chapter to do the following:
1. Use ε_u to calculate $\Delta\sigma_h = \sigma_d$, SL, φ_m, BC, E, and p for sublayers above slip surface.
   The depth of the upper passive wedge is always equal to the depth of slipping mass (Fig. 6.28).
2. Use ε to calculate $\Delta\sigma_h = \sigma_d$, SL, φ_m, BC, E, E_s and p for sublayers below slip (Figs. 6.10 & 6.11)
   surface assuming X_o in the first trial (i.e. E_s profile along the pile for current ε_i)
3. Detemine the pile-head deflection $(Y_o)_{SWM}$ (Eq. 6.53)

1. Use E_s profile to solve the pile problem as a BEF under driving
   forces p_i acting on the pile above the slip surface.
2. Obtain the pile head deflection, $(Y_o)_{BEF}$, and the
   associated point of zero deflection, $(X_o)_{BEF}$ (i.e. h), (Fig.6.10)

IF
$(X_o)_{SWM} = (X_o)_{BEF}$

No

Adjust X_o

Yes

IF
$(Y_o)_{SWM} = (Y_o)_{BEF}$

No

IF$(Y_o)_{SWM} > (Y_o)_{BEF}$ Increase ε_u
IF$(Y_o)_{SWM} < (Y_o)_{BEF}$ Increase ε

Yes

1. Accepted loading increment, p_i, Y_o and E_s profile
2. Calculate Bending Deflection, Moment, Shear Force,
   Distribution of Driving Forces (p_i), and Safety Factor
3. Current Driving Force(P_c) = Σp_i above the slip surface

IF
$P_c < P_D$

Yes

Increase the value
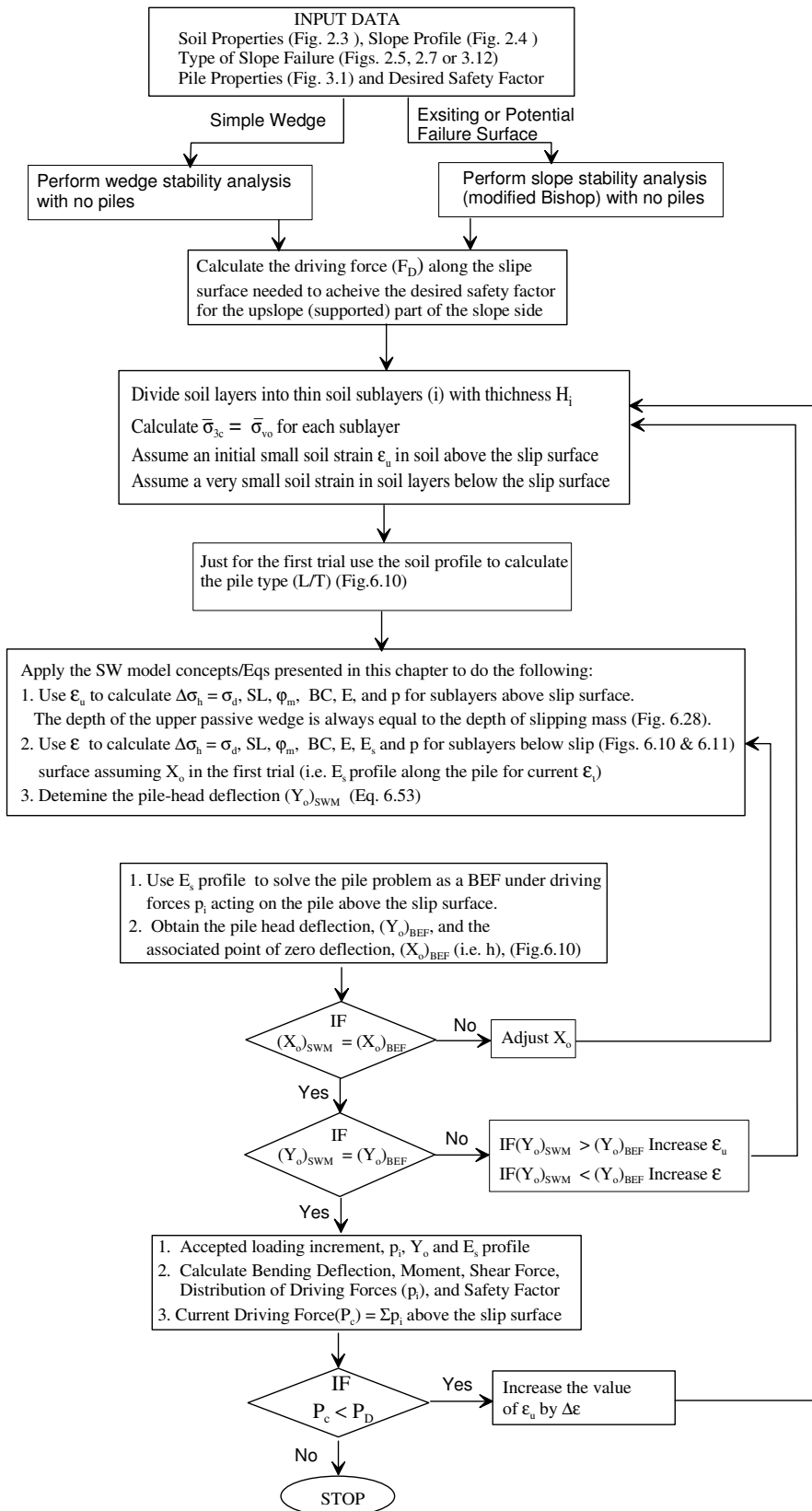of ε_u by $\Delta\varepsilon$

No

STOP

Figure 6-22. Flowchart for the pile-stabilized slopes as presented in the PSSLOPE-G

63

The Flowchart shown in Figure 6-22 demonstrates the calculation process performed in the PSSLOPE-G program. The Flowchart shows:

- The slope-stability analysis without piles.
- The amount of driving forces to be transferred to the stable soil below the slip surface along with the consideration of desired factor of safety.
- Soil resistance/deformation/strain developed above and below the slip surface to achieve global equilibrium along the whole pile at any increment of loading.
- Pile deflection, moment, shear force, and line load distribution at the final increment of stable loading that meets the desired factor of safety and pile distribution along the side of the slope (pile spacings).

Two Stabilizing Pile Rows in Staggered Distribution

The procedure presented by Ashour, *et al.* (2004) is utilized to assess the response of piles installed in the front and back pile rows used to stabilize the slope side. Figure 6-23 shows the locations of the staggered pile rows in the slope side. The down slope pile is called the front pile and the up slope pile is called the back pile.
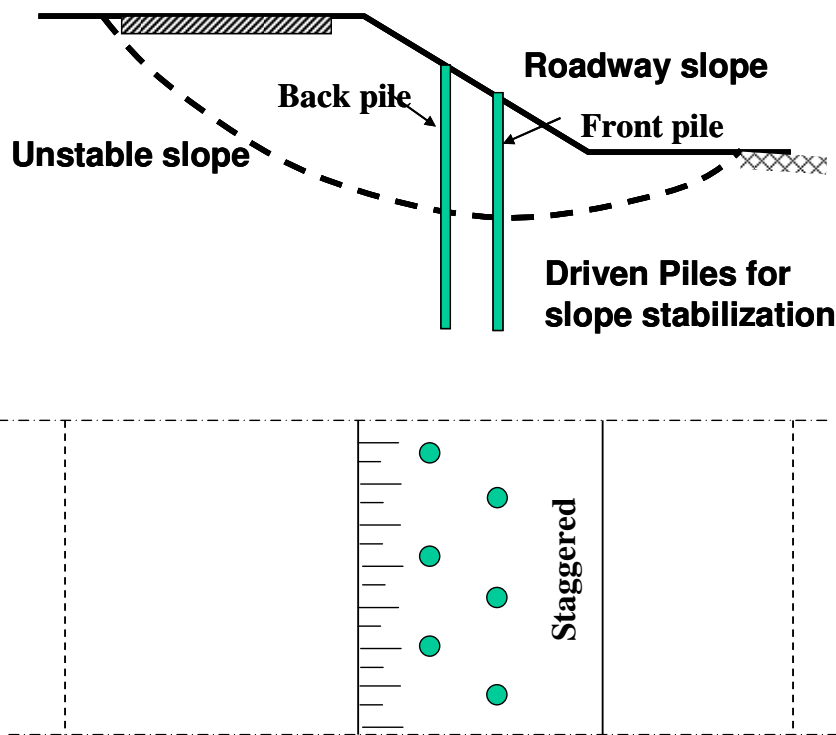

Figure 6-23. Staggered distribution of stabilizing piles

As seen in Figure 6-24, the staggered piles (i.e. passive soil wedges) in the pile rows along the slope side interact horizontally in an amount that varies with depth. Therefore, the varying overlap of the wedges of neighboring (side and front) piles in different sublayers over the depth of the interference and the associated increase in soil stress/strain can be determined as a

64

function of the amount of overlap. As pile lateral load increases, the wedges grow deeper and fan out horizontally, thus causing further changes in overlap and group interference, all of which vary with a change in soil and pile properties.

The current average value of horizontal stress change, $(\Delta\sigma h)_g$, and the associated stress level and strain (SL_g and ε_g) accumulated at the face of the passive wedge at a particular soil sublayer i (sand or clay) (Figure 6-24) are

$$(\Delta\sigma_h)_g = SL_g \, \Delta\sigma_{hf} \tag{6-20}$$

$$(SL_g)_i = SL_i (1 + \sum R_j)^{0.5} \leq 1 \tag{6-21}$$

where j equals the number of neighboring passive wedges in soil layer that overlap the wedge of the pile in question. R (a value less than 1) represents the ratio between the length of the overlapped portion of the face of the passive wedge and the total length of the face of the passive wedge (BC) and derives from all neighboring piles on both sides and in front of the pile in question (Figure 6-24). The SW model assesses SL_g and the associated soil strain (ε_g) in each soil sublayer in the passive soil wedge of each pile in the group. Here ε_g is $\geq \varepsilon$ of the isolated pile and is determined based on the stress-strain relationship ($\Delta\sigma h$ vs ε) presented earlier. The induced soil strain ε_g and Young's modulus E_g related to the pile in question are determined as follows:

$$(\varepsilon_g)_i = \varepsilon_i + \Delta\varepsilon_i \tag{6-22}$$

$$(E_g)_i = \frac{(SL_g)_i (\Delta\sigma_{hf})_i}{(\varepsilon_g)_i} \tag{6-23}$$

The angles and dimensions of the passive wedge (φ_m, β_m, and BC) are modified for group effect according to the estimates of SLg and ε_g. The new $(Es)_g$ of soil layer (Figure 6-25), i, is expressed as

$$\left[(E_s)_g \right]_i = \frac{(A_g)_i \, D \, (\varepsilon_g)_i \, (E_g)_i}{\delta_i (h - x_i)} \tag{6-24}$$

Over the depth of interference (stress overlapping) among the piles, as shown in Figure 6-25, $(Es)_g$ of the pile in question, will be less than Es of the isolated pile. The new profile of $(Es)_g$ will be used to analyze the pile as a BEF (Figure 6-25). The parameter A_g of sublayer i at depth x is a function of the pile and passive soil wedge geometry (including the wedge depth h); the shear stress (τ) at the pile side-soil interface; and the deviatoric stress change, $(\Delta\sigma h)_g$. Detailed information is provided by Ashour, *et al.* (2004).
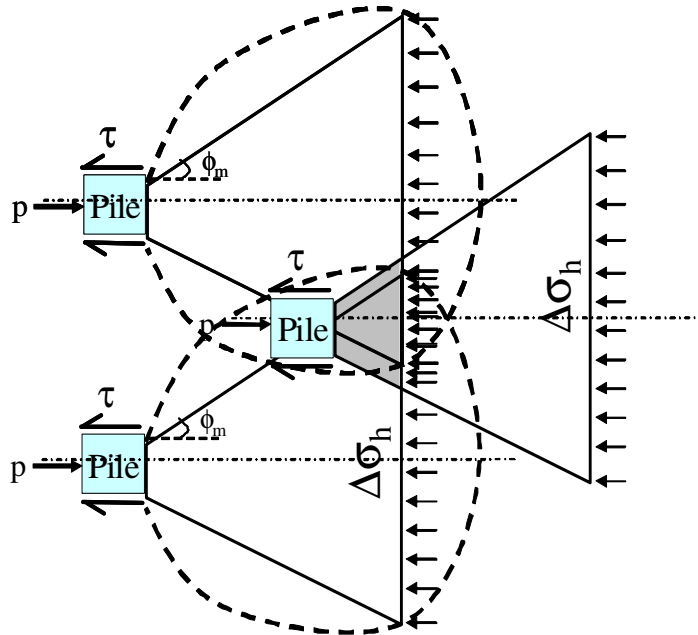
(a) Pile initial interference and soil wedge overlap

Pile   Pile

Overlap of stresses based on elastic theory
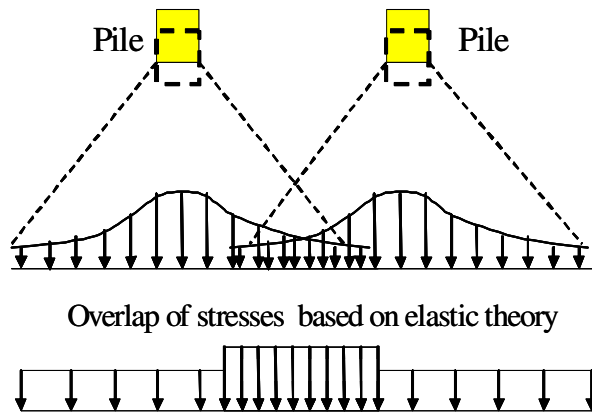
(b) uniform stress overlap in the SW model

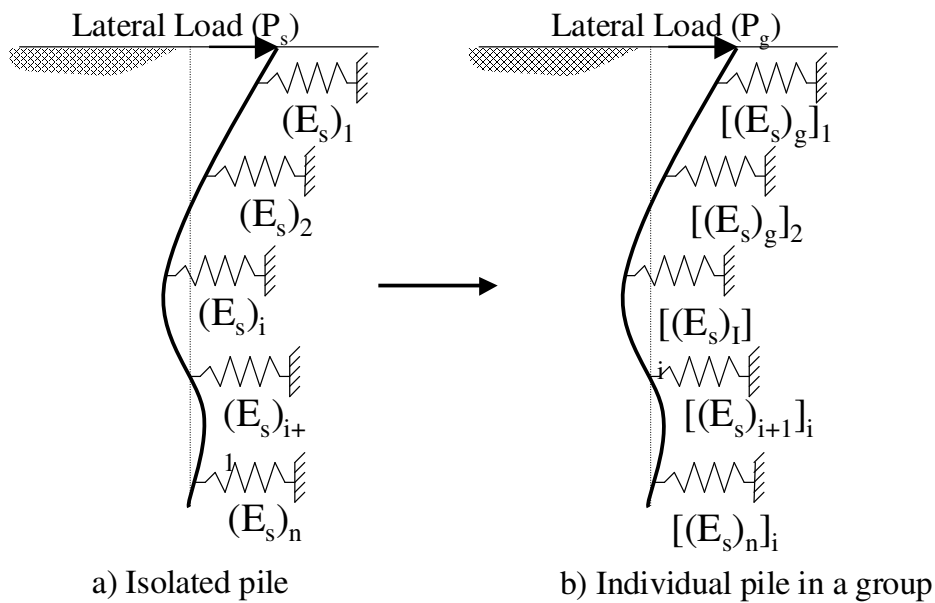**Figure 6-24. Interaction among staggered piles in two rows**

Figure 6-25. Modulus of subgrade reaction profiles for an isolated pile and individual pile in pile rows

Summary

The design procedure presented in this study employs the SW model approach as an effective method for solving the problem of pile-stabilized slopes by calculating the value and distribution of the mobilized driving force induced by a slipping mass of soil. The developed technique also assesses the profile of the nonlinear modulus of subgrade reaction (i.e. p-y curves) for the soil-pile along the length of the pile embedded in the stable soil (below the slip surface). The SW model allows the assessment of the nonlinear p-y curve response of a laterally loaded pile based on the envisioned relationship between the three-dimensional response of a flexible pile in the soil to its one-dimensional beam on elastic foundation parameters. In addition, the SW model employs stress-strain-strength behavior of the soil/weathered rock as established from the triaxial test in an effective stress analysis to evaluate mobilized soil behavior. Moreover, the required parameters to solve the problem of the laterally loaded pile are a function of basic soil properties that are typically available to the designer.

The presented procedure estimates the interference among neighboring piles in the same pile row and the effect of the back pile row on the front one. The pile spacing along the slope embankment (same pile row) governs the magnitude of the driving force carried by the pile and lateral interference among those pile. Furthermore, the soil flow-around plays an important role in limiting the amount of driving force that could be transferred by the pile. It should be noted that the pile-stabilized slope analysis presented in this study assumes that the displacement of the slipping mass of soil is always equal to or larger than the pile deflection.

Section 7
Finite Element Analysis

A comprehensive computation of the loads acting on slope stabilizing piles requires 3D modeling of the problem. It is thought that the 3D piled slope model including a sliding zone is a better representation of the actual field conditions and provides a better insight into the load-transfer mechanisms of piled slopes. The finite element analysis program, PLAXIS-3D Foundation Version 2 (Brinkgreve and Broere 2007), is used for the analysis.

The basic soil elements of a 3D finite element mesh are the 15-node wedge elements (Figure 7-1). These elements are generated from the 6-node triangular elements as generated in a PLAXIS-2D mesh. Due to the presence of non-horizontal soil layers, some 15-node wedge elements may degenerate to 13-node pyramid elements or even to 10-node tetrahedral elements.
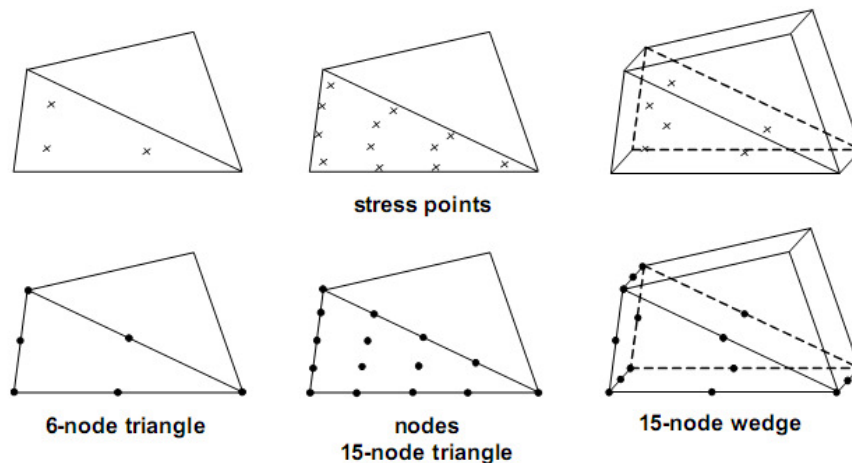

Figure 7-1. Comparison of 2D and 3D soil elements

In addition to the soil elements, special types of elements are used to model structural behavior. For beams (i.e. pile), 3-node line elements are used, which are compatible with the 3-node sides of a soil element. In addition, 12-node and 16-node interface elements are used to simulate soil-structure interaction.

Boreholes are used to define the soil stratigraphy and ground surface level. Soil layers and ground surface may be non-horizontal by using several boreholes at different locations. It is also possible in a calculation phase to assign new material data sets to soil volume clusters or structural objects. This option may be used to simulate the change of material properties with time during the various stages of construction. The option may also be used to simulate soil

improvement processes, e.g. removing poor quality soil and replacing it with soil of a better quality.

The soil mass is modeled using Mohr-Coulomb model (MC model). This linear elastic perfectly plastic model requires five basic input parameters: Young's modulus E, Poisson's ratio ν, the cohesion c, the friction angle φ, and the dilatancy angle ψ.

The reinforcing piles are modeled using the embedded pile element. An embedded pile consists of beam elements with special interface elements providing the interaction between the beam and the surrounding soil. The beam elements are 3-node line elements with six degrees of freedom per node: Three translational degrees of freedom (u_x, u_y, and u_z) and three rotational degrees of freedom (Θ_x, Θ_y, and Θ_z). Element stiffness matrices are numerically integrated from the four Gaussian integration points (stress points). The element allows for beam deflections due to shearing as well as bending. In addition, the element can change length when an axial force is applied.

The material properties of embedded piles include the pile stiffness, the unit weight of the pile material γ, the cross section geometry parameters, the skin resistance, and the foot resistance. In contrast to normal beams, the beam elements of embedded piles cannot have non-linear structural properties. Pile forces (structural forces) are evaluated at the beam element integration points and extrapolated to the beam element nodes and can be viewed graphically and tabulated in the output.

It should be noted that the embedded pile material data set contains neither 'p-y curves' nor equivalent spring constants. In fact, the stiffness response of an embedded pile subjected to loading is the result of the specified pile length, equivalent radius, stiffness and bearing capacity, and the stiffness of the surrounding soil.

Safety Analysis by Strength Reduction Method (SRM)

The shear strength reduction method (called the Phi-c reduction approach in PLAXIS) has been used in the analysis of slopes without piles by Zienkiewicz, *et al.* (1975); Matsui and San (1992); Ugai and Leshchinsky (1995); Dawson, *et al.* (1999); Griffiths and Lane (1999); Cheng, *et al.* (2007); Wei, *et al.* (2009); and others. Also, for pile stabilized slopes, Cai and Ugai (2000); Won, *et al.* (2005); and Wei, *et al.* (2009) have considered the effects of stabilizing piles on the stability of a slope by a three-dimensional finite element analysis using the SRM. However, the use of the SRM with piles results in the development of a new critical failure surface different from the original one induced before pile installation.

In the Phi-c reduction approach the strength parameters tan φ and c of the soil are successively reduced until failure of the structure occurs. The strength of interfaces, if used, is reduced in the same way. The strength of structural objects like plates and anchors is not influenced by the Phi-c reduction.

The total multiplier ΣMsf is used to define the value of the soil strength parameters at a given stage in the analysis:

$$\sum Msf = \frac{\tan\phi_{input}}{\tan\phi_{reduced}} = \frac{c_{input}}{c_{reduced}}$$

where the strength parameters with the subscript 'input' refer to the properties entered in the material sets and parameters with the subscript 'reduced' refer to the reduced values used in the analysis. A Phi-c reduction is performed using the load advancement number of steps procedure. The strength parameters are successively reduced automatically to reach failure. In this case, the factor of safety is given by

$$SF = \frac{available\ strength}{strength\ at\ failure} = value\ of\ \sum Msf\ at\ failure$$

The best way to evaluate the factor of safety is to plot a curve in which the parameter ΣMsf is plotted against the displacement of a certain point. In this way it can be checked whether a constant value is obtained while the deformation is continuing; in other words, whether a failure mechanism has fully developed. Although displacements are not relevant, they indicate whether the failure mechanism developed. Also, incremental displacement plot at failure gives an indication of the likely failure mechanism.

Reinforced Concrete Piles Used to Stabilize a Railway Embankment

Slope model and finite element mesh for the case conducted by Smethurst and Powerie (2007), which is presented in Section 5, is shown in Figure 7-2. The same case study is reanalyzed via the FE method using program PLAXIS. Same pile and soil properties presented in Section 5 are employed in the FE analysis. It should be noted that the pile cracked section properties are used in current analysis.

The Strength Reduction Method (SRM) is used to investigate potential failure surface and measure SF for the slope before using stabilizing piles. Although exact location of critical slip surface cannot be calculated by SRM, but displacement zones for potential critical surfaces can be seen in Figures 7-3 and 7-4. As given in Figure 7-5, the factor of safety for the slope (without piles) is around 1.09.
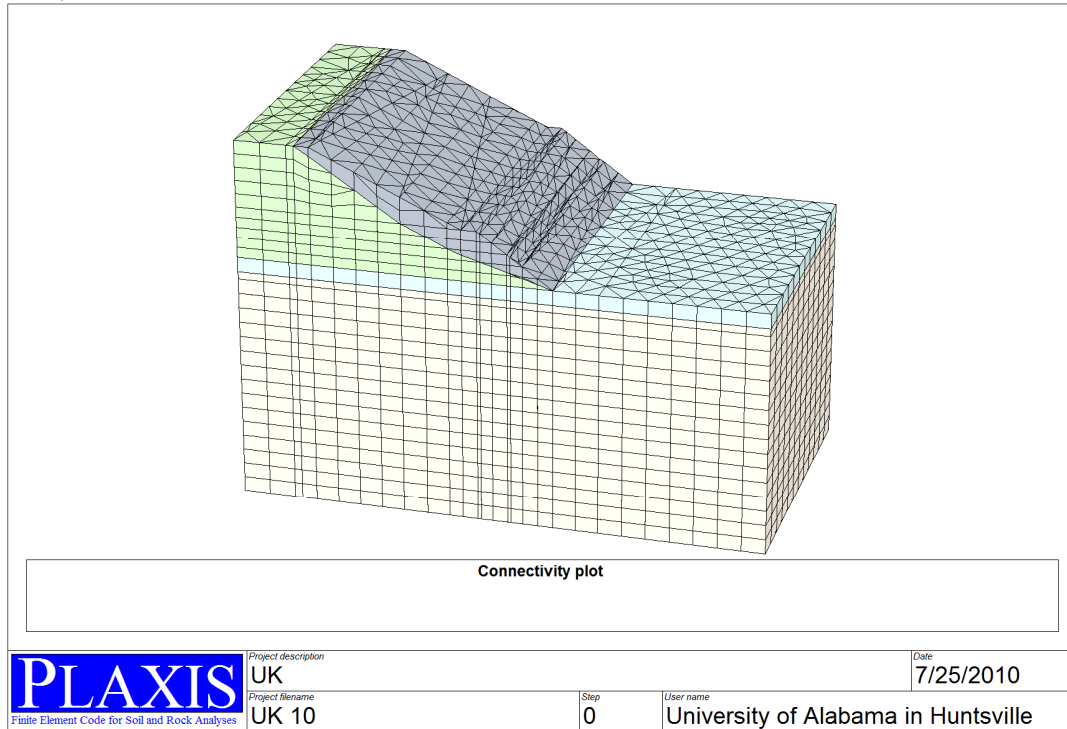
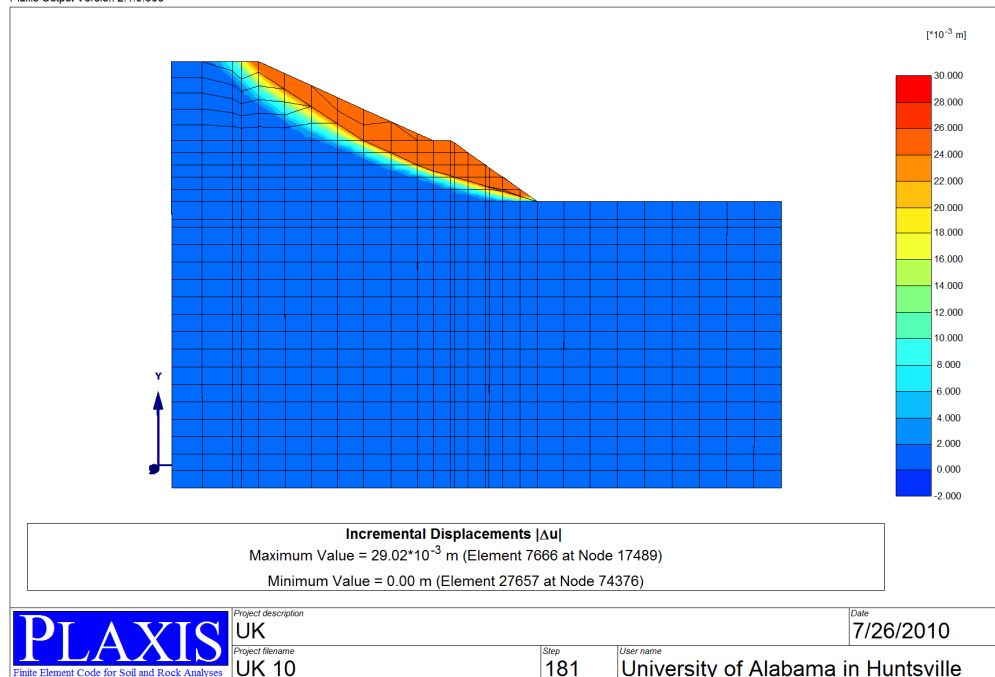**Figure 7-2. Slope model and finite element mesh**

Figure 7-3. Displacement zones for potential critical surfaces before stabilization

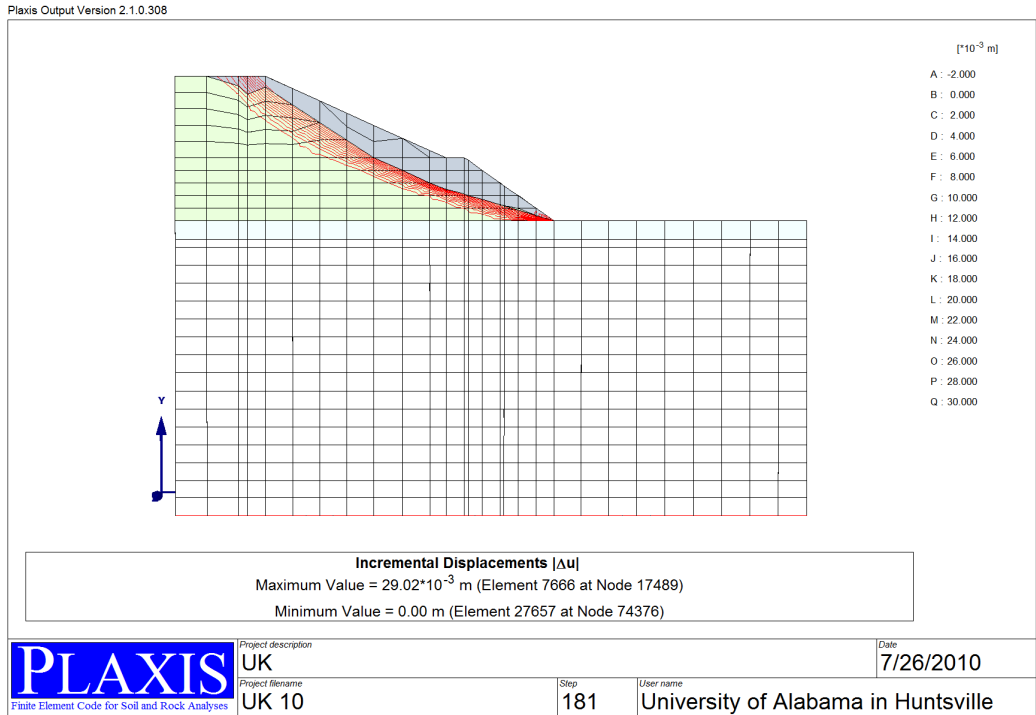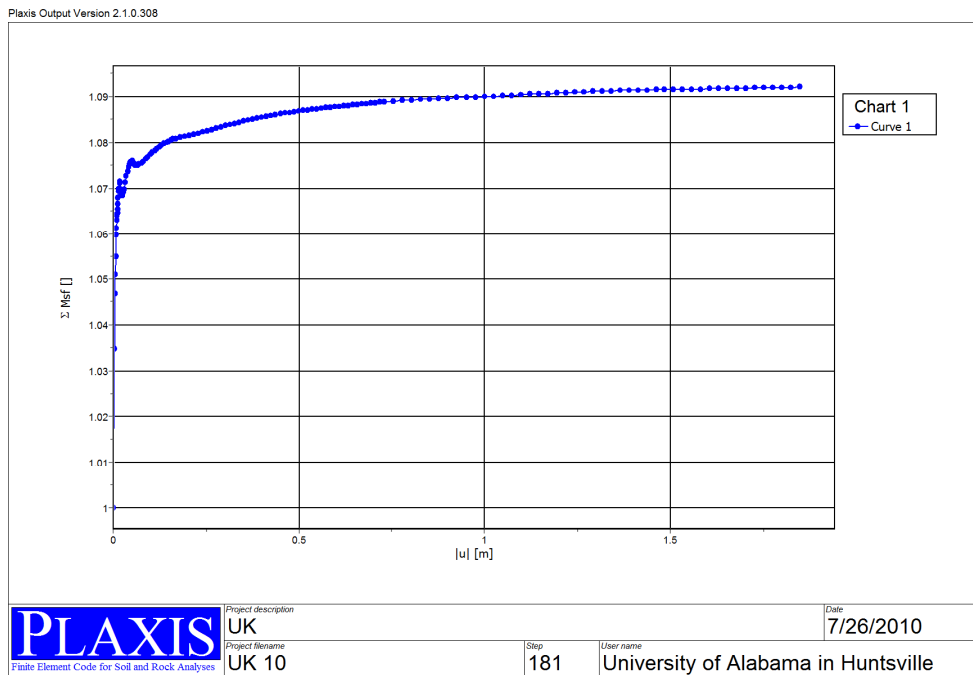**Figure 7-4. Displacement contours for potential critical surfaces before stabilization**

Figure 7-5. Slope stability factor of safety assessed in PLAXIS
using the phi-c reduction approach before stabilization

To model the suggested slip surface by Smethurst and Powerie (2007), a thin weak layer was considered along the critical surfaces (Figure 7-6). The instrumented discrete reinforced

72

concrete piles used to stabilize a 26-ft high railway embankment of weald clay at Hildenborough, Kent, UK, are modeled in Figure 7-7. The soil strength parameters used in design, which are based on data from the site investigation and associated triaxial tests, are given in Table 7-1.

Table 7-1. Design soil parameters

Soil type	Unit weight, γ : lb/ft^3	Friction angle, ϕ' : degrees	Effective cohesion, c' : lb/ft^3
Weald Clay embankment fill	121	25	20.9
Softened Weald Clay embankment fill	121	19	20.9
Weathered Weald Clay	121	25	20.9
Weald Clay	127	30	104.4
Rockfill	121	35	0

Plaxis Output Version 2.1.0.308

Connectivity plot

PLAXIS Finite Element Code for Soil and Rock Analyses	Project description UK		Date 7/25/2010
	Project filename UK 13	Step 0	User name University of Alabama in Huntsville

Figure 7-6. Modeling the critical failure surface suggested by Smethurst and Powerie (2007)

Connectivity plot

	Project description			Date
PLAXIS	UK			7/25/2010
Finite Element Code for Soil and Rock Analyses	Project filename UK 13	Step 5	User name University of Alabama in Huntsville	
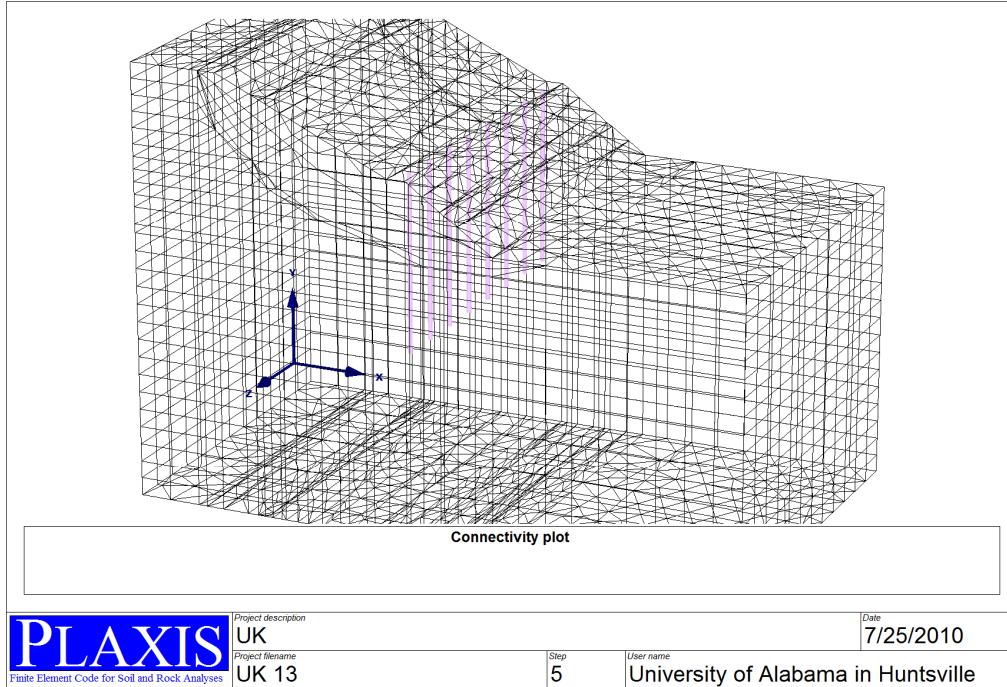
Figure 7-7. FE modeling of pile stabilized slope tested by Smethurst and Powerie (2007)

$[*10^{-3}$ m$]$

Total Displacements |u|

Maximum Value = $46.04*10^{-3}$ m (Element 9961 at Node 27424)

Minimum Value = 0.00 m (Element 34768 at Node 92306)

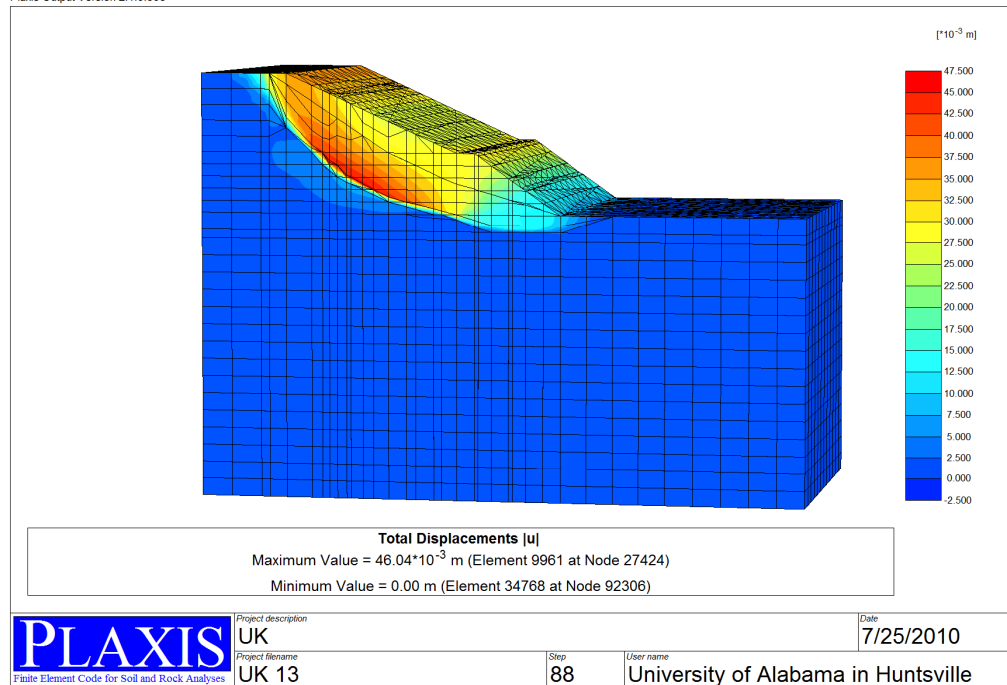|	Project description			Date
PLAXIS	UK			7/25/2010
Finite Element Code for Soil and Rock Analyses	Project filename UK 13	Step 88	User name University of Alabama in Huntsville	

Figure 7-8. Total displacement of the pile stabilized slope as obtained from PLAXIS

Figure 7-8 shows the total displacement developed into the slope after pile stabilization. The critical spots in the slope are highlighted to show the concentration of displacements of the soil mass behind the pile row.

Figures 7-9 and 7-10 present a comparison between measured and computed pile deflection and moment using the SW model technique (Section 5) and the FE method (PLAXIS).
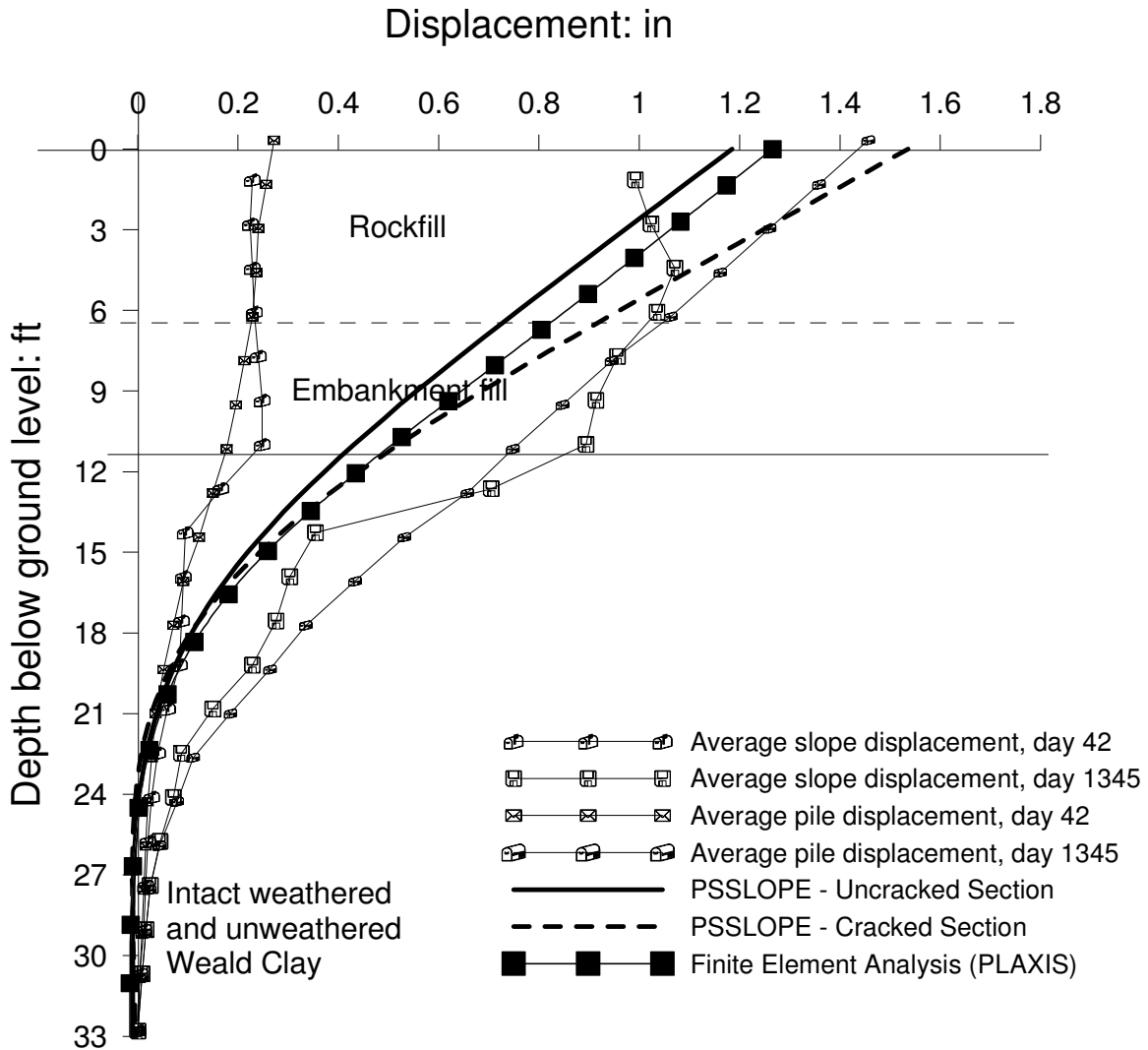

Figure 7-9. Averaged measured and computed pile and soil displacements (after Smethurst and Powerie 2007)
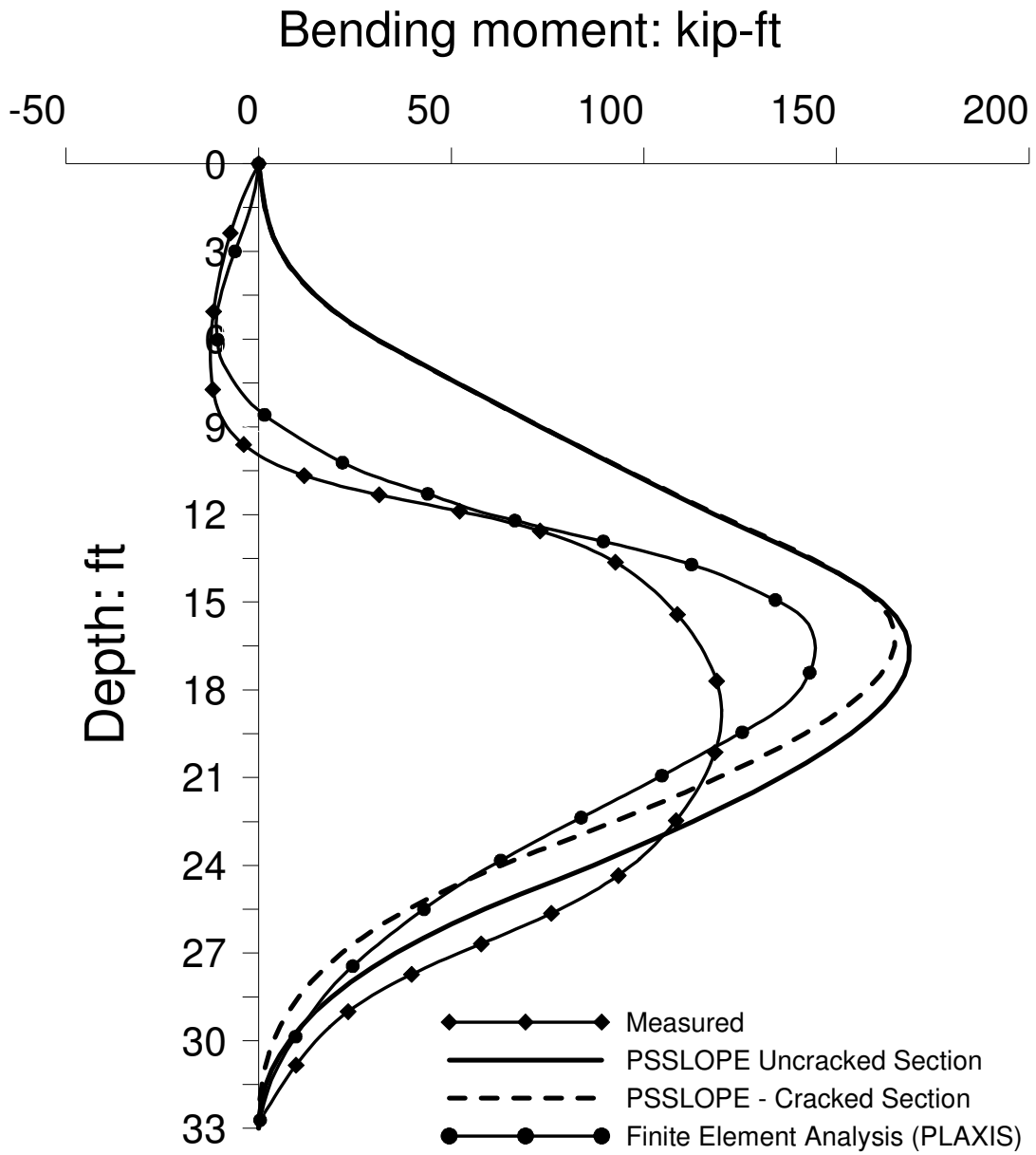
Bending moment: kip-ft

Depth: ft

Measured

PSSLOPE Uncracked Section

PSSLOPE - Cracked Section

Finite Element Analysis (PLAXIS)

Figure 7-10. Measured and computed bending moment in pile c
(after Smethurst and Powerie 2007)

76

Section 8
References

AASHTO (American Association of State Highway and Transportation Officials). *AASHTO LRFD Bridge Design Specifications*. Section C.10.7.2.4. 2007.

Ashour, M. and G.M. Norris. "Modeling lateral soil-pile response based on soil-pile interaction." *Journal of Geotechnical and Geoenvironmental Engineering*. Vol. 126, no. 5, pp. 420-428. 2000.

Ashour, M. and G.M. Norris. *Strain Wedge Model Computer Program for Piles and Large Diameter Shafts with LRFD Procedure*. Nevada Department of Transportation, Contract No. 2007-P498-07-803. 2007.

Ashour, M., G.M. Norris, and P. Pilling. Lateral loading of a pile in layered soil using the strain wedge model." *Journal of Geotechnical and Geoenvironmental Engineering*. Vol. 124, no. 4, pp. 303-315. 1998.

Ashour, M., G.M. Norris, and A. Shamsabadi. "Effect of the non-linear behavior of pile material on the response of laterally loaded piles." Presented at the *Fourth International Conference on Recent Advances in Geotechnical Earthquake Engineering and Soil Dynamics*. San Diego, CA. March 26-31, 2001. Paper 6.10. 2001.

Ashour, M., G.M. Norris, S. Bowman, H. Beeston, P. Billing, and A. Shamsabadi. "Modeling pile lateral response in weathered rock." *Proceedings of the 36th Engineering Geology and Geotechnical Engineering Symposium*. Las Vegas, NV. March 2001.

Ashour, M., P. Pilling, and G.M. Norris. "Lateral behavior of pile group in layered soils." *Journal of Geotechnical and Geoenvironmental Engineering*. Vol. 130, no. 6, pp. 580-592. 2004.

Ashour, M., P. Pilling, G. Norris, and H. Perez. *Development of Strain Wedge Model Program for Pile Group Interference and Pile Cap Contribution Effects*. Department of Civil Engineering, University of Nevada, Report no. CCEER-94-4, Reno, NV. Federal Study no. F94TL16C, Submitted to State of California Department of Transportation (CalTrans). 1996.

Briaud, J.L., T. Smith, and B. Mayer. "Laterally loaded piles and the pressuremeter: comparison of existing methods." *Laterally Loaded Deep Foundations*. STP 835, pp. 97-111. 1984.

Brinkgreve, R.B.J. and W. Broere. *Plaxis 3D Foundation Manual: Version 2*. Delft University of Technology and PLAXIS bv, The Netherlands. 2007.

Broms, B.B. "Lateral resistance of piles in cohesive soils." *Journal of the Soil Mechanics and Foundation Division*. Vol. 90, no. SM2, pp. 27-63. 1964.

Cai, F. and K. Ugai. "Numerical analysis of the stability of a slope reinforced with piles." *Soils and Foundations*. Vol. 40, no. 1, pp. 73–84. 2000.

Cheng, Y.M., T. Lansivaara, and W.B. Wei. "Two-dimensional slope-stability analysis by limit equilibrium and strength reduction methods." *Computers and Geotechnics*. Vol. 34, no. 3, pp. 137–50. 2007.

Coyle, H.M. and L.C. Reese. "Load transfer for axially loaded piles in clay." *Journal of the Soil Mechanics and Foundations Division*. Vol. 92, no. SM2. 1966.

Dawson, E.M., W.H. Roth, and A. Drescher. "Slope-stability analysis by strength reduction." *Geotechnique*. Vol. 49, no. 6, pp. 835–840. 1999.

Evans Jr., L.T. and G.M. Duncan. *Simplified Analysis of Laterally Loaded Piles*. University of California, Berkeley Report Number USB/GT/82-04. 1982.

Gowda, P. *Laterally Loaded Pile Analysis for Layered Soil Based on the Strain Wedge Model*. M.S. Thesis, University of Nevada, Reno. 1991.

Griffiths, D.V. and P.A. Lane. "Slope-stability analysis by finite elements." *Geotechnique.* Vol. 49, no. 3, pp. 387–403. 1999.

Hughes, J.M.O., P.R. Goldsmith, and H.D.W. Fendall. *The Behavior of Piles to Lateral Loads*. Department of Civil Engineering, University of Auckland, Report no. 178, Auckland, New Zealand. 1978.

Matlock, H. and L.C. Reese. "Generalized solution for laterally loaded piles." *Journal of the Soil Mechanics and Foundations Division*. Vol. 86, no. SM5, pp. 673-694. 1961.

Matsui, T. and K.C. San. "Finite element slope-stability analysis by shear strength reduction technique." *Soils and Foundations.* Vol. 32, no. 1, pp. 59–70. 1992.

NAVFAC (Naval Facilities Engineering Command). *Foundations and Earth Retaining Structures Design Manual*. Department of the Navy, DM 7.2, Alexandria, VA. 1982.

Norris, G.M. *The Drained Shear Strength of Uniform Quartz Sand as Related to Particle Size and Natural Variation in Particle Shape and Surface Roughness*. PhD dissertation, University of California, Berkeley. 1977.

Norris, G.M. "Theoretically based BEF laterally loaded pile analysis." Presented at the *Third International Conference on Numerical Methods in Offshore Piling*. Nantes, France, pp. 361-386. 1986.

Reese, L.C. "Discussion of 'Soil modulus for laterally loaded piles'." *Transactions*. Vol. 123, pp. 1071. 1958.

Reese, L.C. *Behavior of Piles and Pile Groups Under Lateral Load*. Office of Research, Development, and Technology, Federal Highway Administration, US Department of Transportation, Washington, DC, September 1983.

Rowe, P.W. "The single pile subject to horizontal force." *Geotechnique*. Vol. 6, no. 2, pp. 70-85. 1956.

Skempton, A.W. "The pore pressure coefficients A and B." *Geotechnique*. Vol. 4, no. 4, pp. 143-147. 1954.

Smethurst, J.A. and W. Powrie. "Monitoring and analysis of the bending behavior of discrete piles used to stabilize a railway embankment." *Geotechnique*. Vol. 57, no. 8, pp. 663–677. 2007.

Tomlinson, M.J. "The adhesion of piles driven in clay soils." *Proceedings of the Fourth International Conference on Soil Mechanics and Foundation Engineering*, Vol. II. London, UK, pp. 66-71. 2007.

Ugai, K. and D. Leshchinsky. "Three-dimensional limit equilibrium and finite element analysis: A comparison of results." *Soils and Foundations*. Vol. 35, no. 4, pp. 1–7. 1995.

US Army Corps of Engineers. *Design of Sheet Pile Walls*. ASCE Press. 1996.

Wei, W.B., Y.M. Cheng, and L. Li. "Three-dimensional slope failure analysis by the strength reduction and limit equilibrium methods." *Computers and Geotechnics*. Vol. 36, pp. 70–80. 2009.

Wei, W.B. and Y.M. Cheng. "Strength reduction analysis for slope reinforced with one row of piles." *Computers and Geotechnics*. Vol. 36, pp. 1176–1185. 2009.

White, D., H. Yang, M. Thompson, and V.R. Schaefer. *Innovative Solutions for Slope Stability Reinforcement and Characterization*. Center for Transportation Research and Education, Iowa State University, IHRB Project TR-489, Ames, IA, 2005.

Won, J., K. You, S. Jeong, and S. Kim. "Coupled effects in stability analysis of pile-slope systems." *Computers and Geotechnics*. Vol. 32, no. 4, pp. 304–315. 2005.

Wu, T.H. *Soil Mechanics*. Boston: Allyn and Bacon. 1966.

Zienkiewicz, O.C., C. Humpheson, and R.W. Lewis. "Associated and non-associated visco-plasticity and plasticity in soil mechanics." *Geotechnique*. Vol. 25, no. 4, pp. 671–89. 1975.